Award Number: W81XWH-12-1-0311

TITLE: Early Intervention with cdk9 Inhibitors to Prevent Post-Traumatic Osteoarthritis

PRINCIPAL INVESTIGATOR: Dominik R. Haudenschild. Ph.D.

CONTRACTING ORGANIZATION: University of California, Davis
Davis, CA 95618

REPORT DATE: October 2014

TYPE OF REPORT: Annual

PREPARED FOR: U.S. Army Medical Research and Materiel Command
Fort Detrick, Maryland 21702-5012

DISTRIBUTION STATEMENT: Approved for Public Release;
Distribution Unlimited

The views, opinions and/or findings contained in this report are those of the author(s) and should not be construed as an official Department of the Army position, policy or decision unless so designated by other documentation.

REPORT DOCUMENTATION PAGE

Form Approved
OMB No. 0704-0188

Public reporting burden for this collection of information is estimated to average 1 hour per response, including the time for reviewing instructions, searching existing data sources, gathering and maintaining the data needed, and completing and reviewing this collection of information. Send comments regarding this burden estimate or any other aspect of this collection of information, including suggestions for reducing this burden to Department of Defense, Washington Headquarters Services, Directorate for Information Operations and Reports (0704-0188), 1215 Jefferson Davis Highway, Suite 1204, Arlington, VA 22202-4302. Respondents should be aware that notwithstanding any other provision of law, no person shall be subject to any penalty for failing to comply with a collection of information if it does not display a currently valid OMB control number. **PLEASE DO NOT RETURN YOUR FORM TO THE ABOVE ADDRESS.**

1. REPORT DATE	2. REPORT TYPE	3. DATES COVERED
October 2014)	Annual	30 Sep 2013 - 29 Sep 2014

4. TITLE AND SUBTITLE

Early Intervention with cdk9 Inhibitors to Prevent Post-Traumatic Osteoarthritis

5a. CONTRACT NUMBER

5b. GRANT NUMBER
W81XWH-12-1-0311

5c. PROGRAM ELEMENT NUMBER

6. AUTHOR(S)
Dominik R. Haudenschild

E-Mail: Dominik.Haudenschild@ucdmc.ucdavis.edu or drhaudenschild@ucdavis.edu

5d. PROJECT NUMBER

5e. TASK NUMBER

5f. WORK UNIT NUMBER

7. PERFORMING ORGANIZATION NAME(S) AND ADDRESS(ES)

University of California, Davis
1850 Research Park Drive, Suite 300
Davis, CA 95618-6134

8. PERFORMING ORGANIZATION REPORT NUMBER

9. SPONSORING / MONITORING AGENCY NAME(S) AND ADDRESS(ES)
U.S. Army Medical Research and Materiel Command
Fort Detrick, Maryland 21702-5012

10. SPONSOR/MONITOR'S ACRONYM(S)

11. SPONSOR/MONITOR'S REPORT NUMBER(S)

12. DISTRIBUTION / AVAILABILITY STATEMENT
Approved for Public Release; Distribution Unlimited

13. SUPPLEMENTARY NOTES

14. ABSTRACT
We proposed to test (in aim 1) whether inhibition of Cdk9 would reduce the early transcriptional response to joint injury, and (in aim 2) whether this would delay or prevent the subsequent development of post-traumatic osteoarthritis. We made significant progress on aim 1 during the past 18 months. The first manuscript describing the in-vitro results on the chondroprotective effects of Cdk9 inhibitors is published in Arthritis&Rheumatology. We next began testing whether inhibition of Cdk9 in mouse knees protects against the acute inflammatory response at early times post-injury. At first we tested the transcription of early response genes since that process is directly controlled by Cdk9. These tests were very successful: a single intraperitoneal injection of Cdk9 inhibitor significantly reduced the acute response, and multiple injections reduced the acute response to baseline levels. Next, we looked at proteinase activity within the joints, which is initiated by the acute response and is responsible for cartilage degeneration. These tests were also successful. We are currently following through with additional analyses including in-vivo imaging and cytokine profiling as described in the proposal. This will be the material for our second manuscript, which we also expect to submit to Arthritis&Rheumatology. Given these positive results during the acute phase, we are well-positioned to initiate the longer-term studies we proposed in aim 2 in the near future.

15. SUBJECT TERMS
PTOA, acute injury response, inflammation, transcriptional elongation, Cdk9

16. SECURITY CLASSIFICATION OF:			17. LIMITATION OF ABSTRACT	18. NUMBER OF PAGES	19a. NAME OF RESPONSIBLE PERSON
a. REPORT	b. ABSTRACT	c. THIS PAGE			USAMRMC
U	U	U	UU	101	19b. TELEPHONE NUMBER *(include area code)*

TABLE OF CONTENTS

INTRODUCTION:

We propose that a fundamental flaw in current OA management is its focus on treating an irreversibly damaged joint during end-stage organ failure, rather than preventing the onset of cartilage and bone degeneration following traumatic joint injury. Our **GLOBAL HYPOTHESIS** is that OA is initiated at the molecular and cellular level shortly after an injury occurs, thus the optimal time frame for therapeutic intervention is also shortly after the injury. The **goal** of this research proposal is to develop an early therapeutic strategy, delivered just after a joint injury, which will prevent or delay the onset of joint degradation and OA.

Joint Injury induces an acute cellular response, which occurs on a time-scale of minutes to hours after injury. This acute cellular response is characterized by mRNA transcription of early response genes and release of inflammatory mediators, which initiate a destructive cascade of events leading to the degradation of joint matrix and osteoarthritis. The mRNA transcription of these early response genes is controlled by a central checkpoint, where Cdk9 kinase activity is the rate-limiting step. We hypothesized that inhibitors of Cdk9 would reduce mRNA transcription of the early response genes, and therefore prevent the destructive cascade of events leading to osteoarthritis.

In aim 1of this proposal we test whether inhibition of Cdk9 reduces the early mRNA transcriptional response to joint injury. For aim 1 we examine early responses (1 hour to 1 week after joint injury), and we test short-term outcomes (mRNA expression, local protease activity, cytokine production). The goal of aim 1 is to determine a treatment window (time and dose) wherein we can reduce the acute response to injury by inhibition of Cdk9. In aim 2 we test whether this early intervention delays or prevents the subsequent development of post-traumatic osteoarthritis using long-term outcomes (joint degradation, arthritis grade, proteoglycan loss). These experiments are performed in our recently developed non-invasive mouse model of joint injury in mice.

BODY:

Scientifically we made significant progress on Aim 1and Aim 2.

The first manuscript describing the in-vitro results on the chondro-protective effects of Cdk9 inhibitors is published in Arthritis & Rheumatology (A&R), which is the highest-impact journal dedicated to arthritis research and has stringent peer review. Many of these results in this manuscript were preliminary data of this grant application, but a good number of additional experiments were still required to get the story published in A&R. Many of these experiments are included in the Statement of Work as Task 1. As a follow up to our first published manuscript on the chondro-protective effects of Cdk9 inhibitors in an in-vitro cell culture system, we have submitted another manuscript describing the protective effects of Cdk9 inhibitors in an ex-vivo cartilage explant system. This study provides additional evidence of Cdk9 inhibition on preventing the detrimental effects of injury-induced damage to cartilage, which include apoptosis and cartilage matrix degradation.

In addition, towards the completion of Aim 2, we have published the second and third manuscripts describing the in-vivo imaging of protease activities in the injured knee joint to monitor post-traumatic osteoarthritis progression are pubished in the peer-reviewed journal Osteoarthritis and Cartilage (OC&A), and in the journal Biochemical and Biophysical Research Communications (BBRC). The accepted manuscripts are attached in appendix 6 and 7.

As proposed in Aim 1, we began testing whether inhibition of Cdk9 in mouse knees protects against the acute inflammatory response at early times post-injury. At first we tested the transcription of early response genes since that process is directly controlled by Cdk9. *These tests were very successful: a single intraperitoneal injection of Cdk9 inhibitor significantly reduced the acute response, and multiple injections reduced the acute response to baseline levels.* We have performed additional analyses on the tissue inflammatory responses and catabolic protease activities, and the remodeling of subchondroal bone microstructure within

the injured joints. These preliminary results are accepted as a poster abstract and will be presented in the upcoming annual meeting of the Orthopaedic Research Society in Las Vegas from March 27-30, 2015. We are currently collecting data on the ability of Cdk9 inhibitors to prevent development of osteoarthritis in the long-term as proposed in Aim 2. Detailed description of the observations and results is presented in bullet format in the next section.

KEY RESEARCH ACCOMPLISHMENTS

SPECIFIC AIM 1 – SHORT TERM EXPERIMENTS TO REDUCE INJURY-RESPONSE

TASK 1 – GENE EXPRESSION ANALYSIS AT BASELINE AND AT 1-240 HOURS POST-INJURY

A. Injure Mice According to the Schedule, with n=6 for each data point.

   Progress: We have completed most of this task. See notes below.

B. Sacrifice mice at given times and dissect out the injured and contralateral uninjured knee joints, and also harvest and store blood for Task 2.

   Progress: We have completed most of this task. Mice were injured according to the schedule provided in the proposal, and joints harvested for RNA extraction at hours 1, 2, 3, 4, 6, and days 1, 2, 3, 5, 7, and 10 after injury.

C. Isolate total RNA and perform PCR-Array quantitative gene expression analysis on 84 NFkB dependent primary response genes.

   Progress: We have successfully isolated total RNA from all the harvested joints, and used this total RNA to synthesize cDNA. We performed quantitative RT-PCR on select primary response genes to determine the quality of the RNA, and estimate the responsiveness of the genes. The results are presented in the appendices. Specifically, Appendix 2 (Fig 1, 2) and Appendix 3 (Fig 3, 4)

D. Perform statistical analysis of the results.

   Progress: Complete for the data collected.

Milestone: We identified a peak response of gene expression at 4-6 hours post-injury. This peak response is rapidly induced by the injury, with some genes (such as IL-6) responding with approximately 80-fold induction in the injured leg compared to the uninjured contralateral knee. The peak is also rapidly resolved by 8 hours for most genes analyzed to date, with gene expression returning to 1-5 times that in the uninjured contralateral knee. Inhibition of Cdk9 with a single dose of inhibitor greatly reduces the injury-related increase of primary response gene expression. Two injections, 0 and 6 hours post-injury, effectively prevents the injury-related increase of the primary response genes assayed.

TASK 2 – ANALYSIS OF SERUM CYTOKINE LEVELS AT BASELINE AND AT 1-240 HOURS POST-INJURY

A. Blood/serum has been collected as part of Task 1A, with n=6 for each data point

   Progress: Blood/serum has been collected and stored appropriately

B. Multiplexed bead immunoassay analysis to quantify 32 pro-and anti-inflammatory cytokines

   Progress: Analysis is underway, see notes below.

C. Statistical analysis of the results

   Progress: Initial results showed statistically insignificant changes of circulating cytokines in the plasma samples, with the exception of IL-6 that showed a mild increase. This is shown in Supporting Data 1. In light of this, we propose a revised approach using homogenized knee

joints to extract cytokines. This data would provide insight into the local cytokine response, presumably with greater sensitivity because only local tissue is analyzed (not diluted into the systemic circulation). The revised approach has not yet been started.

Milestone: We identified a mild increase in serum levels of IL-6, but not other cytokines, in response to joint injury.

TASK 3 – IN-VIVO IMAGING OF JOINT PROTEASE ACTIVITY AT BASELINE AND AT 1-240 HOURS POST-INJURY

A. Mice will be injected with Imaging Reagents prior to imaging

   Progress: Done for all time points.

B. Mice will be injured according to the protocol

   Progress: Done for all time points.

C. Non-invasive functional imaging of Joint Protease activity will be performed on live mice.

   Progress: Done for all time points. Data is shown in Appendix 2 (fig 3), Appendix 4, Appendix 6 (fig 6), and Appendix 7 (fig 2, 4, 5).

D. Mice will be sacrificed for uCT analysis in Task 4.

Milestone: Protease activity within the joint is induced within 1 hour, peaks at 2-4 days post-injury, and remains elevated out to at least 8 weeks after injury. Inhibition of Cdk9 at the time of injury effectively prevents joint protease activity for the first 24 hours. Based on our experience (Task 2) with gene expression, we expect that multiple injections will be required to reduce injury-induced joint protease activity.

TASK 4 – MICROCT ANALYSIS OF THE REMODELING IN SUBCHONDRAL BONE AT BASELINE AND AT 1-240 HOURS POST-INJURY

A. The same mice will be used for both imaging studies (tasks 3 and 4), n=5 for each data point.

   Progress: Done for most time points.

B. Mice will be scanned 1 day before injury to obtain a baseline measurement, and then again at the indicated times.

   Progress: We have obtained scan data from sufficient animals to establish a baseline measurement. This baseline will be used as normal uninjured bone density for comparison to all other measurements.

   Progress: A single dose of Cdk9 inhibitor significantly prevented bone loss after injury at day 3 post-injury, and analyses performed at day 7 and week 8 showed a similar trend but did not reach statistical significance. This is shown in Supporting Data 2. The Cdk9 inhibitor has an in-vivo half-life of under 6 hours. We are repeating the experiments with multiple doses of Cdk9 inhibitor and are analyzing the micro CT scans to measure the degree of bone loss and the amount of osteophyte formation due to the knee injury

Milestone: Inhibition of Cdk9 activity post-injury prevents or reduces bone loss at day 3 post-injury. Day 7 analysis is inconclusive with one injection, multiple injections will be tried.

SPECIFIC AIM 2 – LONG TERM EXPERIMENTS TO PREVENT OA

TASK 1 – HISTOLOGICAL ASSESSMENT OF OA AT TIMES 2, 3, 4 MONTHS POST-INJURY

A. Injured mice will be sacrificed at the indicated times, joints processed for histology, and stained with Safranin-O with a Fast-Green Counter-stain.

Progress: We have encountered a difficulty in completing this aim. Specifically, because our injury model ruptures the ACL, and due to the bent position of the knee in mice, we substantially alter the biomechanics of the joint and in-effect establish a new articulation point. The result of the altered biomechanics is that all animals develop arthritis, even though the initial injury is relatively mild. This is evident in the publication shown in Appendix 5, in figure 8. We have taken two approaches to address this: The first approach is to use our existing model of ACL rupture, but examine earlier time points for intervention efficacy. We have chosen to assess OA progression at the 6-week time point, with the Cdk9 inhibitor administered 3-times per week for up to 3-week post-injury. The drugs were given at a reduced dosage to prevent long-term toxicity in this experiment, which is still in progress. The second approach is to use an even milder mechanical injury model that does not alter the biomechanics of the knee joint. We use our existing instrumentation to apply repeated sub-rupture stress to the ACL. Two other laboratories have used such an approach to generate mild OA without altering the biomechanics of the joint.

2. SUBSTANTIAL PROGRESS TOWARDS OVERALL GOAL:

- We established a cartilage explant injury model, where we mechanically compress bovine cartilage explants to 30% strain at a rate of 100% strain/second. Using this model we observed increased expression of injury response genes within 2 hours, including IL-6 (shown in Appendix 8 in the AR&T manuscript figure 1), iNOS, and others. Treatment with flavopiridol prevented elevation of these genes by injury at 2, 6, and 24 hours after injury.
- We have shown that mechanical injury in cartilage explant leads to chondrocyte apoptosis that is prevented by Cdk9 inhibitor treatment. These data for the first time connects mechanical injury to cartilage explant causes direct cellular damage to chondrocytes but this detrimental effect is prevented by Cdk9 inhibition (Appendix 8 manuscript figures 2 &3).
- In the cartilage explant injury model, we observed that mechanical injury causes degradation of the cartilage matrix and results in a decrease in the mechanical properties of injured cartilage compared to uninjured control. Treatment with flavopiridol prevented this loss of mechanical properties by the simulated injury (Aappendix 8 manuscript figures 4 & 5). In fact, even uninjured controls in the presence of flavopiridol had greater mechanical properties than in the absence of flavopiridol.
- Using our in-vivo mouse model of joint injury, we found a peak of inflammatory gene expression at about 2 hours post-injury. This timing was conserved between many genes, including iNOS, IL-6, MMP13, ADAMTS, TNFa, and others, suggesting a common regulatory mechanism (we presume Cdk9 is involved). Since many of these genes follow a similar pattern of induction after joint injury, we focused on the most highly induced genes, IL-6 and iNOS, for cost saving.
- In the mouse model of joint injury, a single injection of flavopiridol reduced and delayed the activation of inflammatory genes. However, a single injection of flavopiridol did not completely prevent the activation of inflammatory genes. This is not surprising given the half-life of flavopiridol is under 6 hours.
- In the mouse model of joint injury, a single injection of flavopiridol did not reduce the extent of remodeling in subchondral bone as measured by micro-CT within 1 week. We therefore switched to multiple post-injury injections of flavopiridol from here on.

- Multiple injections of flavopiridol completely prevented the activation of pro-inflammatory cytokines and catabolic proteases at the mRNA level after knee injury at all times measured (figure 2 of ORS poster).
- In-vivo imaging of MMP activity after injury showed elevated MMP activity in the injured joint became detectable perhaps as soon as 1 hour after injury. The 1 hour time point did not quite reach statistical significance with n=8 mice, but all other time points (2h, 3h, 4h, 6h, 8h, 12h, 1day, 2day, 4days, 7 days) showed significantly elevated in-vivo MMP activity in the injured joint. (figure 3 of ORS poster, open triangles).
- A single injection of flavopiridol after injury substantially reduced in-vivo MMP activity to near baseline levels during the first 24 hours, and MMP activity remained lower at all time points tested (figure 3 of ORS poster).
- Injury-induced inflammation and synovial hypertrophy both appear reduced if flavopiridol is administered after injury. An anecdotal image is shown as figure 4 of the ORS poster, but this result is preliminary because we still need to perform a full blinded scoring of the histological sections followed by statistical analysis.
- Multiple injections of flavopiridol after injury prevents subchondral bone loss at 3 days post-injury (figure 5 of ORS poster).

In **summary**, the results from these experiments are very positive. The data conclusively demonstrates that Cdk9 inhibition strongly reduced or even completely prevented every one of the acute local responses to joint injury that we tested. Given these positive results during the acute phase, we are well-positioned to initiate the longer-term studies we proposed in aim 2, namely to ask whether reducing the acute response will slow or prevent the development of osteoarthritis.

Given these very positive results in the context of joint injury, we are pursuing a similar Cdk9-inhibition strategy in additional injury situations, such as preventing systemic inflammation upon severe trauma, etc.

2. NEGATIVE FINDINGS AND PROBLEMS IN ACCOMPLISHING TASKS:

Overall the progress has been substantial, in some respects faster and much better than anticipated. The results have been universally very positive, almost without exception. A few minor difficulties are below:

2.a: Deaths of mice: We attribute the following negative events to our own mistakes, but we feel obligated to report them for the sake of transparency. Four mice died in the groups where mice received single or multiple injections of flavopiridol, while no deaths occurred in the vehicle-control or un-injected groups. The deaths occurred at 1 to 2 days after intraperitoneal injection of flavopiridol, and we believe it was because the needle accidentally punctured an internal organ rather than staying within the intraperitoneal space. This is from a total of 519 mice used so far in the study, of which between 1/3 and ½ of received flavopiridol injections. We also discovered that repeated administering of the Cdk9 inhibitors at the maximum dose is not tolerated by the mice and resulted in death due to severed peritoneal infection. We have used a lower dosage of the drug in the current experiment with multiple injections at a schedule that still effectively prevented the short-term adverse effects of the knee injury, and none of the animals show adverse effects from the drug.

2.b: Effort and budget underestimated: I underestimated the amount of effort, and also the budget, required for the proposed studies.

With respect to the effort - in the first year, I was able to recruit unpaid manpower onto this project. Without the uncompensated help of these individuals, progress would not have been as fast. A student from Zhejiang University (a University with which UC Davis has a close connection) joined the project as his PhD Thesis. He was appointed a Research Associate without Salary position here for 13 months ending in December 2013, and worked full-time (>50hrs/wk) on this project. In addition, two first-year medical students in the UC Davis School of Medicine were awarded research fellowships to complete aspects of this project, and four undergraduate interns put in many hours during the school year and even more hours during the

summer to help complete aspects of this project. In addition, contributions from members of other labs were required. Many of these contributors are listed as co-authors in the ORS abstract.

With respect to the budget - prices of everything increased substantially since the original budget proposal, this includes salaries & benefit rates, reagents & supplies, animals, internal recharge rates for services such as in-vivo imaging and microCT, and external services such as histology. In addition, in the original proposal I over-estimated the number of assays we could practically perform on the same animals. It turned out that transferring the mice from the vivarium near my lab in Sacramento (where we perform the injury) to the facility for in-vivo imaging in Davis was a 15-mile one-way trip. For quarantine reasons animals are not allowed back into the Sacramento vivarium, a detail that I did not realize when writing the original proposal. It was unpractical to transport sufficient laboratory equipment from my lab to the imaging facility to perform assays other than imaging at that location. Therefore, given that most of our assays are performed at short time points after injury, we had to perform these experiments on additional sets of mice. Another reason that more mice were required is that imaging the early time points (as in ORS Poster figure 3) could not practically be done on the same mice. In our initial protocol we proposed imaging the mice 3 at a time, so we thought we could easily perform n=6 images within one hour. It turned out that an unexpected limitation of the imaging instrument (IVIS200 by Perkin Elmer) introduced a systemic error based on the location of the mouse and the resulting angle of the illumination on the injured knees. After consulting with the Perkin-Elmer technicians, the only solution was to image one animal at a time, centered directly under the illumination source and camera. While this modification allowed us to get great data, it also greatly increased the number of animals required for the study, and the associated effort and costs.

In retrospect I attribute the effort/budget underestimation to my own inexperience. My original proposal was an honest (not over-inflated) estimate for doing the proposed work at the time of budget preparation. However, I did not include the additional requirements for publication of the results in high-impact journals, I did not sufficiently anticipate the steep inflation of costs, and I did not expect that the constraints of injuring mice at one facility while imaging at another facility would require the early time point experiments to be performed on as many mice.

Freezer Loss: In November we had a catastrophic failure of our -80 freezer, resulting in the loss of all archived RNA and serum samples. This is a serious setback, necessitating the repeat of several key experiments.

Long term mouse injury model: Our mouse PTOA model is ideally suited for studying short-term acute responses to injury. However, the injury inevitably leads to PTOA in 8-12 weeks due to altered biomechanics of the joint, making it less than ideal for long-term experiments to evaluate therapeutic efficacy. We are working on a new milder model, wherein the ACL is stretched repeatedly and the cartilage is impacted, but no changes in biomechanics occur because the ACL stays intact. We will use this model for long term (8-12 week studies) and use our original ACL rupture model for shorter time points (under 6 weeks).

In summary, at the end of year 2 we are scientifically on track with excellent results and only very minor setbacks, but somewhat over budget and over-worked.

REPORTABLE OUTCOMES

MANUSCRIPTS, ABSTRACTS, AND PRESENTATIONS

- Manuscript published in Arthritis & Rheumatology, title "Cyclin-Dependent Kinase 9 inhibition protects cartilage from the catabolic effects of pro-inflammatory cytokines", PMID: 24470357. Included as Appendix 1. Much of the work for this manuscript was directly funded by this award.
- Manuscript published in Journal of Orthopaedic Research, title "Comparison of Loading Rate-Dependent Injury Modes in a Murine Model of Post-Traumatic Osteoarthritis", PMID: 24019199. Included as Appendix 5. No funds from this grant were used, but the work was greatly facilitated by the expertise we developed through this grant.
- Manuscript published in Osteoarthritis and Cartilage, title "In Vivo Fluorescence Reflectance Imaging to Quantify Sex-Based Differences in Protease, MMP, and Cathepsin K Activity in a Mouse Model of Post-Traumatic Osteoarthritis". Included as Appendix 6. No funds from this grant were used, but the work was greatly facilitated by the expertise we developed through this grant.
- Manuscript published in Biochemical and Biophysical Research Communications, title "In-vitro and In- vivo Imaging of MMP Activity in Cartilage and Joint Injury". Included as Appendix 7. No funds from this grant were used, but the work was greatly facilitated by the expertise we developed through this grant.
- Abstracts
    - Poster presentation at Orthopaedic Research Society's 60th Annual Meeting in New Orleans, March 2014. Title "CDK9 inhibition attenuates acute inflammatory response and reduces bone loss in a non-invasive post- traumatic osteoarthritis mouse model." Included as Appendix 2.
    - Poster presentation at World Congress of Osteoarthritis (OARSI) 2013, title "Early Transient Induction of IL-6 in a Mouse Joint Injury Model." Included as Appendix 3.
    - Poster presentation at World Congress of Osteoarthritis (OARSI) 2013, title "Fluorescence Reflectance Imaging of Early Processes of Post-Traumatic Osteoarthritis in Male and Female Mice." Included as Appendix 4.
    - Poster presentation at Orthopaedic Research Society's 61th Annual Meeting in Las Vegas, March 2015. Title "CDK9 inhibition attenuates inflammatory response and apoptosis in cartilage explants to preserve matrix integrity in a single impact mechanical injury model" Included as Appendix 9.

- Presentations:
    - 2012 November 20, ACL Damage as a Model for Early Osteoarthritis, UC Davis Medical Center Osteoarthritis Meeting, headed by Nancy Lane.
    - 2013 January 23, Early Molecular Events in Joint Injury, Invited Seminar at the UC Davis Veterinary Orthopaedic Research Laboratory seminar series.
    - 2013 January 28, CDK9 Inhibition Protects Cartilage from the Catabolic Effects of Pro-Inflammatory Cytokines, by Yik JHN (presenting), Kumari R, Christiansen BA, and Haudenschild DR., Session 42 - "MMP Regulation in Articular Chondrocytes" at the 2013 Meeting of the Orthopaedic Research Society in San Antonio, TX.
    - 2013 June 5, Osteoarthritis: The need for Imaging Early Stages of Disease, Given at the "Frontiers in Biomedical Imaging" seminar series held by the Radiology Department of UC Davis.
    - 2013 June 20, "Early Response to Joint Injury", University of California Davis Department of Orthopaedic Surgery Research Symposium, Lawrence J. Ellison Musculoskeletal Research Center.

- 2013 October 15, "Early Response to Joint Injury and Osteoarthritis", UC Davis Department of Orthopaedic Surgery Grand Rounds invited Seminar
- 2014 November 11, "Cdk9, a revolutionary molecular target for suppressing inflammation after knee trauma", UC Davis Department of Biophysics invited Seminar

LICENSES APPLIED FOR AND/OR ISSUED

- None during the last 12 months

DEGREES OBTAINED THAT ARE SUPPORTED BY THIS AWARD

- None during the last 12 months

DEVELOPMENT OF CELL LINES, TISSUES, OR SERUM REPOSITORIES

- None during the last 12 months

INFORMATICS SUCH AS DATABASES AND ANIMAL MODELS

- None during the last 12 months

FUNDING APPLIED FOR BASED ON WORK SUPPORTED BY THIS AWARD

- We applied for an R21 grant to test whether we could reduce systemic inflammation after severe trauma, using similar inhibition of Cdk9 with flavopiridol as in this award. The grant was favorably reviewed (priority score 33) but not funded. We plan a revision.

EMPLOYMENT OR RESEARCH OPPORTUNITIES APPLIED FOR AND/OR RECEIVED BASED ON EXPERIENCE/TRAINING SUPPORTED BY THIS AWARD

- None during the last 12 months

CONCLUSION

In **conclusion**, the results from these experiments are very positive. Our goal in Aim 1 was to inhibit the early response to joint injury. The data collected thus far conclusively demonstrates that Cdk9 inhibition strongly reduced or even completely prevented every one of the acute local responses to joint injury that we tested. These results are currently being finalized, and readied for submission as a manuscript to Arthritis & Rheumatism.

Given these positive results during the acute phase, we are well-positioned and currently at the midway point of the longer-term studies we proposed in aim 2, namely to ask whether reducing the acute response will slow or prevent the development of osteoarthritis.

Given these very positive results in the context of joint injury, we are pursuing a similar Cdk9-inhibition strategy in additional injury situations, for example preventing systemic inflammation upon severe trauma.

REFERENCES

None

APPENDICES

1. Arthritis & Rheumatism Manuscript, Accepted Manuscript
2. ORS 2014 Poster on chondroprotective effect of Cdk9 inhibitors in joint injury

3. OARSI 2013 Poster on transcriptional response to joint injury
4. OARSI 2013 Poster on in-vivo imaging of joint-injury proteolytic activity
5. JOR Manuscript, Published manuscript
6. OA&C published manuscript
7. BBRC published manuscript
8. AR&T submitted manuscript
9. ORS 2015 Abstract on chondroprotective effect Cdk9 inhibitors in a explant injury model

SUPPORTING DATA

All supporting data is contained in the appendices.

ARTHRITIS & RHEUMATOLOGY
Vol. 66, No. 6, June 2014, pp 1537–1546
DOI 10.1002/art.38378
© 2014, American College of Rheumatology

Cyclin-Dependent Kinase 9 Inhibition Protects Cartilage From the Catabolic Effects of Proinflammatory Cytokines

Jasper H. N. Yik,[1] Zi'ang Hu,[2] Ratna Kumari,[3] Blaine A. Christiansen,[1] and Dominik R. Haudenschild[1]

Objective. **Cyclin-dependent kinase 9 (CDK-9) controls the activation of primary inflammatory response genes. The purpose of this study was to determine whether CDK-9 inhibition protects cartilage from the catabolic effects of proinflammatory cytokines.**

Methods. **Human chondrocytes were challenged with different proinflammatory stimuli (interleukin-1β [IL-1β], lipopolysaccharides, and tumor necrosis factor α) in the presence or absence of either the CDK-9 inhibitor flavopiridol or small interfering RNA (siRNA). The expression of messenger RNA (mRNA) for inflammatory mediator genes, catabolic genes, and anabolic genes were determined by real-time quantitative reverse transcription–polymerase chain reaction (qRT-PCR) analysis. Cartilage explants were incubated for 6 days with IL-1β in the presence or absence of flavopiridol. Cartilage matrix degradation was assessed by the release of glycosaminoglycan (GAG) and cleaved type II collagen (COL2A) peptides.**

Results. **CDK-9 inhibition by flavopiridol or knockdown by siRNA effectively suppressed the induction of mRNA for inducible nitric oxide synthase by all 3 proinflammatory stimuli. Results from NF-κB–targeted PCR array analysis showed that flavopiridol suppressed IL-1β induction of a broad range of inflammatory mediator genes (59 of 67 tested). CDK-9 inhibition also suppressed the induction of catabolic genes (matrix metalloproteinase 1 [MMP-1], MMP-3, MMP-9, MMP-13, ADAMTS-4, and ADAMTS-5), but did not affect the basal expression of anabolic genes (COL2A, aggrecan, and cartilage oligomeric matrix protein) and housekeeping genes. Flavopiridol had no apparent short-term cytotoxicity, as assessed by G6PDH activity. Finally, in IL-1β–treated cartilage explants, flavopiridol reduced the release of the matrix degradation product GAG and cleaved COL2A peptides, but did not affect long-term chondrocyte viability.**

Conclusion. **CDK-9 activity is required for the primary inflammatory response in chondrocytes. Flavopiridol suppresses the induction of inflammatory mediator genes and catabolic genes to protect cartilage from the deleterious effects of proinflammatory cytokines, without affecting cell viability and functions.**

Osteoarthritis (OA) affects more than half of the US population over the age of 65 years. OA is a degenerative disease of the articular joints characterized by slow but progressive loss of cartilage. The main protein component of articular cartilage is a fibrillar network of type II collagen (COL2A), which provides tensile strength to the cartilage. The compressive stiffness of the cartilage is provided by the proteoglycan components, through their attraction of water molecules. Although the cause of OA remains incompletely understood, various inflammatory conditions that cause

Supported by the National Natural Science Fund of China (grants 81101378 and 81271971 to Dr. Hu), University of California Davis (Departmental Startup Funds to Drs. Christiansen and Haudenschild), the Arthritis Foundation (2012 IRG award to Dr. Haudenschild), the US Department of Defense (PRMRP IIRA award PR110507 to Dr. Haudenschild), and the NIH (National Institute of Arthritis and Musculoskeletal and Skin Diseases grant R21-AR-063348 to Dr. Haudenschild).

[1]Jasper H. N. Yik, PhD, Blaine A. Christiansen, PhD, Dominik R. Haudenschild, PhD: University of California Davis, Sacramento, California; [2]Zi'ang Hu, MD: Sir Run Run Shaw Hospital and Zhejiang University, Hangzhou, China, and University of California Davis, Sacramento, California; [3]Ratna Kumari, PhD: University of California Davis, Sacramento, California, and KIIT University, Bhubaneswar, India.

Drs. Yik, Christiansen, and Haudenschild have submitted a patent application for the use of a cyclin-dependent kinase 9 inhibitor in posttraumatic osteoarthritis.

Address correspondence to Dominik R. Haudenschild, PhD, University of California Davis, Department of Orthopaedic Surgery, Lawrence J. Ellison Musculoskeletal Research Center, Research Building 1, Suite 2000, 4635 Second Avenue, Sacramento, CA 95817. E-mail: Dominik.Haudenschild@ucdmc.ucdavis.edu.

Submitted for publication July 2, 2013; accepted in revised form January 21, 2014.

damage to the collagens and proteoglycans in cartilage are suspected of initiating OA.

Proinflammatory cytokines are induced by a variety of stress conditions in cartilage, including joint overloading and physical damage such as occurs in sports-related injuries. Proinflammatory cytokines, such as interleukin 1β (IL-1β) and tumor necrosis factor α (TNFα), elicit a cascade of events that activate inflammatory mediator genes and apoptosis in chondrocytes (for review, see ref. 1). Proinflammatory cytokines can also induce the expression of proteinases that degrade cartilage matrix, including matrix metalloproteinases (MMPs), aggrecanases, and cathepsins (for review, see ref. 2). Therefore, a strategy for effectively suppressing the inflammatory response in cartilage may prevent or delay the onset of OA.

Acute tissue stress and inflammatory signaling activate primary response genes that do not require de novo protein synthesis. Recent advances demonstrate that despite their initiation by diverse signaling pathways, the transcriptional activation of most, if not all, primary response genes is similarly controlled by a general transcription factor (3,4), namely, cyclin-dependent kinase 9 (CDK-9). It was believed for many years that the rate-limiting step in the transcriptional activation of primary response genes is the recruitment of transcription factors and RNA polymerase II (Pol II) complex to the promoters. However, recent studies have shown that in order for these primary response genes to be rapidly activated, the Pol II complex is already preassembled and producing short messenger RNA (mRNA) transcripts in their basal, unstimulated states (3,4). In the absence of inflammatory signals, Pol II remains paused ~40 bp downstream of the transcription start site. Upon inflammatory stimulus, CDK-9 is recruited to the transcription complex by bromodomain-containing protein 4 (BRD-4) through its association with acetylated histones (3,4). Once recruited, CDK-9 phosphorylates Pol II to induce a conformational change that allows Pol II to enter possessive elongation to efficiently transcribe full-length mRNAs (for review, see ref. 5). Thus, CDK-9 regulation represents a central mechanism for activating primary response gene transcription and has a broad impact on many aspects of biologic functions.

Given that CDK-9 controls a common mechanism of all primary response gene activation, it is an attractive target for antiinflammatory therapy (for review, see ref. 6). The objective of this study was to determine whether CDK-9 inhibition effectively suppresses the inflammatory response in chondrocytes and protects cartilage from the catabolic effects of proinflammatory cytokines in vitro.

MATERIALS AND METHODS

Articular chondrocytes and cartilage explants. Human primary chondrocytes and cartilage explants were isolated from cartilage tissues obtained (with Institutional Review Board approval) at the time of total knee arthroplasty from 15 donors with end-stage OA (ages 44–80 years). Samples were cultured in Dulbecco's modified Eagle's medium (DMEM) with 10% fetal bovine serum (FBS) as described elsewhere (7). The chondrocytes were used in experiments within 3–5 days, without passaging (to avoid dedifferentiation). Samples from 5 of the 15 OA cartilage explant donors were used for the matrix degradation studies. All other experiments were performed with chondrocytes from at least 3 of the 15 OA donors.

Full-thickness bovine cartilage explants from the stifle joints of young veal calves were obtained by 6-mm punch biopsy. Samples were maintained in DMEM with 10% FBS.

Treatment of chondrocytes with inflammatory stimuli and small-molecule inhibitors. Primary chondrocytes were seeded in 12-well plates at a density of 2×10^4 cells/cm^2 and allowed to reach ~80% confluence (~4×10^4 cells/cm^2). The cells were treated with 10 ng/ml of lipopolysaccharide (LPS; Sigma), 10 ng/ml of IL-1β (R&D Systems), or 10 ng/ml of TNFα (R&D Systems) for various times, with or without pharmacologic inhibitors. The inhibitors used in this study included flavopiridol (Sigma), JQ-1 (a kind gift from Dr. James Bradner, Harvard University, Boston, MA [8]), BS-181 HCl (Selleckchem), and SNS-032 (Selleckchem). After treatment, the cells were washed 3 times with phosphate buffered saline and harvested for gene and protein expression analyses.

Lentiviral small interfering RNA (siRNA) constructs. The CDK-9–targeting siRNA used in this study (AGGGACATGAAGGCTGCTAAT) was inserted into the *Age* I and *Eco* RI sites of the lentiviral vector pLKO.1 (plasmid no. 8453; Addgene). An siRNA targeting green fluorescent protein (GFP) was used as control. Lentiviral particles were generated and titered as described previously (9). Human chondrocytes were seeded at 1×10^4 cells/cm^2 in 12-well plates. Lentiviral particles harboring CDK-9– or GFP-targeting siRNA were then added at a multiplicity of infection of 10, in the presence of 1 μg/ml of Polybrene (American Bioanalytical). The medium was replaced after 16 hours, and the cells were used for experiments after 5 days. Knockdown of CDK-9 was confirmed by Western blotting.

Real-time quantitative reverse transcription–polymerase chain reaction (qRT-PCR). For the determination of individual mRNA expression, cytokine/inhibitor-treated chondrocytes in 12-well plates were harvested by scraping, transferred to Eppendorf tubes, and subjected to cell lysis and reverse transcription to generate complementary DNA (cDNA) using a Cells-to-C_T kit (Ambion) according to the manufacturer's instructions. A total of 2 μl of cDNA was used for qRT-PCR (in a final volume of 10 μl), which was performed in triplicate using a 7900HT RT-PCR system with gene-specific TaqMan probes (Applied Biosystems) according to the manufacturer's instructions. Results were normalized to 18S ribosomal RNA (rRNA) and calculated as the fold change

in mRNA expression relative to untreated controls, using the $2^{-\Delta\Delta C_t}$ method. The probes used are as follows: for inducible nitric oxide synthase (iNOS), Hs01060345_m1; for MMP-1, Hs00899658_m1; for MMP-3, Hs00968305_m1; for MMP-9, Hs03234579_m1; for MMP-13, Hs0023992_m1; for ADAMTS-4, Hs00192708_m1; for ADAMTS-5, Hs00199841_m1; for aggrecan, Hs00202971_m1; for cartilage oligomeric matrix protein (COMP), Hs00154339_m1; for COL2A, Hs01060345_m1; and for 18S rRNA, 4319413E.

For PCR array analysis, IL-1β/flavopiridol–treated chondrocytes grown in 10-cm plates were harvested, and total RNA was isolated using an RNeasy Mini kit (Qiagen). RNA quality and quantity were assessed with a NanoDrop 2000 spectrophotometer (Thermo Scientific), and ~500 ng of total RNA was reverse transcribed using a SuperScript First-Strand kit (Invitrogen). RT-PCR was performed using a 7900HT RT-PCR system and PCR Arrays for Human NF-κB Signaling Targets (catalog no. 330231; Qiagen) according to the manufacturer's protocol. PCR array data were analyzed by the accompanying online analysis software provided by Qiagen (available online at www.qiagen.com).

Cytotoxicity/viability assays. To determine the short-term cytotoxic effects of flavopiridol, chondrocytes were seeded in 96-well plates at 1, 5, or 10×10^3 cells/well and treated for 5 hours with 300 n*M* flavopiridol. Cytotoxicity was assessed using a Vybrant cytotoxicity assay kit (catalog no. V23111; Invitrogen) according to the manufacturer's protocol, measuring soluble and total G6PD activity with resazurin as substrate. Fluorescence was detected using a Synergy HT plate reader (BioTek Instruments) with excitation and emission filters set at 528 nm and 635 nm, respectively.

To determine the long-term effects of flavopiridol on the viability of chondrocytes in cartilage, bovine cartilage explants (6-mm disk) in 6-well plates were cultured for 6 days in DMEM and 10% FBS, in the presence or absence of 300 n*M* flavopiridol, with medium changes every other day. The live and dead cells were stained using a Live/Dead Viability/Cytotoxicity kit (catalog no. L3224; Invitrogen) according to the manufacturer's protocol. The percentages of live and dead cells were determined by counting the cell numbers in 3 random fields of the cross-sectional images of explants captured using a fluorescence microscope. A total of 3 different donors were used.

Western blot analysis. Chondrocytes grown in 12-well plates were harvested and lysed with sample loading buffer (50 m*M* Tris HCl, pH 6.8, 100 m*M* dithiothreitol, 4% 2-mercaptoethanol, 2% sodium dodecyl sulfate [SDS], and 10% glycerol). Lysates were resolved by 4–12% SDS-polyacrylamide gels and transferred onto nitrocellulose membranes (Bio-Rad). The membranes were blocked with 3% skim milk in TBST (25 m*M* Tris HCl, pH 7.5; 125 m*M* NaCl; 0.1% Tween 20), followed by overnight incubation at 4°C with rabbit anti–CDK-9 (0.6 μg/ml) (10), mouse anti–MMP-13 (1:500 dilution) (catalog no. IM78; Calbiochem), or mouse anti-GAPDH (1:5,000 dilution) (catalog no. AM4300; Ambion). Blots were then probed with horseradish peroxidase–conjugated secondary antibody (Santa Cruz Biotechnology), and reactive protein bands were visualized with Western Lightning Plus-ECL (PerkinElmer) on radiographic films.

Assessment of cartilage degradation. Human cartilage explants (~3-mm cubes) were treated for 6 days with 1 ng/ml of IL-1β, in the presence or absence of 6 n*M* or 300 n*M* flavopiridol (with medium change on day 3). The amount of glycosaminoglycan (GAG) released into the medium from day 3 to day 6 was determined by colorimetric assay using dimethylmethylene blue dye, with chondroitin sulfate as standard (11). The release of COL2A degradation products into the medium was determined by measuring the amount of cleaved COL2A peptides (12) with the use of a C2C enzyme-linked immunosorbent assay kit (Ibex Pharmaceuticals) according to the manufacturer's protocol.

Statistical analysis. Values of all measurements were expressed as the mean ± SD. Changes in gene expression were analyzed by one-way analysis of variance (ANOVA) using SPSS version 16.0 software. The fold change in mRNA was used as variables to compare samples between different treatment groups. The least significant difference post hoc analysis was conducted using a significance level of $P < 0.05$.

RESULTS

Role of CDK-9 in the induction of the primary response gene iNOS. Although the rate-limiting step for transcriptional activation of primary inflammatory response genes in lymphocytes is controlled by CDK-9 (3,4), whether CDK-9 plays a similar role in articular chondrocytes has not been investigated. Therefore, we took advantage of a widely used and well-characterized pharmacologic CDK-9 inhibitor, flavopiridol, to determine the role of CDK-9 in the activation of primary response genes in chondrocytes. To activate primary response genes, chondrocytes in culture were treated with IL-1β in the presence or absence of 300 n*M* flavopiridol (the effective plasma concentration determined in clinical trials [13]). The induction of the stress response gene iNOS (14) was determined at various time points. The results showed that the level of mRNA for iNOS was unchanged after 1 hour of IL-1β treatment but was induced to significant levels after 3 and 5 hours (Figure 1A). However, cotreatment with flavopiridol completely suppressed the induction of iNOS by IL-1β (Figure 1A). These results indicate a time-dependent induction of iNOS by IL-1β that is sensitive to flavopiridol treatment.

The above findings demonstrated the effects of flavopiridol administered concurrently with the inflammatory cytokines. We next tested whether a delay in the addition of flavopiridol could still suppress iNOS induction by IL-1β. Chondrocytes were treated with IL-1β for a total of 5 hours, with either no delay or a 1- or 3-hour delay in the addition of flavopiridol. The data showed that when compared to no flavopiridol treatment (~235-fold iNOS induction), the addition of flavopiridol markedly repressed iNOS induction if administered without

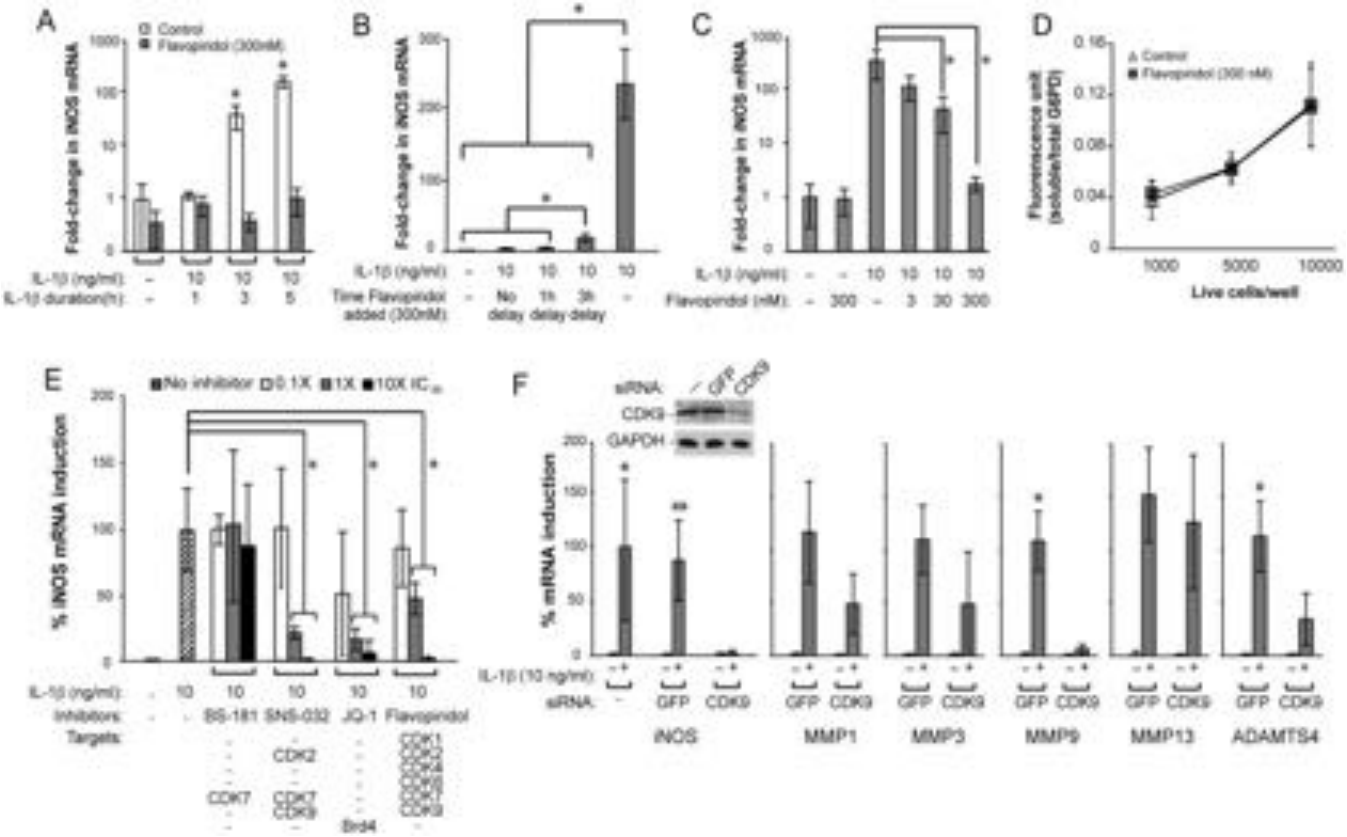

Figure 1. Characterization of the effects of flavopiridol-induced cyclin-dependent kinase 9 (CDK-9) inhibition on the induction of inducible nitric oxide synthase (iNOS). **A,** Kinetics of interleukin-1β (IL-1β)–induced iNOS expression. Human chondrocytes were treated with 10 ng/ml of IL-1β in the presence or absence of 300 n*M* flavopiridol for the indicated times. The fold induction of mRNA for iNOS relative to the untreated control was determined by quantitative reverse transcription–polymerase chain reaction (qRT-PCR) analysis. **B,** Time window of flavopiridol administration for iNOS suppression. Chondrocytes were treated for 5 hours with IL-1β and flavopiridol was added at the indicated time points to determine the window of opportunity for effective suppression of iNOS induction. **C,** Dose-dependent suppression of iNOS induction by flavopiridol. Chondrocytes were treated for 5 hours with IL-1β and flavopiridol was added at the indicated concentrations to determine the dose-response for suppressing iNOS induction. **D,** Cytotoxicity assays. Chondrocytes were seeded in 96-well plates at the indicated cell density, treated for 5 hours with 300 n*M* flavopiridol, and then soluble/total G6PD activity was measured to determine the cytotoxic effects of flavopiridol. **E,** Suppression of iNOS induction by different inhibitors. Chondrocytes were treated for 5 hours with IL-1β in the presence or absence of the indicated concentrations of various small-molecule inhibitors, and IL-1β induction of mRNA for iNOS was determined (maximum induction in the absence of inhibitor was set at 100%). The selected 50% inhibition concentrations (IC_{50}) of various drugs based on their kinase inhibition are as follows: for BS-181, 21 n*M* for CDK-7; for SNS-032, 60 n*M* for CDK-7 (used in this experiment) and 4 n*M* for CDK-9; and for flavopiridol, 30 n*M* for CDK-9. JQ-1 is not a kinase inhibitor but prevents CDK-9 recruitment to primary response gene promoters through suppression of the binding of bromodomain-containing protein 4 (BRD-4) to acetylated histones at an IC_{50} of 300 n*M*. **F,** Impairment of iNOS and catabolic gene induction by small interfering RNA (siRNA)–mediated depletion of CDK-9. Chondrocytes were transduced with lentiviral particles harboring siRNA against CDK-9 or green fluorescent protein (GFP; control). After 5 days, cells were treated for 5 hours with IL-1β and harvested for Western blotting for protein levels and qRT-PCR for mRNA expression. While IL-1β induction of iNOS was not significantly different between the control (*) and GFP siRNA (**) groups, iNOS induction was markedly suppressed by CDK-9 knockdown. IL-1β–induced expression of mRNA for matrix metalloproteinases (MMPs) 1, 3, 9, and 13 as well as ADAMTS-4 in cells with GFP siRNA was similar to that of the control (data not shown), but their induction was reduced by CDK-9 siRNA. Values are the mean ± SD of 3 different donors. * = $P < 0.05$ versus all other conditions and for the indicated comparisons.

delay (~2.7-fold induction) or with a 1-hour delay (~4-fold induction) (Figure 1B). Although less effective, a 3-hour delay still allowed significant repression of iNOS induction (~18-fold) (Figure 1B). These results indicate that there is at least a 3-hour window of opportunity for administering flavopiridol in order to suppress iNOS induction after initial treatment with IL-1β.

We next demonstrated that flavopiridol suppressed iNOS induction by IL-1β in a dose-dependent manner, with the most effective dose being 300 n*M* (Figure 1C). Importantly, there was no apparent cytotox-

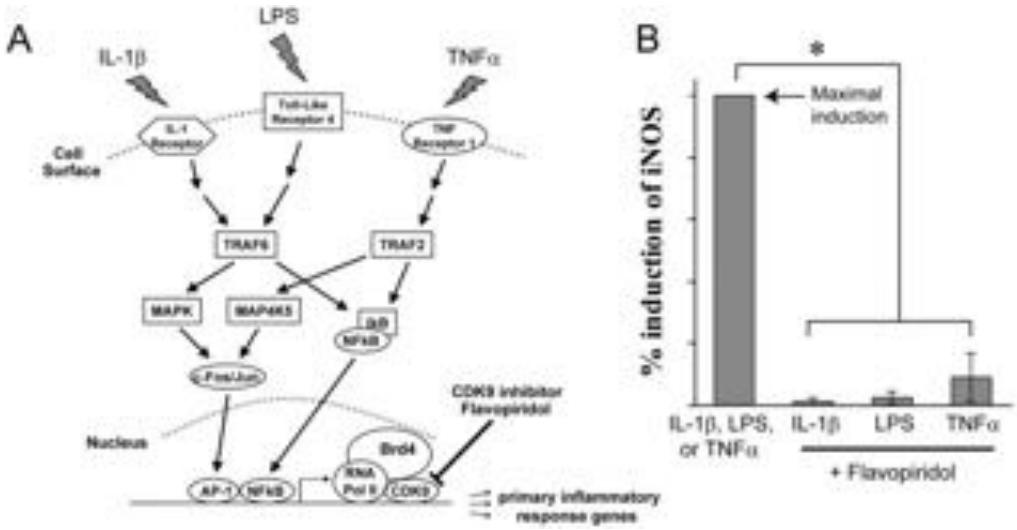

Figure 2. Effectiveness of the cyclin-dependent kinase 9 (CDK-9) inhibitor flavopiridol against different inflammatory stimuli. **A,** Activation of inflammatory genes by diverse signals. Multiple proinflammatory stimuli, such as interleukin-1β (IL-1β), lipopolysaccharide (LPS), and tumor necrosis factor α (TNFα), activate their respective cell surface receptors. These signals are then transmitted through different intracellular mediators/pathways, which ultimately converge on CDK-9–dependent transcription of inflammatory genes. Bromodomain-containing protein 4 (BRD-4) recruits CDK-9 to the activated promoters. TRAF6 = TNF receptor–associated factor 6; AP-1 = activator protein 1; RNA Pol II = RNA polymerase II. **B,** Effectiveness of flavopiridol against multiple inflammatory stimuli. Human chondrocytes in monolayer culture were treated for 5 hours with 10 ng/ml of the indicated inflammatory stimuli in the presence or absence of 300 n*M* flavopiridol. Expression of mRNA for iNOS was determined by real-time quantitative reverse transcription–polymerase chain reaction analysis as a measure of the inflammatory response. The induction of iNOS by each stimulus alone was arbitrarily set at 100% (left bar) and was compared to the value obtained in the samples cotreated with the respective inflammatory stimulus plus flavopiridol. Values are the mean ± SD of 3 different donors. $* = P < 0.05$ for the indicated comparisons.

icity of flavopiridol when administered at the highest dose on cultured chondrocytes in terms of G6PD activity within the 5-hour period tested (Figure 1D).

Besides CDK-9, flavopiridol has off-target effects that include other CDKs (see Figure 1E). While these CDKs do not affect primary response gene activation directly, we nevertheless used additional CDK inhibitors to rule out their involvement in the suppression of iNOS induction. To this end, we tested the ability of the following 3 small-molecule inhibitors to suppress iNOS induction: BS-181 HCl (specific for CDK-7) (15), SNS-032 (targets CDKs 2, 7, and 9) (16), and JQ-1 (specific for BRD-4, which is required for the function of CDK-9 [8]). The data showed that only SNS-032, JQ-1, and flavopiridol, but not BS-181, suppressed iNOS induction in a dose-dependent manner (Figure 1E), thus effectively ruling out the involvement of CDK-7 in IL-1β–induced iNOS transcription. It is important to note that unlike the other CDK inhibitors we tested, JQ-1 does not directly inhibit the kinase activity of CDK, but rather, it prevents the association of acetylated histones with BRD-4 (8), which specifically recruits CDK-9 to the promoters for activation of the transcription of primary response genes (4,5). Therefore, the above results strongly suggest that CDK-9 is involved in iNOS induction.

To definitively prove this, we used siRNA to specifically knockdown CDK-9 expression in chondrocytes and then determined the effects on iNOS induction. The results showed that in CDK-9–depleted cells (confirmed by Western blotting [Figure 1F, inset]), IL-1β failed to induce iNOS. Similar results were obtained when other catabolic genes, such as MMPs 1, 3, 9, and 13 as well as ADAMTS-4, were examined (Figure 1F), thus demonstrating the requirement of CDK-9 in catabolic gene induction. Taken together, our results clearly show the specific involvement of CDK-9, but not other CDKs, in the induction of iNOS by IL-1β.

Since flavopiridol is the first small-molecule CDK inhibitor in clinical trials with well-characterized pharmacokinetics, it has the highest potential for translation into clinical studies. Therefore, we used flavopiridol exclusively in the remainder of this study.

CDK-9 control of the activation of the inflammatory response from diverse signals. Primary response genes are activated by diverse inflammatory signals. Regardless of the sources, however, most inflammatory signals converge on the rate-limiting step of transcrip-

tional elongation of primary response genes, which is controlled by CDK-9. In order to illustrate this, 3 different inflammatory signaling pathways were selected, namely, IL-1β, lipopolysaccharide, and TNFα. The cellular response to IL-1β, LPS, or TNFα is mediated by 3 distinct pathways: activation of the IL-1 receptor, Toll-Like receptor 4, or TNF receptor type I, respectively (Figure 2A).

Chondrocytes were treated independently with 3 inflammatory stimuli, in the presence or absence of the CDK-9 inhibitor flavopiridol. The expression of mRNA for iNOS, a common effector gene for all 3 pathways (14), was then determined. The results showed that flavopiridol greatly suppressed the activation of iNOS expression by all 3 pathways (Figure 2B), demonstrating the effectiveness and broad range of flavopiridol in preventing the inflammatory response from diverse signals. Thus, our data confirmed previous findings in other cellular systems (4,5) and established CDK-9 as a central regulatory point for the primary inflammatory response in chondrocytes.

Prevention of the activation of a broad spectrum of inflammatory response genes by inhibition of CDK-9. To further investigate the effects of CDK-9 inhibition on the activation of other mediators of inflammation, the gene expression profiles of chondrocytes treated for 5 hours with IL-1β were determined by real-time PCR arrays. The PCR array contained 84 key genes responsive to NF-κB signal transduction (Qiagen), which is central to the regulation of multiple cellular processes, such as the inflammatory response, the immune response, and the stress response. The gene expression profiles from 3 chondrocyte donors were averaged and are presented as heat maps, in which low and high relative expression values are represented by green and red colors, respectively (Figure 3). (The array data are available in numerical format upon request from the corresponding author.)

The results showed that IL-1β strongly activated the majority of the 84 NF-κB target genes tested (Figure 3), while CDK-9 inhibition by flavopiridol almost completely abolished the effects of IL-1β. On average, across the 3 chondrocyte donors, CDK-9 inhibition repressed IL-1β activity by more than 86% and suppressed 59 of 67 NF-κB target genes that were activated at least 1.5-fold by IL-1β. Importantly, housekeeping genes, as well as genes not induced by IL-1β, were not affected by flavopiridol. These data demonstrated that CDK-9 can be targeted to effectively suppress only the activation of a cascade of downstream inflammatory response genes, without affecting the basal expression of nonresponsive genes.

Figure 3. Effectiveness of flavopiridol (flavo.) in suppressing the induction of a broad range of inflammatory mediators. Primary human chondrocytes (n = 3 different donors) in monolayer culture were treated for 5 hours with 10 ng/ml of interleukin-1β (IL-1β) in the presence or absence of 300 n*M* flavopiridol. Gene expression was analyzed using real-time polymerase chain reaction arrays for NF-κB targets, and the results are shown as heat maps, where green indicates minimum expression and red indicates maximum expression. Of the 84 NF-κB target genes tested, 67 were induced >1.5-fold by IL-1β (compare lane 1 with lane 2). Flavopiridol almost completely abolished the effects of IL-1β in 59 of these 67 genes (lane 3). Importantly, housekeeping genes and noninducible genes were unaffected by either IL-1β or flavopiridol.

Prevention of catabolic gene activation, but no effect on basal expression of anabolic genes, by inhibition of CDK-9 in chondrocytes. Besides activating the acute-phase inflammatory response genes, proinflammatory cytokines, such as IL-1β and TNFα, can also stimulate the expression of catabolic genes in chondrocytes (2,17). These catabolic genes include the various matrix MMPs and ADAMTS genes that degrade the cartilage matrix. Given the role of CDK-9 in the activation of inflammatory genes, we next examined the effects of CDK-9 inhibition on the induction of MMPs and ADAMTS in chondrocytes treated independently with IL-1β, LPS, and TNFα for 5 hours. The results showed that the IL-1β–mediated up-regulation of mRNA for MMPs 1, 3, 9, and 13 as well as ADAMTS-4 was markedly suppressed by cotreatment with flavopiri-

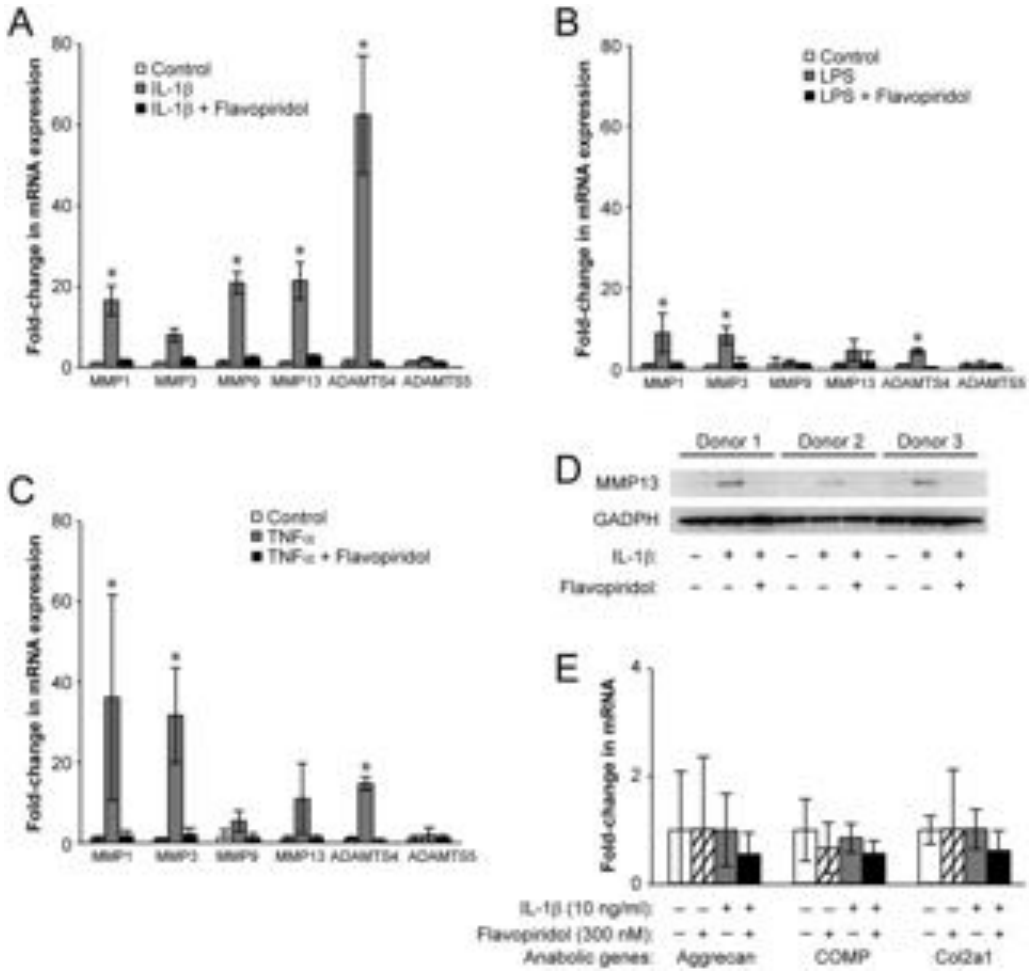

Figure 4. Cyclin-dependent kinase 9 inhibition and prevention of the induction of matrix metalloproteinase (MMP) and ADAMTS expression by various inflammatory stimuli. **A–C,** Primary chondrocytes were treated for 5 hours with 10 ng/ml of interleukin-1β (IL-1β) (**A**), lipopolysaccharide (LPS) (**B**), or tumor necrosis factor α (TNFα) (**C**) in the presence or absence of 300 n*M* flavopiridol, and the relative expression of mRNA for the cartilage-degrading enzymes MMPs 1, 3, 9, and 13 as well as ADAMTS-4 and ADAMTS-5 was determined by real-time quantitative reverse transcription–polymerase chain reaction (qRT-PCR) analysis. **D,** Human chondrocytes from 3 different donors were grown in 6-well plates and treated for 2 days with 10 ng/ml of IL-1β in the presence or absence of 300 n*M* flavopiridol. Expression of cell-associated active MMP-13 protein (~48 kd) was suppressed by flavopiridol, as determined by Western blotting. GAPDH was included as a loading control. **E,** Chondrocytes were treated for 5 hours with IL-1β and/or flavopiridol, and the expression of mRNA for the cartilage matrix genes aggrecan, cartilage oligomeric matrix protein (COMP), and type II collagen (COL2A) was determined by qRT-PCR analysis. Basal expression of these anabolic genes was not affected by treatment with flavopiridol. Values are the mean ± SD of 3 different donors. $* = P < 0.05$ versus the other experimental conditions and for the indicated comparisons.

dol (Figure 4A). Similar trends were observed in LPS- or TNFα-treated samples (Figures 4B and C). These data indicated that CDK-9 inhibition prevented the transcriptional activation of catabolic genes in chondrocytes.

Next, we sought to confirm the up-regulation of MMP-13 at the protein level, which is implicated in collagen degradation and osteoarthritis (18). Chondrocytes were treated for 2 days with IL-1β, with or without flavopiridol. Cell-associated active MMP-13 protein (~48 kd) was then detected by Western blotting. The data showed that MMP-13 protein expression was elevated in all 3 donors treated with IL-1β, but remained at basal levels with IL-1β plus flavopiridol treatment (Figure 4D). Thus, the results of the protein expression analysis corroborated the mRNA expression profiles of MMP-13. In contrast, the mRNA expression of selected anabolic genes (aggrecan, COMP, and COL2a) in chondrocytes was not significantly affected by IL-1β or flavopiridol within the same 5-hour time frame (Figure 4E). Taken together, these results demonstrate that

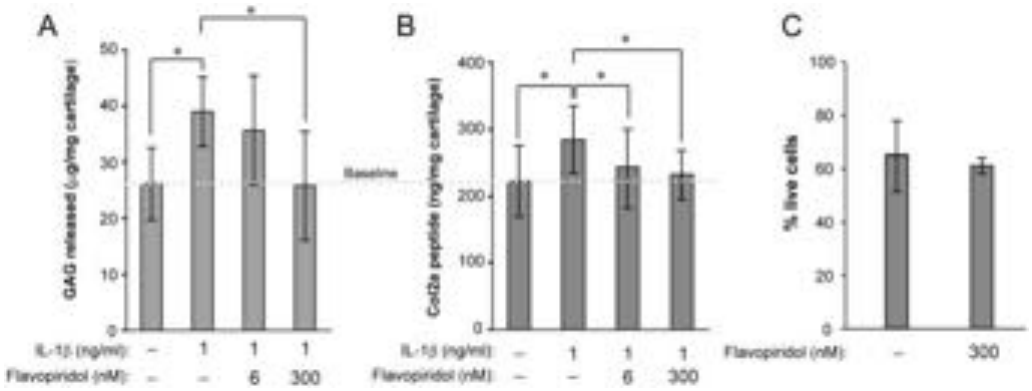

Figure 5. Protection of cartilage from the catabolic effects of interleukin-1β (IL-1β) by inhibition of cyclin-dependent kinase 9. **A,** Breakdown of glycosaminoglycans (GAGs) in cartilage explants. Explants of human arthritic cartilage samples (3-mm cubes) were treated for 6 days with 1 ng/ml of IL-1β and the indicated concentrations of flavopiridol (medium change on day 3). The amount of GAG released into the medium was measured by dimethylmethylene blue dye binding assay. Results were normalized to the wet weight of the explants. Treatment with IL-1β alone caused cartilage degradation, as indicated by increased GAG release. In the presence of 300 n*M* flavopiridol, levels of GAG release returned to baseline. **B,** Degradation of type II collagen (COL2A) in human cartilage explants. Samples from 5 donors were treated for 6 days with 1 ng/ml of IL-1β with the indicated concentrations of flavopiridol (medium change on day 3). The amount of cleaved COL2A peptides released into the medium was measured by enzyme-linked immunosorbent assay for a serum biomarker of type II collagen degradation (C2C). Results were normalized to the wet weight of the explants. Treatment with IL-1β alone caused cartilage degradation, as indicated by increased levels of COL2A peptides. In the presence of flavopiridol, the levels returned to baseline. Values in **A** and **B** are the mean ± SD of 5 different donors. $* = P < 0.05$ for the indicated comparisons. **C,** No reduction in chondrocyte viability following long-term treatment of bovine cartilage explants with flavopiridol. Bovine cartilage explants (6-mm full-thickness disks; n = 3 donors) were treated for 6 days in the presence or absence of 300 n*M* flavopiridol. The explants were sliced in half and stained with Live/Dead stain as described in Materials and Methods. The numbers of live and dead cells in 3 random fields were counted, and the percentages of live cells were calculated. Values are the mean ± SD.

flavopiridol selectively suppresses only the induction of catabolic genes by proinflammatory stimuli while having negligible effects on the basal expression of anabolic genes.

Protection of cartilage from the catabolic effects of IL-1β by inhibition of CDK-9. Since CDK-9 inhibition suppresses the activation of inflammatory genes and catabolic enzymes in chondrocytes, we next determined whether flavopiridol could protect cartilage from the deleterious effects of proinflammatory cytokines. Explants of human arthritic cartilage samples were isolated and cultured for 6 days in medium containing 1 ng/ml of IL-1β in the presence or absence of flavopiridol. Note that the concentration of IL-1β was reduced from the 10 ng/ml used in the short-term monolayer cultures, to a level similar to those detected in the synovial fluid samples from inflamed joints (19–21). Degradation of cartilage matrix was then assessed by measuring the release of GAG and COL2A cleavage peptides into the culturing medium.

As expected, IL-1β treatment increased the amount of both GAG (Figure 5A) and COL2A peptides (Figure 5B) released by human cartilage samples into the medium. However, the concentrations of both GAG and COL2A peptides were reduced by treatment with 6 n*M* flavopiridol and returned to baseline levels by treatment with 300 n*M* flavopiridol (Figures 5A and B). Thus, our data provide evidence that CDK-9 inhibition prevents the catabolic destruction of cartilage by IL-1β.

Importantly, the percentages of live/dead cells in bovine cartilage explants were similar in both untreated and flavopiridol-treated samples (Figure 5C). This result indicates that prolonged treatment of cartilage with flavopiridol did not have an adverse effect on the viability of chondrocytes in cartilage explants. Taken together, our data indicate that CDK-9 inhibition protects cartilage explants from the catabolic effects of IL-1β.

DISCUSSION

The cause of primary OA remains incompletely understood, and involvement of the inflammatory response is a subject of some controversy. However, it is well established that damage to the collagen network originates around chondrocytes at the cartilage matrix surface (22). Since the inflammatory response induces chondrocyte apoptosis and cartilage matrix breakdown (2), there are several anti-OA strategies that target either specific branches of the inflammatory signaling cascade (e.g., IL-1, IL-6, TNFα, and NF-κB inhibitors) (17,23,24) or downstream events (e.g., apoptosis with

caspase inhibitors) (1). However, because inflammation can be induced by a variety of stimuli, the above individual approaches would have limited effectiveness in handling the diverse simultaneous challenges in a biologic system, as well as limited abilities in efficiently suppressing a broad range of inflammatory mediator expression. A novel approach to addressing these limitations is to directly target CDK-9, which activates transcription of primary inflammatory response genes. Using the pharmacologic CDK-9 inhibitor flavopiridol, we showed that cartilage can be protected from the harmful effects of proinflammatory cytokines.

Our study is the first to demonstrate in chondrocytes that flavopiridol effectively suppresses the acute response to multiple inflammatory stimuli (Figure 2) and prevents the induction of a broad range of inflammatory mediators (Figure 3), as well as catabolic genes that contribute to the degradation of the cartilage matrix (Figure 4). In most cases, flavopiridol almost completely abolished the activation of inflammatory mediator expression. For example, with the PCR array data (Figure 3 and data available in numerical format upon request from the corresponding author), IL-1β induced the expression of IL-6 by 492-fold, but by only 4.2-fold in the presence of flavopiridol, representing a 99.2% repression of IL-1β–dependent transcription.

Importantly, our data demonstrate the selectivity of flavopiridol-mediated inhibition, in which only the IL-1β–inducible genes are suppressed, but not the basal expression of noninducible genes, housekeeping genes (Figure 3), and the anabolic genes (COL2A, COMP, and aggrecan) in chondrocytes (Figure 4E). The gene expression profiles are further supported by the experiments demonstrating flavopiridol can effectively prevent cartilage degradation induced by IL-1β (Figures 5A and B). The reduction in matrix degradation products was not due to changes in cell viability in cartilage treated with flavopiridol, since staining for live/dead cells revealed similar chondrocyte viabilities in control and flavopiridol-treated bovine cartilage explants (Figure 5C). Bovine cartilage was used instead of human cartilage because normal, healthy human cartilage is not routinely available and because the ratio of live to dead cells in arthritic human cartilage obtained at the time of knee surgery was erratic even when adjacent areas were examined.

Flavopiridol is an ATP analog that preferentially inhibits CDK-9 kinase activity (K_i = 30 nM) by a high-affinity interaction with its ATP-binding pocket (25). Although flavopiridol can potentially inhibit other CDKs, numerous studies using a combination of specific inhibitors and siRNA have demonstrated that only CDK-9 inhibition is responsible for the antiinflammatory action of flavopiridol (26,27). We have also shown that both JQ-1–mediated inhibition of BRD-4, which does not directly interact with other CDKs (10), and siRNA-mediated inhibition of CDK-9 lead to the loss of IL-1β–mediated induction of iNOS in chondrocytes (Figures 1E and F). In addition, we did not document a pronounced effect of other CDKs involved in cell cycle regulation on the transcriptional activation of a broad range of primary response genes within the 5-hour time frame used in this study. Therefore, our results provide strong evidence that only CDK-9 is responsible for the activation of primary response genes in chondrocytes.

Flavopiridol was originally known for its antiproliferation properties by suppressing cell-cycle progression in rapidly dividing cells (e.g., cancers) or in cells with a short lifespan (e.g., neutrophils). Its pharmacologic activity has been well-documented over the last 2 decades because of its use in clinical trials as an antiproliferation/anticancer agent (for review, see ref. 28). Sekine et al (29) demonstrated that systemic administration of flavopiridol reduced synovial hyperplasia without inducing apoptosis, and as a result, it prevented the development of rheumatoid arthritis in a collagen-induced mouse model. However, it is not known whether the antiarthritic activity of flavopiridol is due to the systematic suppression of the leukocyte-mediated immune response to the injected collagen or to the localized suppression of the inflammatory response of chondrocytes in cartilage.

Our group of investigators has developed a noninvasive knee injury mouse model for posttraumatic OA (30). Preliminary data indicate that systemic administration of flavopiridol effectively suppresses the production of proinflammatory cytokines locally at the injured knee, thus confirming our in vitro findings detailed in the present study. Future experiments are needed to determine whether flavopiridol treatment will prevent or delay the development of posttraumatic OA in our mouse model or in other existing models of posttraumatic OA (31,32).

In summary, our data for the first time demonstrate the absolute requirement of CDK-9 activity in the activation of primary response genes in human chondrocytes. In addition, our data strongly indicate that flavopiridol is an effective agent to prevent the activation of acute inflammatory response and catabolic pathways in cartilage. Our results thus may provide a new strategy to prevent or delay the onset of OA.

AUTHOR CONTRIBUTIONS

All authors were involved in drafting the article or revising it critically for important intellectual content, and all authors approved the final version to be published. Dr. Haudenschild had full access to all of the data in the study and takes responsibility for the integrity of the data and the accuracy of the data analysis.

Study conception and design. Yik, Hu, Kumari, Christiansen, Haudenschild.

Acquisition of data. Yik, Hu, Kumari, Haudenschild.

Analysis and interpretation of data. Yik, Hu, Kumari, Haudenschild.

REFERENCES

1. Lotz MK, Kraus VB. New developments in osteoarthritis: posttraumatic osteoarthritis: pathogenesis and pharmacological treatment options [review] [published erratum appears in Arthritis Res Ther 2010;12:408]. Arthritis Res Ther 2010;12:211.
2. Goldring MB, Otero M, Tsuchimochi K, Ijiri K, Li Y. Defining the roles of inflammatory and anabolic cytokines in cartilage metabolism. Ann Rheum Dis 2008;67 Suppl 3:iii75–82.
3. Hargreaves DC, Horng T, Medzhitov R. Control of inducible gene expression by signal-dependent transcriptional elongation. Cell 2009;138:129–45.
4. Zippo A, Serafini R, Rocchigiani M, Pennacchini S, Krepelova A, Oliviero S. Histone crosstalk between H3S10ph and H4K16ac generates a histone code that mediates transcription elongation. Cell 2009;138:1122–36.
5. Zhou Q, Yik JH. The Yin and Yang of P-TEFb regulation: implications for human immunodeficiency virus gene expression and global control of cell growth and differentiation. Microbiol Mol Biol Rev 2006;70:646–59.
6. Krystof V, Baumli S, Furst R. Perspective of cyclin-dependent kinase 9 (CDK9) as a drug target. Curr Pharm Des 2012;18: 2883–90.
7. Li H, Haudenschild DR, Posey KL, Hecht JT, Di Cesare PE, Yik JH. Comparative analysis with collagen type II distinguishes cartilage oligomeric matrix protein as a primary TGFβ-responsive gene. Osteoarthritis Cartilage 2011;19:1246–53.
8. Filippakopoulos P, Qi J, Picaud S, Shen Y, Smith WB, Fedorov O, et al. Selective inhibition of BET bromodomains. Nature 2010;468: 1067–73.
9. Dull T, Zufferey R, Kelly M, Mandel RJ, Nguyen M, Trono D, et al. A third-generation lentivirus vector with a conditional packaging system. J Virol 1998;72:8463–71.
10. Yang Z, Yik JH, Chen R, He N, Jang MK, Ozato K, et al. Recruitment of P-TEFb for stimulation of transcriptional elongation by the bromodomain protein Brd4. Mol Cell 2005;19:535–45.
11. Farndale RW, Buttle DJ, Barrett AJ. Improved quantitation and discrimination of sulphated glycosaminoglycans by use of dimethylmethylene blue. Biochim Biophys Acta 1986;883:173–7.
12. Poole AR, Ionescu M, Fitzcharles MA, Billinghurst RC. The assessment of cartilage degradation in vivo: development of an immunoassay for the measurement in body fluids of type II collagen cleaved by collagenases. J Immunol Methods 2004;294: 145–53.
13. Fornier MN, Rathkopf D, Shah M, Patil S, O'Reilly E, Tse AN, et al. Phase I dose-finding study of weekly docetaxel followed by flavopiridol for patients with advanced solid tumors. Clin Cancer Res 2007;13:5841–6.
14. Maier R, Bilbe G, Rediske J, Lotz M. Inducible nitric oxide synthase from human articular chondrocytes: cDNA cloning and analysis of mRNA expression. Biochim Biophys Acta 1994;1208: 145–50.
15. Ali S, Heathcote DA, Kroll SH, Jogalekar AS, Scheiper B, Patel H, et al. The development of a selective cyclin-dependent kinase inhibitor that shows antitumor activity. Cancer Res 2009;69:6208–15.
16. Heath EI, Bible K, Martell RE, Adelman DC, Lorusso PM. A phase 1 study of SNS-032 (formerly BMS-387032), a potent inhibitor of cyclin-dependent kinases 2, 7 and 9 administered as a single oral dose and weekly infusion in patients with metastatic refractory solid tumors. Invest New Drugs 2008;26:59–65.
17. Kobayashi M, Squires GR, Mousa A, Tanzer M, Zukor DJ, Antoniou J, et al. Role of interleukin-1 and tumor necrosis factor α in matrix degradation of human osteoarthritic cartilage. Arthritis Rheum 2005;52:128–35.
18. Wang M, Sampson ER, Jin H, Li J, Ke QH, Im HJ, et al. MMP13 is a critical target gene during the progression of osteoarthritis. Arthritis Res Ther 2013;15:R5.
19. Fiocco U, Sfriso P, Oliviero F, Roux-Lombard P, Scagliori E, Cozzi L, et al. Synovial effusion and synovial fluid biomarkers in psoriatic arthritis to assess intraarticular tumor necrosis factor-α blockade in the knee joint. Arthritis Res Ther 2010;12:R148.
20. McNiff PA, Stewart C, Sullivan J, Showell HJ, Gabel CA. Synovial fluid from rheumatoid arthritis patients contains sufficient levels of IL-1β and IL-6 to promote production of serum amyloid A by Hep3B cells. Cytokine 1995;7:209–19.
21. Deirmengian C, Hallab N, Tarabishy A, Della Valle C, Jacobs JJ, Lonner J, et al. Synovial fluid biomarkers for periprosthetic infection. Clin Orthop Relat Res 2010;468:2017–23.
22. Hollander AP, Pidoux I, Reiner A, Rorabeck C, Bourne R, Poole AR. Damage to type II collagen in aging and osteoarthritis starts at the articular surface, originates around chondrocytes, and extends into the cartilage with progressive degeneration. J Clin Invest 1995;96:2859–69.
23. Attur M, Millman JS, Dave MN, Al-Mussawir HE, Patel J, Palmer G, et al. Glatiramer acetate (GA), the immunomodulatory drug, inhibits inflammatory mediators and collagen degradation in osteoarthritis (OA) cartilage. Osteoarthritis Cartilage 2011;19:1158–64.
24. Attur MG, Dave M, Cipolletta C, Kang P, Goldring MB, Patel IR, et al. Reversal of autocrine and paracrine effects of interleukin 1 (IL-1) in human arthritis by type II IL-1 decoy receptor: potential for pharmacological intervention. J Biol Chem 2000;275:40307–15.
25. Ni W, Ji J, Dai Z, Papp A, Johnson AJ, Ahn S, et al. Flavopiridol pharmacogenetics: clinical and functional evidence for the role of SLCO1B1/OATP1B1 in flavopiridol disposition. PLoS One 2010; 5:e13792.
26. Wang K, Hampson P, Hazeldine J, Krystof V, Strnad M, Pechan P, et al. Cyclin-dependent kinase 9 activity regulates neutrophil spontaneous apoptosis. PLoS One 2012;7:e30128.
27. Schmerwitz UK, Sass G, Khandoga AG, Joore J, Mayer BA, Berberich N, et al. Flavopiridol protects against inflammation by attenuating leukocyte-endothelial interaction via inhibition of cyclin-dependent kinase 9. Arterioscler Thromb Vasc Biol 2011; 31:280–8.
28. Wang LM, Ren DM. Flavopiridol, the first cyclin-dependent kinase inhibitor: recent advances in combination chemotherapy. Mini Rev Med Chem 2010;10:1058–70.
29. Sekine C, Sugihara T, Miyake S, Hirai H, Yoshida M, Miyasaka N, et al. Successful treatment of animal models of rheumatoid arthritis with small-molecule cyclin-dependent kinase inhibitors. J Immunol 2008;180:1954–61.
30. Christiansen BA, Anderson MJ, Lee CA, Williams JC, Yik JH, Haudenschild DR. Musculoskeletal changes following non-invasive knee injury using a novel mouse model of post-traumatic osteoarthritis. Osteoarthritis Cartilage 2012;20:773–82.
31. Glasson SS, Blanchet TJ, Morris EA. The surgical destabilization of the medial meniscus (DMM) model of osteoarthritis in the 129/SvEv mouse. Osteoarthritis Cartilage 2007;15:1061–9.
32. Furman BD, Strand J, Hembree WC, Ward BD, Guilak F, Olson SA. Joint degeneration following closed intraarticular fracture in the mouse knee: a model of posttraumatic arthritis. J Orthop Res 2007;25:578–92.

Department of Orthopaedic Surgery, Lawrence J. Ellison Musculoskeletal Research Center, Sacram

Objective

Although joint injuries often lead to post-traumatic osteoarthritis (PTOA), few studies have focused on the immediate effects of an acute injury response on the progression and development of PTOA. Acute injury responses are characterized by the transcriptional activation of primary inflammatory genes such as IL-1β, IL-6, and TNFα, and other inflammatory mediators. These events lead to increased production of matrix degrading enzymes that contribute to the catabolic destruction of cartilage and subchondral bone. We **hypothesize** that excessive inflammatory response to joint injuries is a major contributor to the observed cartilage and bone loss preceding the onset of PTOA. Despite being triggered by various inflammatory stimuli, diverse signaling pathways converge onto a single mechanism that activates the transcription of primary inflammatory response genes. **This rate-limiting step of inflammatory gene activation is controlled by the transcription factor cyclin-dependent kinase 9 (CDK9).** CDK9 functions to phosphorylate RNA Polymerase II to overcome its promoter proximal pausing and to stimulate transcriptional elongation of mRNAs. Thus, CDK9 is an attractive and novel target for anti-inflammatory therapy, and we showed that CDK9 inhibition protects cartilage from catabolic cytokines in vitro[1]. Here we investigated the effects of CDK9 inhibition, by the pharmacological small molecule inhibitor Flavopiridol, on:
1) suppressing the acute injury response, and 2) the subsequent cartilage/ bone loss in an in vitro cartilage explant injury model, and in a non-invasive PTOA mouse model.

Methods

Cartilage explant injury: Cartilage explants were harvested by 6mm biopsy punches from bovine stifled joints obtained from a local slaughter house. The explants were trimmed to a height of 3mm and cultured in DMEM+10% FBS for 24 hrs. The explants were then subjected to a single load of compression with 30% strain, and then placed into culturing media with or without 300 nM Flavopiridol (Santa Cruz Biotech). The expression of inflammatory and catabolic/anabolic genes was determined by qPCR described below.

Mechanical properties: After 4 weeks of culture, mechanical properties were measured in a sample of the cartilage (2mm height by 3mm diameter). A Bose Enduratec instrument was used to apply 10% and 20% compressive strain and custom MatLab software to estimate the instantaneous and relaxation moduli.

PTOA mouse model: The right knees of skeletally matured C57BL6 mice were injured with a single mechanical compression as described (2), with the contralateral knees as uninjured control. These knee injuries consistently lead to a rapid bone loss at 1 week and apparent PTOA at 8 weeks. Half of these mice received intra-peritoneal injections of Flavopiridol at a dosage of 7.5mg/kg at 0- and 4-hours post-injury, and the other half received placebo injections. The knee joints and capsules were harvested and dissected at various time points (n=6/time point) and processed for gene expression, histology (H&E staining), and microCT analysis for femoral epiphysis bone volume. All animal procedures were performed according to an IACUC approved protocol.

qPCR: Total RNA from cartilage explants or dissected mouse knees were isolated by the miRNeasy Kit (Qiagen) and reverse transcribed by the QuantiTect Reverse Transcription Kit (Qiagen). Expression of pro-inflammatory cytokines, catabolic and anabolic genes were determined by qPCR in a 7900HT PCR system with gene-specific probes (ABI) and normalized to 18s rRNA.

In vivo Functional Imaging of MMP activity: MMP activities at the knee joints were determined by in vivo fluorescence imaging at 1-hour to 7-days post injury. MMP-Sense 680 probe was systemically administered, the animals were imaged in an IVIS imaging system under isoflurane anesthesia while held in place by a custum built adaptor. For each mouse, fluorescence (MMP activity) was expressed as a ratio of the injured to uninjured knee.

Statistical analysis: One-way ANOVA with Tukey's correction for multiple comparisons was used to determine significance.

Results

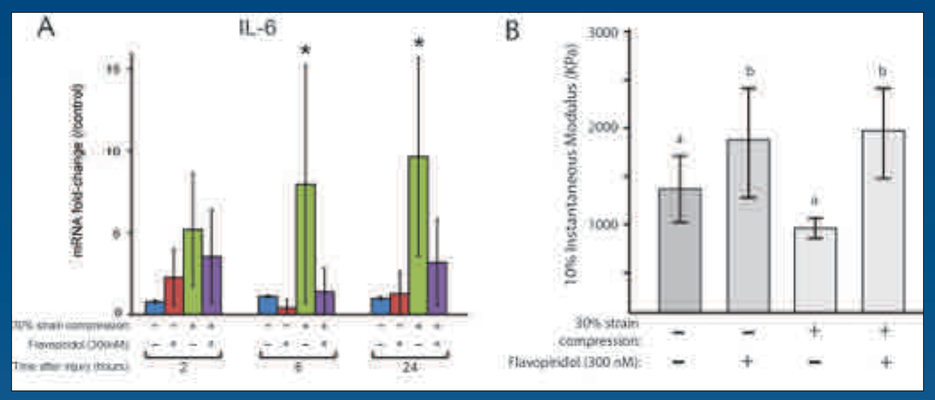

Fig. 1. Mechanically injured cartilage explants express pro-inflammatory cytokines.

A) CDK9 inhibition suppressed IL-6 induction. Bovine cartilage explants were compressed by a single load of 30% strain rate and analyzed for the mRNA expression of the injury marker IL-6. The results showed that IL-6 expression was markedly increased at 6 and 24 hours post-injury, but the increase was suppressed by Flavopiridol ($P<0.05$). Importantly, Flavopiridol did not affect anabolic genes expression nor chondrocyte viabilities (not shown).

B) CDK9 inhibition preserved cartilage mechanical properties. The mechanical properties of the explants were determined 4 weeks post-injury. The results showed that injury caused a reduction in the instantaneous modulus but the effects were reversed by Flavopiridol.

Fig. 2. In vivo CDK9 inhibition suppresses pro-inflammatory cytokine and catabolic gene mRNA induction after traumatic knee injury. In the PTOA mouse model, the expression of IL-6 and MMP13 mRNA increased rapidly 2 hrs after knee injury and peaked at 4 hrs, then returned gradually to baseline after 3-7 days. However, their induction was greatly reduced by Flavopiridol (*$P<0.05$). Similar results were seen in other catabolic genes such as IL-1β and ADAMTS4 (not shown). In contrast, at these time points the expression of anabolic genes Col2a1 and aggrecan were not affected by knee injury or Flavopiridol.

Fig 3. Functional imaging of MMP activity in vivo. C
point) were pre-injected with the MMP-Sense 680 sub
24-hr prior. Their right knees were then injured, w
uninjured control. The mice were then immediately in
Flavopiridol or vehicle. At the indicated times while u
activities at the mouse knees were determined by in
imaging system. **(A)** Representative fluorescence i
uninjured knees. **(B)** For each mouse, fluorescenc
expressed as a ratio of the injured to uninjured knee.

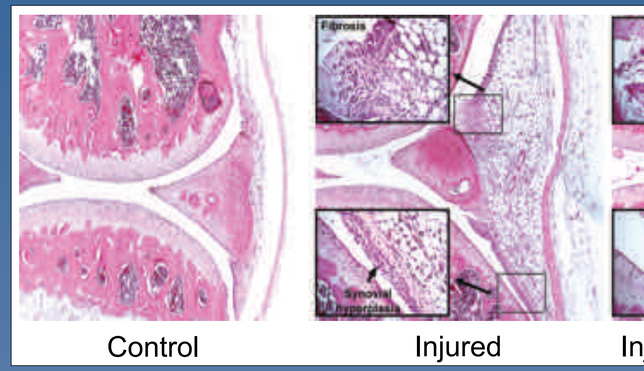

Fig. 4. Cdk9 inhibition reduced inflammation a
Histological analysis of knees 3-days post-injury sh
inflammation, fibrosis, synovial hyperplasia, per
leukocyte infiltration. However, these clinical presen
by Flavopiridol treatment.

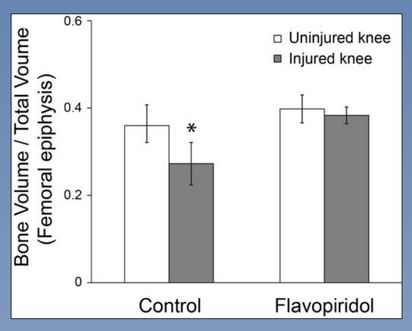

Fig. 5. CDK9 inhi
loss after joint
epiphysis bone volu
by μCT. Injury caus
loss in 3 days but
Flavopiridol treatmer

Discussion

The acute inflammatory reaction to joint injury is largely dependent on CDK9 kinase activity. Inhibition of CDK9 activity after injury will:

- **Reduce pro-inflammatory gene expression in explants and in-vivo**
- **Preserve the mechanical integrity of cartilage explants**
- **Reduce post-injury MMP activity in-vivo**
- **Reduce inflammation, fibrosis, synovial hyperplasia, and leukocyte infiltration**
- **Prevent post-traumatic loss of sub-chondral bone**

Significance: PTOA is commo
injuries in young active patients
clinical treatment available to pr
PTOA. Our studies suggest tha
after injuries can prevent cartil
may prevent or delay the onset o

References

(1) Yik JHN, Hu Z, Kumari R, Christiansen BA, and Haudenschild DR. *Arthritis Rheumatology* 2014, ePublished

(2) Christiansen BA, Anderson MJ, Lee CA, Williams JC, Yik JNH, and Haudenschild DR. *Osteoarthritis Cartilage* 2012, **20**(7): 733-82.

Acknowledgement: This study was supported by the Arthritis Foundation, the Dept. of Defense (PR110507) and NIH (R2

Introduction

Although the etiology of osteoarthritis (OA) is unknown, it is often associated with joint injuries. For example, ~50% of people with knee injuries, such as an anterior cruciate ligament (ACL) tear, develop post traumatic osteoarthritis (PTOA) within 10-20 years. The mechanical damage during joint trauma immediately causes cell death and physical damage to the surrounding tissues. This is followed by an acute cellular response, which occurs within a time-scale of minutes to hours. The acute response phase is characterized by the release of inflammatory mediators from the injured joint tissues, including IL-1, IL-6, TNFa, and iNOS. This causes the transcriptional activation of primary response genes (or inflammatory genes), and leads to increased production of matrix degrading enzymes such as MMPs, collagenases and aggrecanases. The enzymatic degradation of matrix contributes to OA via a cascade of destructive events. We believe that a window for therapeutic intervention exists shortly after injury, during which attenuating the acute cellular response will decrease the production of matrix degrading enzymes and thus decrease the likelihood of developing PTOA.

The acute cellular response within hours of knee injury has not been studied in detail in a mouse model. We have developed a non-invasive knee injury mouse model, in which the ACL is ruptured by a single mechanical compression. These mice consistently develop osteoarthritis in the injured knees within 2-3 months. The non-surgical nature of our model allows us to focus on the acute phase response that initiate the progression of osteoarthritis without the confounding effects of surgery. Using our mouse model, we have examined the short-term temporal expression of pro-inflammatory cytokines and their selected target genes. Our study will characterize the temporal changes in gene expression shortly after knee trauma and identify a window of opportunity for therapeutic intervention.

Methods

Non-invasive knee injury model

Under isoflurane anesthesia, 10-week old C57BL/6 mice were placed into the loading device, and the right leg subjected to a single axial compressive load to -12 N at 1mm/sec. The loading causes anterior subluxation of the tibia relative to the distal femur, demonstrated by the μCT image. Knee injury is evident by the release of compressive force during loading (red line on graph), with continued displacement of the loading actuator (black line). Avulsion fractures of the ACL are typical.

Total RNA was isolated from the injured knee joints shortly after injury, with the contralateral uninjured knee as control. The mRNA expression of pro-inflammatory cytokines and MMP13 was then determined by quantitative PCR and normalized to the 18s rRNA.

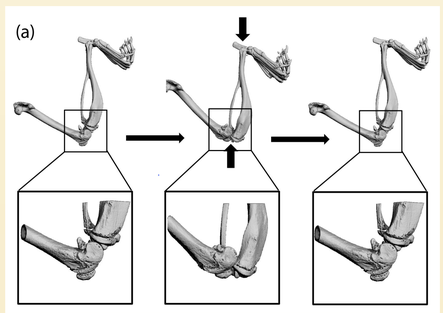

Gene expression analysis of total and partial knee

Two groups of mice were subjected to knee injury. For the first group, tissues were harvested from the entire joint capsule (whole knee), including the synovium, patella, ligaments and tendons, with most of the muscles removed (area within the dotted line). For the second group, only the tissues from the femeral to tibial growth plates were isolated (area within the red line). This partial knee region is composed of mainly articular cartilage and the subchondral bones, as well as the meniscus, ACL, PCL, and lateral ligaments. Total RNA were then isolated by the miRNeasy Kit (Qiagen) and reverse transcribed with First strand cDNA synthesis Kit (Invitrogen). The mRNA levels of the three most characterized pro-inflammatory cytokines, IL-1, IL-6, and TNF, as well as IL-6 receptor, MMP13, were determined by quantitative PCR, with gene-specific probes (ABI). Results were normalized to the 18s rRNA.

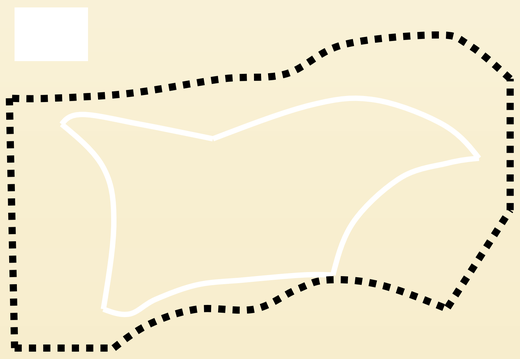

Results

IL-6 mRNA expression is transiently induced at the origin of injury, and s whole joint

Dramatic elevation (~40-fold) of IL-6 mRNA was first detected and peaked at 2-hour po dissection. In contrast, IL-6 induction was delayed in the whole knee dissection, but the magnit (~80-fold). This results indicated that IL-6 was first induced at the inner knee where the ACL inj later spread to the outer region of the knee. The expression of IL-6 receptor, however, did not the entire time course.

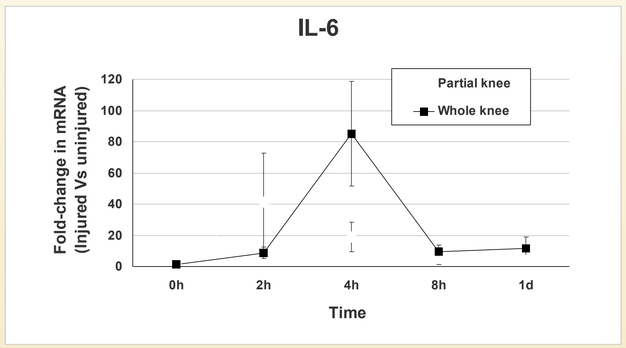

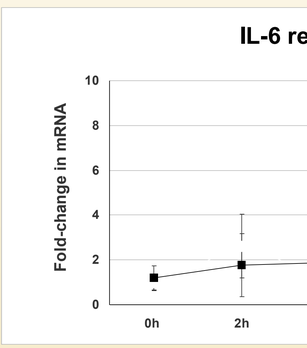

IL-1b mRNA induction is higher in whole knee compared to partial knee

IL-1b mRNA expression was slightly increased in partial knee at 2- and 4-hour post-inj foldrespectively. In contrast, IL-1b induction was only ~2-fold at 2-hour, but was markedly upre in the whole knee. Coincide with the peaked IL-1b induction in whole knee, its downstream tar ~4-fold at 4 hour.

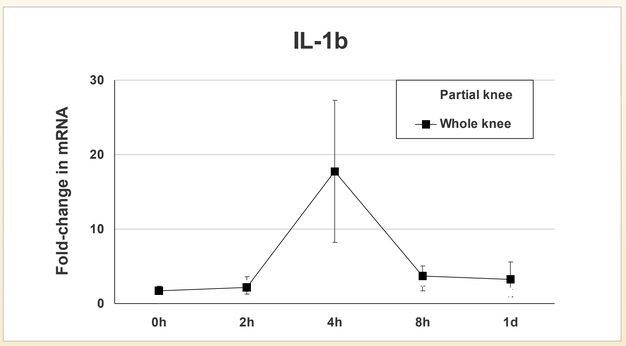

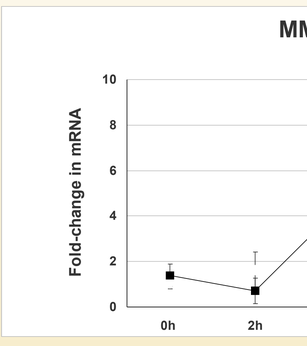

TNF expression does not change significantly after knee injury

Next, we determined the expression of TNF in the injured knee but found that TNF mRNA was not induced within 1-day post-injury (see below), and its level remained the same through a 7-day time course (not shown).

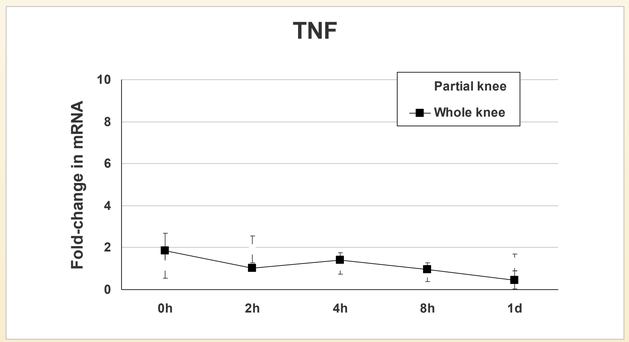

Involvement of IL-6 in cartilage degradation and bone remodeli osteoarthritis

Activation of the IL-6 pathway may contribute to the development of osteoarthritis. Although the precise mechanism remains incompletely understood, IL-6 contributes to cartilage matrix degradation through activation of the NF-kB pathway , leading to upregulation of matrix-degradating enzymes that destroy cartilage. IL-6 also activates the JAK/ STAT3 signaling pathways and enhances bone matrix remodeling, thus contributing to changes in the subchondral bone that may in turn affects the health of the cartilage.

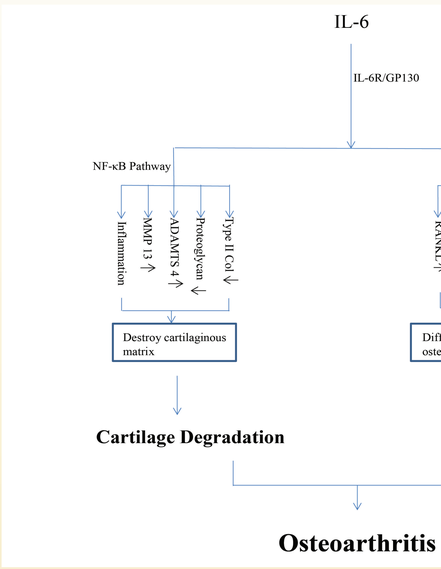

Conclusion

- IL-6 is transiently but markedly elevated in cartilage/subchondral bone tissues shortly after knee injury

- IL-6 may play an important role in the acute phase response to joint injury and the subsequent development of post-traumatic o

Print this Page for Your Records.

Patrick B Satkunananthan
UC Davis Medical Center
4635 2nd Ave
Suite 2000
Sacramento CA 95817

Dear Patrick Satkunananthan:

Thank you for submitting your abstract **FLUORESCENCE REFLECTANCE IMAGING OF EARLY PROCESSES OF POST-TRAUMATIC OSTEOARTHRITIS IN MALE AND FEMALE MICE**, to the 2013 World Congress on Osteoarthritis, being held April 18 – 21, 2013 in Philadelphia, Pennsylvania at the Marriott Philadelphia DowntownOn behalf of the OARSI Program Committee, we are pleased to inform you that your abstract has been accepted as a poster presentation.

As part of the abstract submission process, it is understood that acceptance of your abstract by the program committee would constitute your participation as a presenter.

Please click on the CONFIRM button below. By clicking confirm, you are acknowledging receipt of this notification and your agreement to participate as a poster presenter.

Please respond no later than Friday, February 4, 2013.

Your poster number will be sent to you in the next six weeks.

The poster sessions are taking place at the following times:

Poster Session I
Friday, April 19, 2013
3:30 PM – 5:00 PM

Poster Session II
Saturday, April 20, 2013
3:30 PM – 5:00 PM

It is **important** for you to be present at your poster during these times to answer questions and discuss issues on your research with meeting attendees. (**Please note that you will receive specific presentation times when you receive your poster number)

POSTER FORMAT and SET-UP

Each poster will have a display area of two (2) meters tall by one (1) meter wide (6.5 feet tall by 3 feet wide) to display your materials. The overall area is reduced by a two-inch frame on all four sides.

PLEASE NOTE THAT THE SIZES FOR THE POSTERS ARE TWO (2) METERS HIGH BY ONE (1) METER WIDE.

You may display your information in figures, tables, text, photographs, etc. Please prepare all illustrations neatly and legibly beforehand, in a size sufficient to read at a distance of three (3) feet. A series of typewritten sheets attached to the poster board is not acceptable. Materials will be available to fasten your material to the poster board.

Poster set up is to convene on Thursday, April 18, 2013 from 8:00 AM – 5:00 PM

Posters **MUST** remain on display until 5:00 PM on Saturday, April 20, 2013 at which time authors will be responsible for dismantling. Any posters remaining after 5:00 PM on Saturday will be removed by staff and OARSI cannot be

responsible for your poster.

For your convenience, please visit the OARSI 2012 Congress Website at http://2013.oarsi.org for registration and hotel information. On-line registration is available for the meeting. Please be sure to register prior to March 11, 2013 to receive the Pre-Congress rate.

Please note that all presenters are expected to cover their own travel and lodging and pay the registration fees.

ALL presenters are required to register for the meeting.

If you have any questions, please feel free to contact me at the OARSI Meetings Department.

We look forward to meeting with you at what promises to be an exciting and informative program. For more information regarding the meeting and OARSI, please go to our website at http://2013.oarsi.org.

Sincerely,

Anthony Celenza, CMP
Senior Meeting Manager

Francisco J. Blanco, MD, PhD
Congress Chair

Rita Kandel, MD
Abstract Chair

Your Response: Confirm

OsteoArthritis Research Society International (OARSI)
15000 Commerce Parkway, Suite C
Mt. Laurel, NJ 08054, USA
Tel.: +1/856-439-1385
Fax: +1/856-439-0525
Email: **info@oarsi.org**

Leave OASIS Feedback

The Online Abstract Submission and Invitation System
© 1996 - 2013 Coe-Truman Technologies, Inc. All rights reserved.

Purpose: Approximately 50% of individuals that experience anterior cruciate ligament (ACL) rupture develop post-traumatic osteoarthritis (PTOA) within 10-20 years, resulting in severe joint pain and stiffness. Although females are 4-6 times more likely than males to sustain an ACL injury during exercise or sports, males demonstrate an increased tendency to develop osteoarthritis following injury. ACL rupture initiates a surge of inflammatory cytokines, matrix metalloproteinases (MMPs), and other proteases, as well as cartilage degeneration and rapid bone turnover. It is possible that the magnitude or time course of these early biological responses may differ by sex, making males more likely to develop PTOA, however the quantification of these processes in males and females has not been performed. In this study, we used fluorescence reflectance imaging to quantify the time course of the early biological response to traumatic joint injury in male and female mice in vivo using highly sensitive activatable fluorescent agents that quantify protease activity, MMP activity, and osteoclastic bone resorption in injured and uninjured knees.

Methods: A total of 48 mice were subjected to non-invasive knee injury as previously described (Christiansen et al., Osteoarthritis and Cartilage, 2012). Three groups of 16 mice (8 male, 8 female) were imaged with either ProSense 680, MMPSense 680, or CatK 680 FAST (Perkin Elmer, Waltham, MA) in order to quantify protease activity, MMP activity, or osteoclastic bone resorption, respectively. Injections were administered 24-30 hours prior to imaging, on days 1, 3, 7, 14, 21, 28, and 56 after initial injury. At each time point of interest, mice were anesthetized with isoflurane, and imaged with the IVIS Spectrum system. Fluorescent signals were quantified by evaluating radiant efficiency of the signal within a uniform region of interest (ROI), anatomically selected around the knee on grayscale photograph. Radiant efficiency of the injured knee was normalized by that of the contralateral uninjured knee.

Results: For both male and female mice, protease activity (ProSense), MMP activity (MMPSense), and osteoclastic bone resorption (CatK) were significantly increased in the injured knee relative to the uninjured knee at nearly all time points. For example, Protease activity was significantly increased by day 1, reached a peak between 3 and 14 days, then decreased at later time points (Figure). Males and females displayed similar changes in injury response through the time periods observed, with males averaging a slightly higher normalized radiant efficiency at early time points, although this was not statistically different.

Conclusions: Using commercially available activatable fluorescent agents, we were able to quantify the time course of protease activity, MMP activity, and osteoclastic bone resorption in male and female mice following traumatic knee injury. However, contrary to our hypothesis, we were not able to observe a significant differential response between male and female mice. Our future studies will continue to explore potential mechanisms of the sex-based adaptation to joint injury that may contribute to the greater incidence of PTOA development in males. Our future studies will also continue to use fluorescence reflectance imaging as a method for measuring biological activity in vivo.

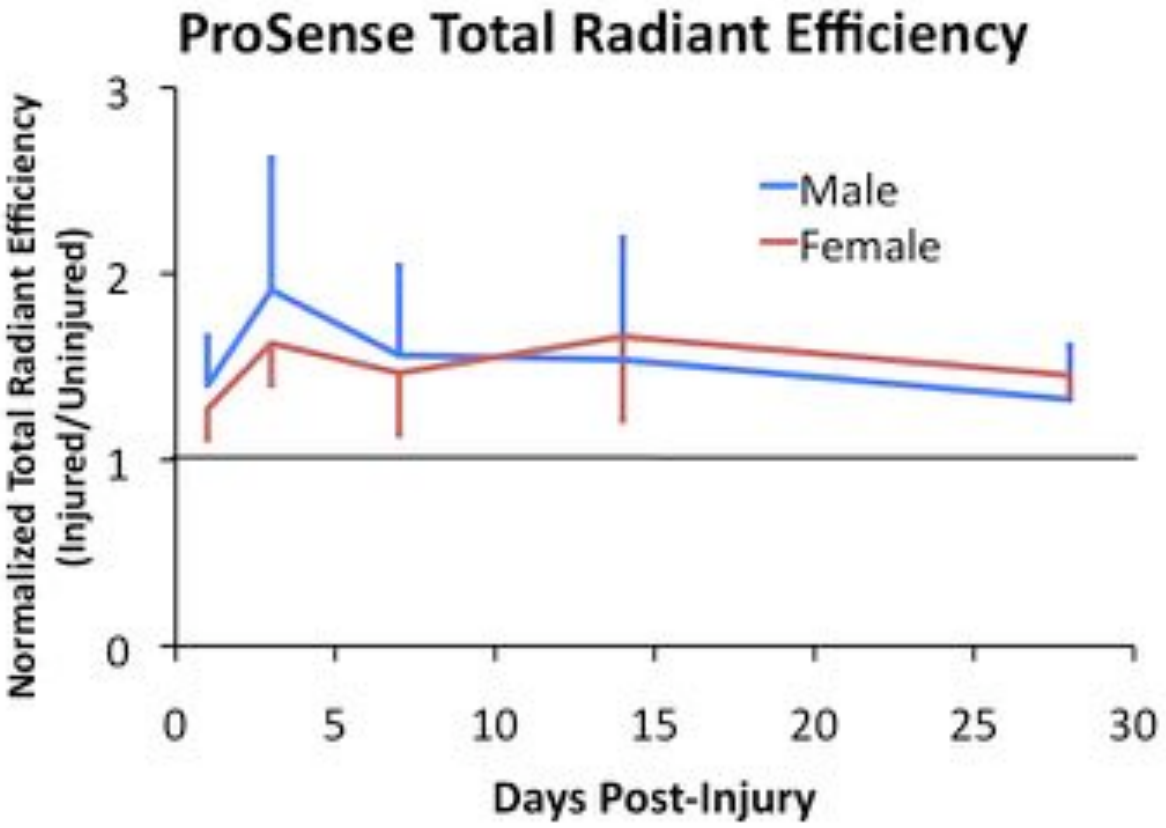
ProSense Total Radiant Efficiency
Normalized Total Radiant Efficiency (Injured/Uninjured)
3
2
1
0
Male
Female
0
5
10
15
20
25
30
Days Post-Injury

Comparison of Loading Rate-Dependent Injury Modes in a Murine Model of Post-Traumatic Osteoarthritis

Kevin A. Lockwood, Bryce T. Chu, Matthew J. Anderson, Dominik R. Haudenschild, Blaine A. Christiansen

Department of Orthopaedic Surgery, University of California-Davis Medical Center, 4635 2nd Ave, Suite 2000, Sacramento, California 95817

Received 19 April 2013; accepted 14 August 2013
Published online in Wiley Online Library (wileyonlinelibrary.com). DOI 10.1002/jor.22480

ABSTRACT: Post-traumatic osteoarthritis (PTOA) is a common long-term consequence of joint injuries such as anterior cruciate ligament (ACL) rupture. In this study we used a tibial compression overload mouse model to compare knee injury induced at low speed (1 mm/s), which creates an avulsion fracture, to injury induced at high speed (500 mm/s), which induces midsubstance tear of the ACL. Mice were sacrificed at 0 days, 10 days, 12 weeks, or 16 weeks post-injury, and joints were analyzed with micro-computed tomography, whole joint histology, and biomechanical laxity testing. Knee injury with both injury modes caused considerable trabecular bone loss by 10 days post-injury, with the Low Speed Injury group (avulsion) exhibiting a greater amount of bone loss than the High Speed Injury group (midsubstance tear). Immediately after injury, both injury modes resulted in greater than twofold increases in total AP joint laxity relative to control knees. By 12 and 16 weeks post-injury, total AP laxity was restored to uninjured control values, possibly due to knee stabilization via osteophyte formation. This model presents an opportunity to explore fundamental questions regarding the role of bone turnover in PTOA, and the findings of this study support a biomechanical mechanism of osteophyte formation following injury.
© 2013 Orthopaedic Research Society. Published by Wiley Periodicals, Inc. J Orthop Res XX:XXX–XXX, 2013.

Keywords: mouse model; post-traumatic osteoarthritis; ACL injury; joint stability; osteophyte

Osteoarthritis (OA) is the most common joint disease, and the knee is the most commonly affected joint.[1] OA causes pain and stiffness in the joint, and severely limits mobility for those people who are affected. Current evidence indicates that after non-contact anterior cruciate ligament (ACL) injury, patients have an increased chance of developing post-traumatic osteoarthritis (PTOA) within 10–20 years after injury.[2,3]

Animal models are useful tools for studying PTOA, since the disease process can be studied in a more controlled environment on a dramatically condensed time line. There have been a number of mouse models developed for studying PTOA,[4–7] but many of these still have significant drawback such as invasive surgery or multiple bouts of mechanical loading. Our lab has developed a non-invasive mouse model that induces ACL rupture in mice in vivo by a single tibial compression overload.[8] This model closely mimics traumatic ACL rupture in humans without the costs and complications of surgery.

Our previous study using this mouse model had limitations, including ACL damage primarily by avulsion fractures rather than midsubstance tears, induction of only mild osteoarthritis by the end of the study (8 weeks post-injury), and little quantification of joint biomechanics.[8] Avulsion fracture is not a common injury mode in adults,[9] therefore a more clinically relevant mouse model would induce a midsubstance tear of the ACL rather than failure by an avulsion fracture. Based on the results from Crowninshield et al.[10] and Noyes et al.,[11] we hypothesized that increasing the loading rate during knee injury would cause midsubstance ACL tears and decrease the likelihood of an avulsion fracture.

In this study we used our non-invasive mouse injury model to compare biomechanical and structural changes in the joint following ACL injury either with avulsion fracture or with midsubstance tear. We examined short term (10 days) and long term (12–16 weeks) structural changes in subchondral bone and epiphyseal trabecular bone, osteophyte formation, articular cartilage degeneration, and biomechanical stability of injured vs. uninjured knees. We hypothesized that injury mode (avulsion vs. midsubstance tear) would not significantly affect structural bone changes, osteoarthritis development, or biomechanical stability.

METHODS

Animals

A total of 80 male C57BL/6N mice (10 weeks old at time of injury) were obtained from Harlan Sprague Dawley, Inc. (Indianapolis, IN). Mice underwent a 1-week acclimation period in a housing facility before injury. Mice were caged individually and were maintained and used in accordance with National Institutes of Health guidelines on the care and use of laboratory animals. All procedures were approved by our Institutional Animal Care and Use Committee.

Non-Invasive Knee Injury

ACL injury was induced as previously described.[8] Briefly, mice were anesthetized using isoflurane inhalation, then the right lower leg was positioned between two loading platens: an upper platen that held the flexed ankle at approximately 30 degrees of dorsiflexion and a lower platen that held the flexed knee. The platens were aligned vertically in an electromagnetic materials testing machine (Bose ElectroForce 3200, Eden Prairie, MN). A preload of 1 N was applied to the knee before a single dynamic axial compressive load was applied to a target displacement of −1.7 mm at a loading rate of either 1 or 500 mm/s. A target displacement was chosen rather than a target compressive load (as in our

Grant sponsor: National Institute of Arthritis and Musculoskeletal and Skin Diseases; Grant sponsor: National Institutes of Health,; Grant numbers: AR062603, AR063348.
Correspondence to: Blaine A. Christiansen (T: 1-916-734-3974, F: 1-916-734-5750; E-mail: bchristiansen@ucdavis.edu)
© 2013 Orthopaedic Research Society. Published by Wiley Periodicals, Inc.

previous study) to minimize overshoot at high loading rates. Compressive loads at ACL rupture were comparable for both 1 and 500 mm/s loading rates, and were similar to those observed in our previous study (8–12 N). After injury, mice were given a subcutaneous injection of buprenorphine (0.5 mg/kg body weight) for analgesia. Mice were allowed normal cage activity until sacrifice.

Characterization of Joint Injury

To determine the effect of tibial compression loading rate on injury mode (avulsion fracture vs. midsubstance tear), both knees of six mice were injured at loading rates of 1 or 500 mm/s ($n = 6$ knees per group). Immediately following injury, mice were sacrificed and injured knees were imaged with micro-computed tomography (μCT) as described below to detect the presence of bone fragments in the joint space indicative of avulsion fracture. To further characterize the injuries induced by High Speed or Low Speed tibial compression loading rate, both knees of 10 mice were injured using 1 mm/s ($n = 7$ knees) or 500 mm/s ($n = 7$ knees) loading rates, or left intact ($n = 6$ knees). Mice were sacrificed immediately after injury. Contrast enhanced μCT was performed on six knees ($n = 2$ per group). Knees were stained with phosphotungstic acid (PTA; 0.3% in 70% ethanol) for 1 week before being scanned with μCT (2 μm nominal voxel size, Micro Photonics, Inc., Allentown, PA). The remaining 14 knees ($n = 4$–5 per group) were decalcified, sectioned in the sagittal plane, and stained with hematoxylin and eosin (H&E) to assess joint structure.

Comparison of High Speed and Low Speed Injury Models

Study Design: A total of 64 mice were used for this study (Table 1). Half of the injured mice were injured with the 1 mm/s load rate (Low Speed injury; $n = 26$); the other half were injured with the 500 mm/s load rate (High Speed injury; $n = 26$). An additional 12 mice underwent sham injury (anesthetized and loaded with the 1 N preload only). Following injury, mice were immediately sacrificed ($n = 12$) or returned to normal cage activity for 10 days ($n = 22$), 12 weeks ($n = 15$), or 16 weeks ($n = 15$), at which point they were euthanized by CO_2 asphyxiation and both hind limbs were excised for analysis. The left limb served as an internal control for each mouse.

Micro-Computed Tomography of Distal Femoral Epiphysis, Tibial Subchondral Bone, and Osteophytosis

Injured and uninjured knees were imaged with micro-computed tomography (SCANCO μCT 35, Bassersdorf, Switzerland) to quantify trabecular bone structure in the distal femoral epiphysis, subchondral bone structure at the proximal tibia, and osteophyte formation around the joint. Dissected limbs were fixed in 4% paraformaldehyde for 24–48 h, then transferred to 70% ethanol. Knees were scanned according to the guidelines for micro-computed tomography (μCT) analysis of rodent bone structure[12] (energy = 55 kVp, intensity = 114 mA, 10 μm nominal voxel size, integration time = 900 ms). Trabecular bone in the distal femoral epiphysis was analyzed by manually drawing contours on 2D transverse slices. The distal femoral epiphysis was designated as the region of trabecular bone enclosed by the growth plate and subchondral cortical bone plate. We quantified trabecular bone volume per total volume (BV/TV), trabecular thickness (Tb.Th), trabecular number (Tb.N), and apparent bone mineral density (Apparent BMD; mg HA/cm^3 TV) using the manufacturer's analysis tools. In our previous study[8] we observed comparable trabecular bone changes at the femoral epiphysis, tibial epiphysis, and tibial metaphysis following knee injury. The current study investigated only the femoral epiphysis, since it has the largest volume for analysis and therefore will yield the most consistent trabecular bone parameters. Subchondral bone of the proximal tibial plateau was analyzed for 12- and 16-week knees. The subchondral bone was segmented for 500 μm (50 slices) distal to the most proximal point of the tibia, excluding the trabecular bone compartment and any osteophytes growing from the tibia. We quantified cortical thickness (Ct.Th) and bone mineral density (BMD; mg HA/cm^3 BV) of the subchondral bone using the manufacturer's analysis tools. We investigated only the tibial suchondral bone because analysis of the subchondral bone of the femoral condyles is technically challenging, as is highly dependent on the orientation of the femur in the μCT scan. Osteophyte volume was calculated for 12- and 16-week knees, and included all mineralized tissue in and around the joint space, excluding naturally ossified structures (patella, fabella, and anterior and posterior horns of the menisci).

Table 1. Animal Numbers and Experimental Groups for "Comparison of High Speed and Low Speed Injury Models"

Time Point	Low Speed	High Speed	Sham
Day 0	6	6	
Day 10	8	8	6
Week 12	6	6	3
Week 16	6	6	3

Anterior–Posterior Joint Laxity

We quantified joint laxity of injured and uninjured mouse knees using a laxity tester based on previous designs.[13,14] This tester was designed to interface with a materials testing machine (Bose ElectroForce 3200). The protocol was similar to that described by Blankevoort et al.[14] for anterior–posterior (AP) laxity. Briefly, after fixation in brass tubes with polymethyl methacrylate (PMMA), the right and left knees of mice at day 0 ($n = 12$), week 12 ($n = 15$), and week 16 ($n = 15$) after injury were tested at 30°, 60°, and 90° of flexion. For each joint angle, knees underwent five loading cycles to a target force of ±1.5 N at a rate of 0.5 mm/s (Fig. 6). The force was applied normal to the longitudinal axis of the tibia. The femur was fixed during testing, but the tibia was allowed to translate and rotate about its longitudinal axis, giving the system three degrees of freedom of motion. Similar to Blankevoort et al., total AP joint laxity was computed based on the difference between displacement at +0.8 N and −0.8 N.

To assess whether fixation in 4% paraformaldehyde and 70% ethanol had an effect on joint laxity, day 0 limbs were tested fresh-frozen, and then retested after being fixed in 4% paraformaldehyde and preserved in 70% ethanol for 4 weeks. Fixed limbs were allowed to rehydrate in a bath of phosphate buffered saline (PBS) for 3 min before potting and testing. During testing, the limbs were continuously hydrated with PBS.

Long Term Whole Joint Histology

Knees were analyzed with whole joint histology to determine the extent of articular cartilage degeneration. Intact joints

were decalcified for 4 days in 10% buffered formic acid and then processed for standard paraffin embedding. For each limb, 6–7 sagittal sections (6 μm thickness) were cut across the entire joint separated by 250 μm. Slides were stained with Safranin-O and Fast Green to assess articular cartilage and other joint structures (meniscus, subchondral bone, osteophytes, etc.). Slides were blinded and graded by four independent readers using the semi-quantitative OARSI scale described by Glasson et al.[15] Grades were assigned to the medial and lateral tibial plateau, and medial and lateral femoral condyles.

Statistical Analysis

Trabecular bone μCT results for High Speed and Low Speed injury modes were compared at each time point by calculating the difference between injured and uninjured knees for each mouse (injured–uninjured) and using analysis of variance (ANOVA) to compare between groups. Joint laxity of uninjured control (UIC), 1, and 500 mm/s injury rate joints were compared at each time point using one-way ANOVA. Differences in joint laxity as a function of knee flexion angle were compared using repeated measures ANOVA. Histology OARSI scores of UIC, 1, and 500 mm/s injured knees were averaged between readers for each slide, then for all slides for each mouse, and were then compared using one-way ANOVA for each joint region (medial femur, medial tibia, lateral femur, lateral tibia). Significance was defined as $p < 0.05$ for all tests. Mean ± standard deviation is presented for all data.

RESULTS

Characterization of Joint Injury

Non-invasive injury of mice using tibial compression overload with increasing loading rates yielded observable differences in injury mode at the high speed loading rate (500 mm/s) compared to the low speed loading rate (1 mm/s). Using μCT imaging of injured mouse knees, we were able to observe bone fragments indicative of avulsion fracture for all mice injured at 1 mm/s, but we observed no bone fragments at a loading rate of 500 mm/s. We concluded that "High Speed injury" at 500 mm/s caused midsubstance disruption of the ligament, while "Low Speed injury" at 1 mm/s caused a combination injury involving ligament disruption with avulsion fracture. Contrast-enhanced μCT and whole joint histology showed disruption of the ACL for both 1 and 500 mm/s injury rates, with no obvious damage to the posterior collateral ligament, menisci, or other structures of the joint (Fig. 1). Consistent with our hypothesis, Low Speed injury (1 mm/s) caused disruption of the ACL with an avulsion fracture from the posterior femur. High Speed injury (500 mm/s) resulted in disruption of the ACL only, with no evidence of avulsion fracture.

Comparison of High Speed and Low Speed Injury Models

Micro-Computed Tomography of Distal Femoral Epiphysis, Tibial Subchondral Bone, and Osteophytosis

Both injury modes initiated a rapid loss of epiphyseal trabecular bone in the distal femur by 10 days post-injury, and long-term joint degeneration and osteophytosis by 12 and 16 weeks post-injury. At all time points, knees injured with either the High Speed or Low Speed loading rates had significantly reduced trabecular BV/TV at the femoral epiphysis compared to uninjured contralateral knees and UIC mice (Fig. 2). At 10 days post-injury, knees injured using the Low Speed loading rate had significantly greater

Figure 1. Imaging of injured and uninjured knee joints. Contrast-enhanced μCT images (left column) show disruption of the ACL in both High Speed and Low Speed injuries. Hemotoxylin and Eosin sections of intact, High Speed, and Low Speed injury modes (middle and right columns) show disruption of the ACL with both injury modes compared to uninjured ligament. Low Speed injury (1 mm/s) caused avulsion of the ACL from the posterior femur (circle). No avulsion was detected in the High Speed (500 mm/s) injury group.

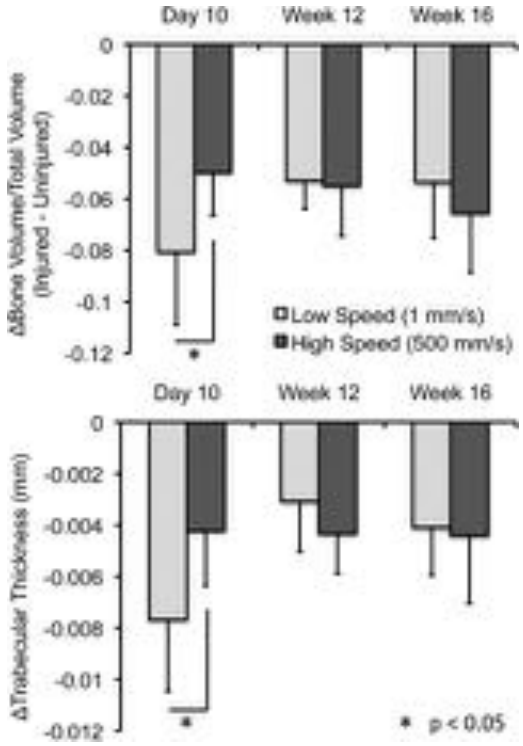

Figure 2. Difference in bone volume fraction (BV/TV) and trabecular thickness (Tb.Th) of the distal femoral epiphyses for Low Speed (1 mm/s) and High Speed (500 mm/s) injury groups. Values are the average difference between injured and contralateral control legs for each mouse. Injured versus uninjured values were significantly different for all groups and all time points ($p < 0.05$). Mice injured at Low Speed, which induced avulsion from the distal femur, exhibited greater trabecular bone loss at 10 days post-injury. After 12–16 weeks, injured knees still had significantly reduced bone volume and trabecular thickness compared to uninjured knees, although there were no differences between High Speed and Low Speed injuries in trabecular structure at these time points.

loss of trabecular BV/TV compared to those injured with the High Speed loading rate (−31% vs. −20%, respectively). By 12 and 16 weeks post-injury, there were no differences in trabecular BV/TV between the High Speed and Low Speed injury modes, although BV/TV of injured knees remained significantly lower than contralateral knees ($p < 0.05$). At 12 weeks post-injury, BV/TV of High Speed and Low Speed injured knees was 20.9% and 19.6% lower than contralateral knees, respectively, while at 16 weeks, BV/TV of injured knees was 22.9% and 21.5% lower, respectively. Trabecular thickness (Tb.Th) and apparent BMD of the femoral epiphysis followed a similar pattern, with the Low Speed injury rate exhibiting a significantly lower thickness and apparent BMD than the High Speed injury rate at 10 days. At 12 and 16 weeks there were no significant differences between injury modes, but injured limbs had reduced Tb.Th and BMD compared to uninjured contralateral limbs.

Analysis of subchondral bone at the proximal tibia revealed significant thickening of the subchondral bone plate in injured knees by 12 and 16 weeks post-injury (Fig. 3). Cortical thickness was 20–26% larger for injured knees compared to contralateral knees for both injury modes and both time points ($p < 0.05$). However, we observed no significant differences in cortical thickness increase between time points or between injury modes. BMD of the subchondral bone plate was significantly higher for Low Speed injured knees compared to contralateral knees at week 12 only (908.7 vs. 891.7 mg HA/cm^3; $p = 0.001$). No significant differences in subchondral bone BMD were observed for High Speed injured knees or for any knees at 16 weeks post-injury.

Injured knees exhibited significant osteophytosis using both the High Speed and Low Speed injury modes by 12 and 16 weeks post-injury (Figs. 4–6). The pattern of osteophyte formation was consistent for all mice at 12 and 16 weeks, regardless of injury mode. Specifically, there was considerable osteophyte formation on the anterior-medial aspect of the distal femur, the menisci (particularly the medial meniscus) exhibited hypertrophy and osteophyte formation, primarily extending in an anteromedial direction from the joint (Fig. 5). The posterior medial tibial plateau exhibited bone formation in the posterior direction, and extreme erosion of the tibial plateau was observable with μCT, exposing the underlying subchondral bone.

Both injury models exhibited increased osteophyte volume from 12 to 16 weeks, although this increase was only significant for the Low Speed injury group (Fig. 6). The High Speed injury group exhibited higher osteophyte volume compared to the low speed injury group at both time points; this difference was statistically significant at 12 weeks ($p = 0.04$). We were able to observe preliminary signs of osteophyte formation on transverse μCT images of injured joints as early as 10 days post-injury, particularly on the anteromedial aspect of the distal femur (Fig. 5).

Anterior–Posterior Joint Laxity

We observed a greater than twofold increases in AP joint laxity immediately following joint injury with both injury modes (Fig. 7). We observed no significant difference in joint laxity between flexion angles for any group at any time point. By 12 and 16 weeks post-injury, AP joint laxity for both injured groups was reduced to control values. During AP laxity testing of week 16 legs, one control leg was broken during potting. Additionally, injured knees of week 16 mice had severely diminished range of motion and were difficult to extend to 30°. As a result, three of the 1 mm/s and two of the 500 mm/s week 16 knees were also fractured. Thirty-degree extension was tested last to ensure that data was collected for 60° and 90° joint angles.

No change in joint laxity was observed for day 0 uninjured joints after fixation in 4% paraformaldehyde and preservation in 70% ethanol for 4 weeks (compared to fresh-frozen joints), but injured joints exhibited significantly increased joint laxity after fixation (+18% AP joint laxity). Subsequently, joint laxity

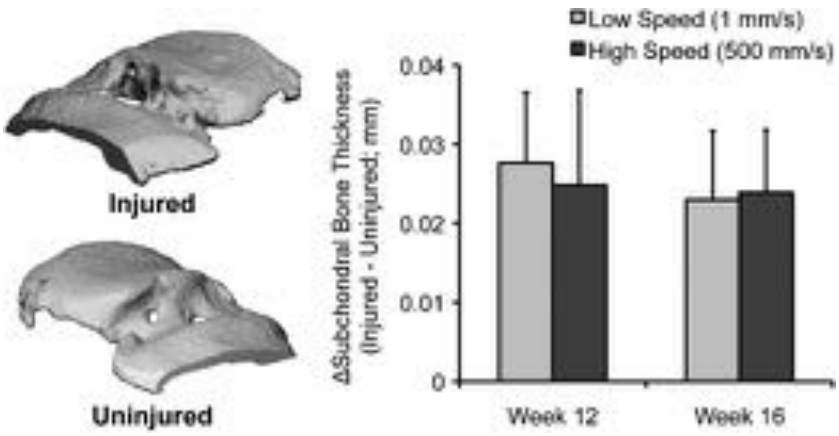

Figure 3. Left: Micro-computed tomography reconstructions of the subchondral bone plate of the tibial plateau of injured and uninjured knees, with a medial cut for visualization of subchondral bone thickness. Right: Difference in subchondral bone thickness of the proximal tibial plateau for Low Speed (1 mm/s) and High Speed (500 mm/s) injury groups. Values are the average difference between injured and contralateral control legs for each mouse. Injured versus uninjured values were significantly different for all groups and all time points ($p < 0.05$). No significant differences were observed between injury modes or time points.

values of day 0 preserved knees were used for all comparisons between day 0, week 12, and week 16 data.

Long Term Whole Joint Histology

Whole joint histology showed extreme degeneration and OA for both injury modes at 12 and 16 weeks post-injury (Fig. 8). OARSI scores were significantly higher than UIC joints at 12 and 16 weeks for both injury modes, however there were no significant differences between High Speed and Low Speed injured joints (Fig. 9). Injured joints exhibited extreme erosion of cartilage on both the medial and lateral aspects of the tibia and femur. Many injured joints had bone-bone contact and even erosion of subchondral bone, sometimes extending as far as the growth plate. There was extreme fibrosis within the joint space and osteophytes present on the tibia and femur. The menisci on both sides were hypertrophied and degenerated. Inspection of individual sections showed the most severe degeneration on the posterior aspect of the tibial plateau of injured joints, while the anterior aspect appeared comparable to UICs. At 16 weeks the UIC joints were given an average OARSI score of approximately 2, indicating mild OA occurring naturally in the mice by 26 weeks of age.

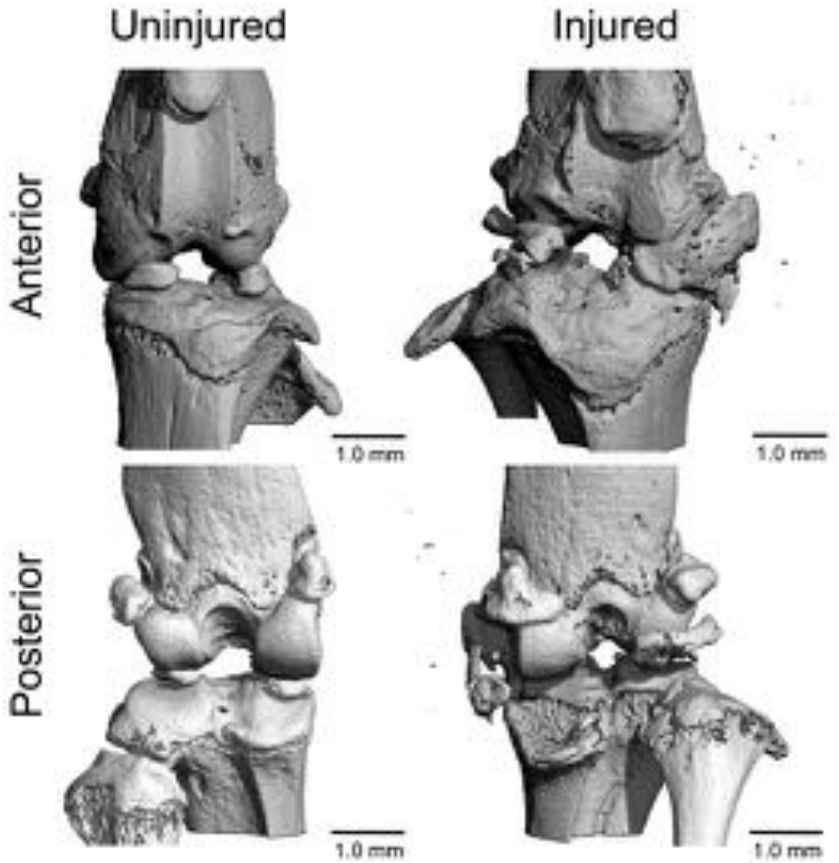

Figure 4. μCT images of injured and uninjured mouse knees at 12 weeks post-injury (Low Speed injury). Substantial osteophytosis and joint degeneration were observed in all injured knees. In particular, osteophytes were observed on the anteriomedial aspect of the distal femur, the posteromedial aspect of the proximal tibia, and the medial meniscus.

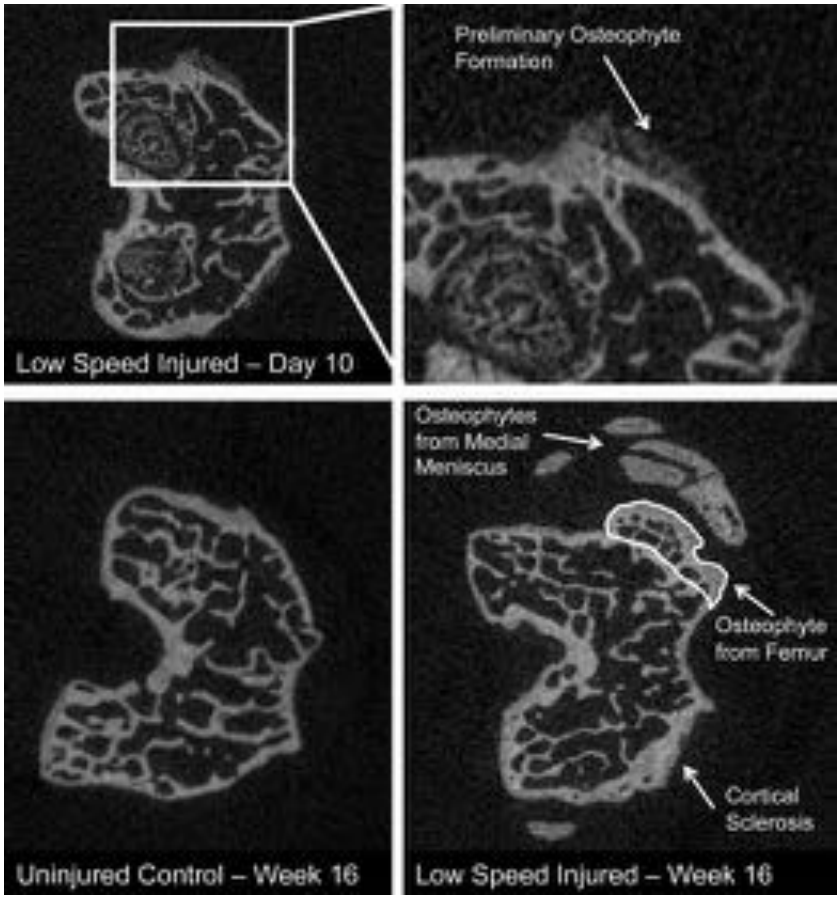

Figure 5. Transverse μCT slices of the distal femur. Top: Femoral epiphysis of an injured joint 10 days postinjury, with expanded image showing early osteophytosis from the anteriomedial femur. Bottom: Uninjured (left) and injured (right) femoral epiphysis at 16 weeks showing considerable osteophyte formation from the anteriomedial femur and medial meniscus, as well as sclerosis of cortical plate on the lateral condyle.

DISCUSSION

In this study we used a non-invasive injury model in mice to compare two similar but distinctly different injury modes, and assess potential differences in PTOA development. Using different tibial compression loading rates, we were able to produce two unique injury modes in the knees of mice: ACL rupture with avulsion fracture ("Low Speed injury", 1 mm/s loading rate) or midsubstance ACL rupture ("High Speed injury", 500 mm/s loading rate). Consistent with our hypothesis, we found that the two injury modes were not significantly different from each other with respect to long-term changes in bone structure, joint laxity, and cartilage degeneration. However, we observed a greater loss of trabecular bone in the distal femoral epiphysis at 10 days post-injury in the Low Speed injury model compared to High Speed injury. This difference is likely due to direct bone damage caused by avulsion of the ACL in the Low Speed injury group. We also observed significant differences in osteophyte formation, with High Speed injured knees developing greater osteophyte volume. Altogether, these results suggest that ACL injury mode in mice is a minor contributing factor to the subsequent joint degeneration that follows traumatic joint injury after 12–16 weeks.

The role of subchondral bone in progression of OA has been an active topic of discussion,[16–18] with authors hypothesizing that cartilage health is influenced by the structure of the underlying subchondral bone. However, early changes in subchondral bone and epiphyseal trabecular bone are not well defined in human subjects, but rather established (severe) OA is

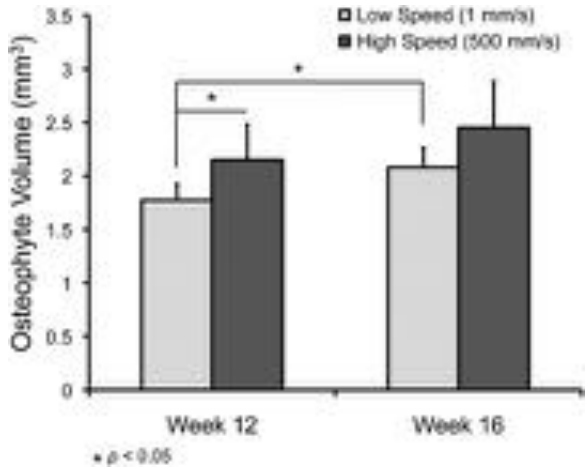

Figure 6. Osteophyte volume of injured joints. Non-native bone formation was quantified for Low Speed (1 mm/s) and High Speed (500 mm/s) injured joints at 12 and 16 weeks post-injury. High Speed injured joints exhibited greater osteophyte volume than Low Speed injured joints at 12 weeks postinjury. Osteophyte volume increased from 12 to 16 weeks for both groups, but this increase was only significant for Low Speed injured mice ($p < 0.05$).

Figure 7. Top left: Joint laxity test setup for 60° of flexion. Top right: Total anterior–posterior joint laxity at 60° for day 0, week 12, and week 16 knees. $^{*}p < 0.05$ between injured and uninjured values. Injured joints had a greater than twofold increase in joint laxity at day 0, but joint stability was returned to control values by 12 and 16 weeks post-injury. Bottom: Total anterior–posterior joint laxity at day 0 (left) and week 16 (right) at 30°, 60°, and 90° of knee flexion. $^{*}p < 0.05$ between injured and uninjured values. There were no significant differences between joint angles, or between injury modes (High Speed vs. Low Speed injury).

typically studied.[19] A few recent studies have investigated epiphyseal trabecular bone changes in the knees of osteoarthritic subjects using MRI imaging,[20,21] and have observed decreased trabecular bone parameters (loss of trabecular bone) in osteoarthritic knees, particularly in the lateral compartment. This is consistent with the current study and our previous study[8] that showed trabecular bone loss from both the medial and lateral compartments in mice, although our previous study found similar magnitudes of trabecular bone loss from the medial and lateral compartments. Subchondral bone sclerosis and osteophyte formation are also common findings in humans with OA.[22] This is consistent with the current study, in which we observed thickening of the tibial subchondral bone plate, and considerable osteophyte formation around the joint by 12 and 16 weeks post-injury. The relatively large scale of osteophytes observed in this study is not typical for OA in humans, although this may be due to the fact that bone features do not scale linearly with body size between mice and humans. For example, body mass in humans is approximately 2,000–4,000 times greater than that of mice, while trabecular thickness in humans is approximately 4–7 times greater (100–350 μm in humans vs. 25–50 μm in mice). Altogether, the subchondral and trabecular bone changes observed in this mouse model of PTOA are generally consistent with the bone changes observed in human OA.

By both 12 and 16 weeks post-injury we observed severe OA in injured knees. This is in contrast to our previous study, in which joints exhibited only mild OA by 8 weeks post-injury, with loss of Safranin-O staining, minor fissuring, and cell death in the superficial

Figure 8. Whole joint histology at 12 weeks. Sagittal sections of the medial condyle stained with Safranin-O and Fast Green. By 12 weeks post-injury we observed significant degeneration of both the tibia and femur. In particular, the posterior aspect of the medial tibia has severe degeneration of cartilage and bone erosion, often extending as far as the growth plate.

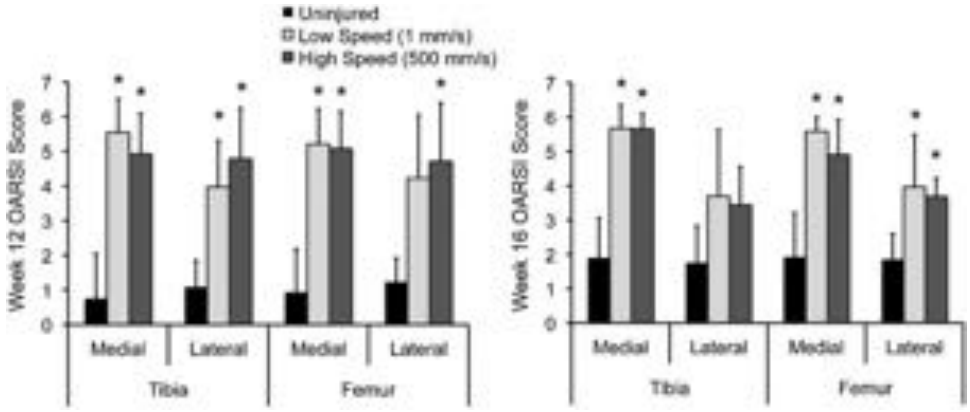

Figure 9. OARSI scores for whole joint histology at 12 and 16 weeks. We observed severe osteoarthritis of both the tibia and femur at both time points, often with degeneration of articular cartilage extending to the subchondral bone (* indicates significant difference from uninjured control. No statistically significant differences were observed in the OARSI score of knees injured with the High Speed versus Low Speed injury mode).

zone.[8] In the current study we found that by only 4 weeks later (12 weeks post injury), injured joints exhibited severe OA with total loss of cartilage tissue. In many joints there was bone on bone contact, extreme fibrosis, and severe meniscal degeneration visible by 12 weeks post-injury, often to a degree that is unnecessary for studies of arthritis development. The severe posterior bone erosion we observed on the tibial plateau, particularly on medial side, is not typical of ACL injury-induced PTOA in other animal species or in humans, although similar erosion has been described with surgical transection of the ACL in mice.[4] This posterior degeneration may therefore be specific to mouse models of ACL-induced PTOA irrespective of how the ACL is ruptured (with or without surgery). In this way, ACL injury in mice may be limited for translation to human injuries. For future studies with this model, we anticipate that an 8–10 weeks end point should be sufficient to show moderate to severe OA, and would be sufficient to detect any improvement in OA development due to treatment. In contrast, the DMM and ACLT models utilized by Glasson et al.[4] were able to induce moderate-to-severe OA by 4 weeks post-injury.

Changes in AP joint laxity of injured knees in this study were similar to values obtained from previous studies using C57BL/6 mice with healthy knees. At ± 0.8 N in healthy ACL intact joints, Blankevoort et al.[14] measured 0.43 ± 0.16 mm and Wang et al.[13] measured 0.50 ± 0.09 mm, compared to 0.57 ± 0.08 mm in our study. The increased joint laxity measured in this study is likely due to the additional degree of freedom in our test fixture, which allowed rotation of the tibia about its longitudinal axis. The previous studies only allowed two degrees of freedom of motion.

In this study we observed consistent and repeatable patterns of osteophytosis around the joint capsule by 12 and 16 weeks post injury for both injury modes. In particular, we observed osteophytes forming from the anteriomedial femur, the posteromedial tibia, and the medial meniscus. It is possible that osteophyte formation around the joint may have contributed to the reduction in joint laxity from day 0 values. The stabilizing effect of osteophytes in osteoarthritic joints was previously studied by Pottenger et al.[23] in humans undergoing total knee arthroplasty (TKA) by measuring varus-valgus (VV) laxity before and after removal of osteophytes. They observed an increase in VV joint laxity from 11.0° to 14.7° after osteophyte removal, showing that osteophytes helped stabilize the joint. These results support the hypothesis that osteophytes form as a response to joint instability. The drawback to restoring joint stability by osteophyte formation is severe reduction in joint range of motion, which was observed in the current study. Twelve- and sixteen-week knees were extremely stiff and resisted extension to 30°. This was supported by a study in humans undergoing TKA, in which residual posterior femoral condyle osteophytes were associated with reduced knee flexion after surgery. Removal of the osteophytes avoided impingement with the implant and allowed more flexion to occur.[24] Unfortunately, our study did not investigate AP joint laxity at intermediate time points between 0 and 12 weeks post-injury. Future analyses could investigate the time course of "re-stabilization" of the joint after ACL rupture, and could confirm the proposed correlation with osteophyte formation.

Future studies using this model should include additional biomechanical analyses to further characterize relationships between joint injury and OA progression. Gait analysis of injured mice could address questions concerning voluntary mechanical loading after injury and whether mice change limb-loading patterns. If the mice are unweighting the injured limb, then loss of bone volume may be partly explained due to disuse. Additionally, future studies could investigate the activity level of mice following joint injury. It is possible that voluntary cage activity is reduced, which would result in further mechanical loading-

related bone atrophy. The opposite is also likely true; increased cage activity or exercise (including fighting) could exacerbate PTOA progression following injury.

This study advances our previous study by analyzing multiple injury modes, quantifying biomechanical changes in the joint, and analyzing time points at which severe OA is present. However, there are still limitations that must be acknowledged. In particular, while anatomical structures between human and mice are similar, the bipedal gait of humans is very different from that of mice, and may result in divergent laxity changes, loading patterns, and locations of degeneration. Additionally, the severe osteophyte formation that we observe with this model is not typical for human joints, although it is comparable to other widely used mouse models,[25] and may be largely explained by the dramatic size difference between mouse and human joints. Finally, these studies used 10-week-old mice with open growth plates (the growth plates in mouse long bones typically remain open throughout the lifetime of the animal). This is a ubiquitous limitation of using mice for studies of bone, and may have contributed to the skeletal adaptation observed in this study. While this model may not be able to overcome all of these limitations, it still has several advantages over other existing mouse models of PTOA, and may be uniquely useful for investigating OA progression in humans.

In conclusion, in this study we found that ACL injury mode does not affect the long term bone changes or OA severity in mice, although it does affect short term trabecular bone turnover, with injury involving direct bone damage (avulsion) exhibiting greater short term trabecular bone loss. We also found that ACL injury dramatically increased AP joint laxity in mice immediately following injury, but joint stability is restored by 12 weeks post-injury, possibly due to extensive osteophyte formation around the joint. These studies further characterize the non-invasive knee injury mouse model developed in our lab, and begin to describe mechanical loading changes initiated by joint injury. The model presented provides an opportunity to explore fundamental questions regarding the role of bone turnover in PTOA progression, and findings from this model may point to bone turnover as a potential target for therapies aimed at slowing or preventing PTOA.

ACKNOWLEDGEMENTS

Research reported in this publication was supported by the National Institute of Arthritis and Musculoskeletal and Skin Diseases, part of the National Institutes of Health, under Award Number AR062603 (B.A.C.) and AR063348 (D.R.H.). The content is solely the responsibility of the authors and does not necessarily represent the official views of the National Institutes of Health.

REFERENCES

1. Felson DT. 1988. Epidemiology of hip and knee osteoarthritis. Epidemiol Rev 10:1–28.
2. Lohmander LS, Englund PM, Dahl LL, et al. 2007. The long-term consequence of anterior cruciate ligament and meniscus injuries: osteoarthritis. Am J Sports Med 35:1756–1769.
3. Oiestad BE, Engebretsen L, Storheim K, et al. 2009. Knee osteoarthritis after anterior cruciate ligament injury: a systematic review. Am J Sports Med 37:1434–1443.
4. Glasson SS, Blanchet TJ, Morris EA. 2007. The surgical destabilization of the medial meniscus (DMM) model of osteoarthritis in the 129/SvEv mouse. Osteoarthritis Cartilage 15:1061–1069.
5. Furman BD, Strand J, Hembree WC, et al. 2007. Joint degeneration following closed intraarticular fracture in the mouse knee: a model of posttraumatic arthritis. J Orthop Res 25:578–592.
6. van Beuningen HM, Glansbeek HL, van der Kraan PM, et al. 2000. Osteoarthritis-like changes in the murine knee joint resulting from intra-articular transforming growth factor-beta injections. Osteoarthritis Cartilage 8:25–33.
7. Poulet B, Hamilton RW, Shefelbine S, et al. 2011. Characterising a novel and adjustable non-invasive murine knee joint loading model. Arthritis Rheum 63:137–147.
8. Christiansen BA, Anderson MJ, Lee CA, et al. 2012. Musculoskeletal changes following non-invasive knee injury using a novel mouse model of post-traumatic osteoarthritis. Osteoarthritis Cartilage 20:773–782.
9. Gottsegen CJ, Eyer BA, White EA, et al. 2008. Avulsion fractures of the knee: imaging findings and clinical significance. Radiographics 28:1755–1770.
10. Crowninshield RD, Pope MH. 1976. The strength and failure characteristics of rat medial collateral ligaments. J Trauma 16:99–105.
11. Noyes FR, DeLucas JL, Torvik PJ. 1976. Biomechanics of anterior cruciate ligament failure: an analysis of strain-rate sensitivity and mechanisms of failure in primates. J Bone Joint Surg Am 56:236–253.
12. Bouxsein ML, Boyd SK, Christiansen BA, et al. 2010. Guidelines for assessment of bone microstructure in rodents using micro-computed tomography. J Bone Miner Res Off J Am Soc Bone Miner Res 25:1468–1486.
13. Wang VM, Banack TM, Tsai CW, et al. 2006. Variability in tendon and knee joint biomechanics among inbred mouse strains. J Orthop Res Off Publ Orthop Res Soc 24:1200–1207.
14. Blankevoort L, van Osch JVM, Janssen B, et al. 1996. In vitro laxity-testers for knee joints of mice. J Biomechanics 29:799–806.
15. Glasson SS, Chambers MG, Van Den Berg WB, et al. 2010. The OARSI histopathology initiative—Recommendations for histological assessments of osteoarthritis in the mouse. Osteoarthritis Cartilage 18:S17–S23.
16. Mansell JP, Tarlton JF, Bailey AJ. 1997. Biochemical evidence for altered subchondral bone collagen metabolism in osteoarthritis of the hip. Br J Rheumatol 36:16–19.
17. Hayami T, Pickarski M, Zhuo Y, et al. 2006. Characterization of articular cartilage and subchondral bone changes in the rat anterior cruciate ligament transection and meniscectomized models of osteoarthritis. Bone 38:234–243.
18. Radin EL, Rose RM. 1986. Role of subchondral bone in the initiation and progression of cartilage damage. Clin Orthop Relat Res 213:34–40.
19. Mastbergen SC, Lafeber FP. 2011. Changes in subchondral bone early in the development of osteoarthritis. Arthritis Rheum 63:2561–2563.
20. Chiba K, Uetani M, Kido Y, et al. 2011. Osteoporotic changes of subchondral trabecular bone in osteoarthritis of the knee: a 3-T MRI study. Osteoporos Int 23:589–597.
21. Bolbos RI, Zuo J, Banerjee S, et al. 2008. Relationship between trabecular bone structure and articular cartilage

morphology and relaxation times in early OA of the knee joint using parallel MRI at 3 T. Osteoarthritis Cartilage 16:1150–1159.
22. Jacobson JA, Girish G, Jiang Y, et al. 2008. Radiographic evaluation of arthritis: degenerative joint disease and variations. Radiology 248:737–747.
23. Pottenger LA, Phillips FM, Draganich LF. 1990. The effect of marginal osteophytes on reduction of varus–valgus instability in osteoarthritic knees. Arthritis Rheum 33:853–858.
24. Yau WP, Chiu KY, Tang WM, et al. 2005. Residual posterior femoral condyle osteophyte affects the flexion range after total knee replacement. Int Orthop 29:375–379.
25. Moodie JP, Stok KS, Muller R, et al. 2011. Multimodal imaging demonstrates concomitant changes in bone and cartilage after destabilisation of the medial meniscus and increased joint laxity. Osteoarthritis Cartilage 19: 163–170.

Osteoarthritis and Cartilage 22 (2014) 1461–1469

Osteoarthritis and Cartilage

In vivo fluorescence reflectance imaging of protease activity in a mouse model of post-traumatic osteoarthritis

P.B. Satkunananthan † ‡, M.J. Anderson †, N.M. De Jesus ‡ §, D.R. Haudenschild † ‡, C.M. Ripplinger ‡ §, B.A. Christiansen † ‡ *

† *Department of Orthopaedic Surgery, University of California-Davis Medical Center, USA*
‡ *Biomedical Engineering Graduate Group, University of California-Davis, USA*
§ *Department of Pharmacology, University of California-Davis Medical Center, USA*

ARTICLE INFO

Article history:
Received 21 May 2014
Accepted 10 July 2014

Keywords:
Fluorescence reflectance imaging
Post-traumatic osteoarthritis
Inflammation
Bone resorption
Protease
Cathepsin

SUMMARY

Objective: Joint injuries initiate a surge of inflammatory cytokines and proteases that contribute to cartilage and subchondral bone degeneration. Detecting these early processes in animal models of post-traumatic osteoarthritis (PTOA) typically involves *ex vivo* analysis of blood serum or synovial fluid biomarkers, or histological analysis of the joint. In this study, we used *in vivo* fluorescence reflectance imaging (FRI) to quantify protease, matrix metalloproteinase (MMP), and Cathepsin K activity in mice following anterior cruciate ligament (ACL) rupture. We hypothesized that these processes would be elevated at early time points following joint injury, but would return to control levels at later time points.
Design: Mice were injured *via* tibial compression overload, and FRI was performed at time points from 1 to 56 days after injury using commercially available activatable fluorescent tracers to quantify protease, MMP, and cathepsin K activity in injured vs uninjured knees. PTOA was assessed at 56 days post-injury using micro-computed tomography and whole-joint histology.
Results: Protease activity, MMP activity, and cathepsin K activity were all significantly increased in injured knees relative to uninjured knees at all time points, peaking at 1–7 days post-injury, then decreasing at later time points while still remaining elevated relative to controls.
Conclusions: This study establishes FRI as a reliable method for *in vivo* quantification of early biological processes in a translatable mouse model of PTOA, and provides crucial information about the time course of inflammation and biological activity following joint injury. These data may inform future studies aimed at targeting these early processes to inhibit PTOA development.
© 2014 Osteoarthritis Research Society International. Published by Elsevier Ltd. All rights reserved.

Introduction

Osteoarthritis (OA) is a primary musculoskeletal health concern, affecting approximately 27 million Americans[1]. Post-traumatic osteoarthritis (PTOA) is commonly observed within 10–20 years following anterior cruciate ligament (ACL) rupture[2–4]. Traumatic joint injuries initiate a surge of inflammatory cytokines, matrix metalloproteinases (MMPs), cathepsin proteases, and other degradative enzymes that contribute to cartilage and subchondral bone degeneration[2,5–11]. Detecting these early biological processes in animal models of OA typically involves analysis of blood serum or synovial fluid biomarkers, or destructive histological analysis of the joint. The ability to quantify these processes non-invasively *in vivo* has the distinct advantages of rapid measurement time, relatively low cost, and the capability to perform repeated longitudinal measurements in the same animals at multiple time points or following therapy. Additionally, non-invasive *in vivo* analyses preclude the possibility of exacerbated inflammation or damage to the joint as a direct result of the sampling procedure.

Near-infrared protease activatable probes combined with fluorescence reflectance imaging (FRI) have become widely used for *in vivo* imaging to visualize and quantify cellular activity. These optical tracers are fluorescently quenched until a linker domain is cleaved by a specific protease of interest, which then produces a robust fluorescent signal. These techniques have been extensively validated and used in studies of cancer[12–15] and atherosclerosis[16–19], but are also potentially useful for studies of the

* Address correspondence and reprint requests to: B.A. Christiansen, UC Davis Medical Center, Department of Orthopaedic Surgery, 4635 2nd Ave, Suite 2000, Sacramento, CA 95817, USA. Tel: 1-916-734-3974; Fax: 1-916-734-5750.
E-mail addresses: psatkun@ucdavis.edu (P.B. Satkunananthan), mjanderson@ucdavis.edu (M.J. Anderson), ndejesus@ucdavis.edu (N.M. De Jesus), drhaudenschild@ucdavis.edu (D.R. Haudenschild), cripplinger@ucdavis.edu (C.M. Ripplinger), bchristiansen@ucdavis.edu (B.A. Christiansen).

http://dx.doi.org/10.1016/j.joca.2014.07.011
1063-4584/© 2014 Osteoarthritis Research Society International. Published by Elsevier Ltd. All rights reserved.

musculoskeletal system to measure markers of inflammation and matrix degradation (cathepsin proteases and MMPs) and bone turnover (cathepsin K), which have vital roles in OA progression. Commercially available fluorescent activatable probes have been validated for use in musculoskeletal applications[20–23]. However, no studies have utilized these methods in an animal model of PTOA to determine the dynamic protease profile following joint injury or to quantify disease severity or progression.

In this study, we used FRI to quantify the time course of biological processes associated with PTOA progression following non-invasive joint injury in mice. We hypothesized that inflammatory biomarkers and degradative processes would be elevated at early time points following traumatic joint injury (1–14 days), but would return to control levels at later time points (4–8 weeks). These results of this study reveal, for the first time, the dynamic time course of protease activity in joints following injury, and establish FRI imaging as a feasible method for *in vivo* quantification of these biological processes in a mouse model of PTOA.

Methods

Animals

A total of 54 C57BL/6 mice (27 male, 27 female; 10 weeks old at the time of injury) were obtained from Harlan Sprague Dawley, Inc. (Indianapolis, IN, USA). Forty-eight mice (24 male, 24 female) were injured using tibial compression overload, while 6 mice (3 male, 3 female) were sham injured. Animals were housed in a compliant facility at UCDMC for a 2-week acclimation period prior to injury. All animals were maintained and used in accordance with National Institutes of Health guidelines on the care and use of laboratory animals, and the study was approved by our institutional Animal Studies Committee.

Tibial compression-induced knee injury

Mice were subjected to non-invasive ACL rupture induced by a single overload cycle of tibial compression as previously described[24]. Briefly, mice were anesthetized and placed in a prone position in a materials testing system (Bose ElectroForce 3200, Eden Prairie, MN, USA) with tibial compression loading platens (Fig. 1). A single dynamic axial compressive load was applied at 1 mm/s to the right lower leg to a target compressive force of 12 N to produce ACL rupture. This loading protocol produces failure of the ACL with avulsion fracture from the distal femur[24,25]. Contralateral limbs remained uninjured, and served as internal controls. Sham injury was performed by anesthetizing mice and loading them into the tibial compression system, then applying a 1–2 N compressive load for ~5 s.

Fluorescent reflectance imaging (FRI)

All mice were imaged on days 1, 3, 7, 14, 28, and 56 after injury using *in vivo* FRI to quantify levels of fluorescence from activated probes in injured knees vs contralateral knees. Three probes were used in this study: ProSense 680, MMPSense 680, and CatK 680 FAST (Table I; PerkinElmer, Waltham, MA). Sixteen injured mice (8 male, 8 female) were analyzed with each of the fluorescent activatable probes; 6 uninjured (sham) mice (3 male, 3 female) were analyzed with ProSense 680 in order to confirm that there were no right/left differences in uninjured mice, and to quantify possible systemic inflammation that may be measureable in contralateral limbs of injured mice. In previous studies, both MMPSense[26,27] and ProSense[13,16] have been shown to localize to sites of inflammation, while CatK has been demonstrated to localize to sites of increased bone resorption and osteoclast activity[28].

Before each imaging time point (24 h prior for ProSense 680 and MMPSense 680, and 6 h prior for CatK 680 FAST), mice were anesthetized via isoflurane inhalation, and 10 μL (~0.1 mg/kg, IV) of probe was administered to each mouse. Hair was removed with a depilatory from the ventral aspect of both legs, and mice were imaged three at a time (22.5 cm field of view) in the imaging system (IVIS Spectrum, PerkinElmer, Waltham, MA). Each mouse was

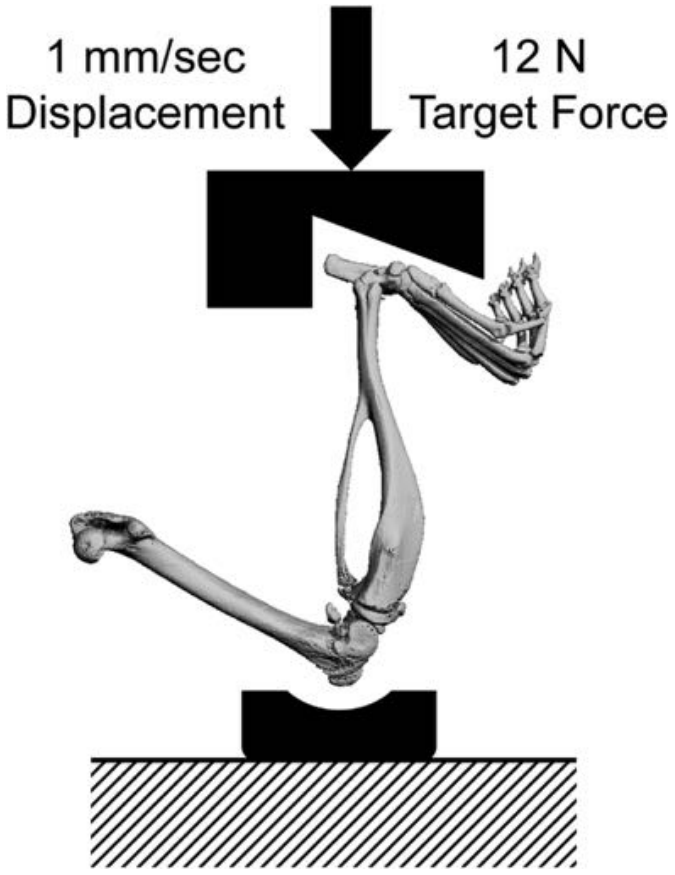

Fig. 1. Tibial compression setup for non-invasive knee injury. A single dynamic axial compressive load was applied at 1 mm/s to the right lower leg to a target compressive force of 12 N to produce ACL rupture. For uninjured mice, sham injury was performed by applying a 1–2 N compressive load.

Table I
Fluorescent tracers used to quantify early processes of PTOA

Imaging agent	Action	Indication
MMPSense 680	Activated by MMPs including MMP-2, -3, -9, -13	Localizes to inflammatory infiltrates involved in the degradation of collagens
ProSense 680	Activated by proteases such as Cathepsin B, L, S and Plasmin	Activated by family of lysosomal cathepsin proteases, allows detection of activated macrophages, neutrophils, eosinophils in the inflammatory response
CatK 680 FAST	Activated by Cathepsin K proteinase (Cat K)	Specific indicator of bone resorption

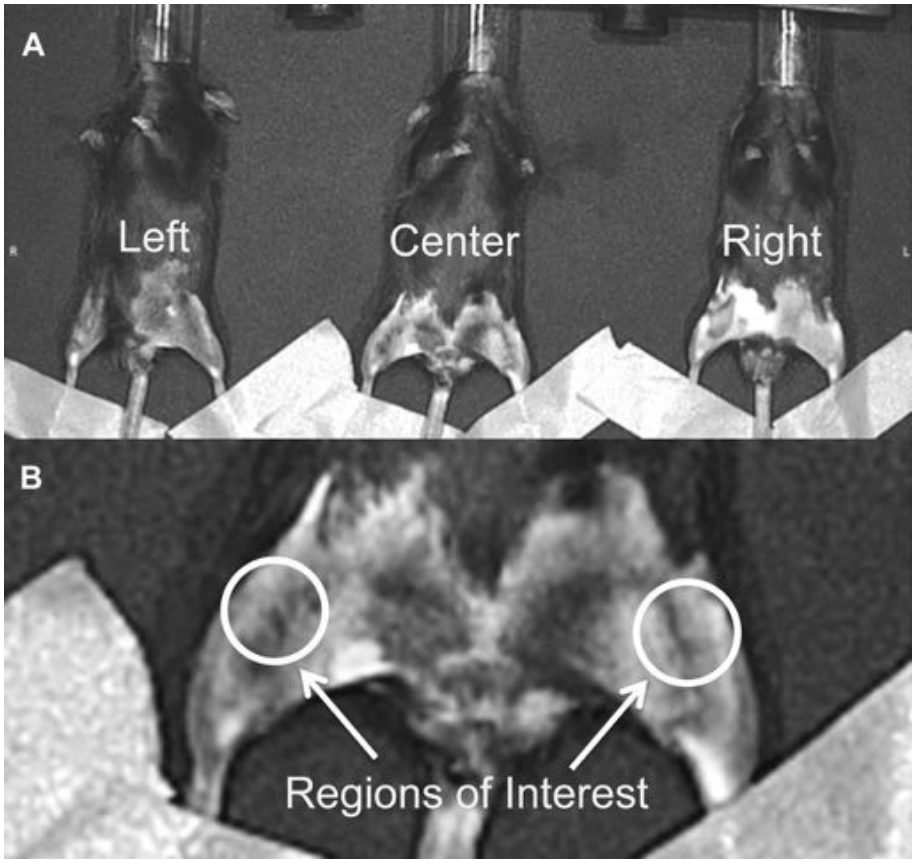

Fig. 2. (A) Imaging positions for mice in the IVIS Spectrum system. Each mouse was imaged twice at each time point in two different positions, and results from the two images were averaged for each mouse/time point. (B) Regions of interest for quantifying fluorescent signals in each knee. The ROI was a uniform circle of 12.3 mm^2 that was anatomically selected around the knee on a grayscale photograph of the mice, such that the selection criteria were unbiased by the fluorescent signals.

imaged twice at each time point in two different positions (left, right, or center; Fig. 2A), and results from the two images were averaged for each mouse/time point. Mouse legs were positioned such that the anterior-medial aspect of the knees was horizontal to allow for even epi-illumination. The legs were taped down across the ankle, and image processing and quantification was performed *via* IVIS *Living Image* software.

The excitation and emission filters for all probes were 675 ± 35 nm and 700 ± 35 nm, respectively, and were chosen based on the peak excitation and emission spectra of the probes (680/700 nm ex/em for ProSense 680 and MMPSense 680; 675/693 nm ex/em for CatK 680 FAST). The exposure time for each probe was 0.75 s for ProSense 680, 0.75 s for MMPSense 680, and 1.0 s for CatK 680 FAST. Spatial binning of pixels was set at the Medium option and the F/Stop was set to 2. Quantification of fluorescence intensity was performed by evaluating the *total radiant efficiency* ([photons/sec]/[μW/cm^2]) of the signal within a region of interest (ROI). The ROI was a uniform circle of 12.3 mm^2 that was anatomically selected around the knee on a grayscale photograph of the mice [Fig. 2(B)], such that the ROI selections encapsulated the entire knee and were unbiased by the fluorescent signals. Subsequently, the total radiant efficiency of the injured knee was normalized to the contralateral uninjured knee of each mouse, to account for mouse-to-mouse variation in delivery of the fluorescent probe.

Micro-computed tomography analysis of epiphyseal trabecular bone and osteophyte formation

Injured and uninjured knees from 8 male and 8 female mice were analyzed with micro-computed tomography (μCT 35, SCANCO, Brüttisellen, Switzerland) to quantify trabecular bone structure of the distal femoral epiphysis and osteophyte formation around the joint. All mice were sacrificed 56 days post-injury following the last time point for FRI imaging. Dissected limbs were fixed in 4% paraformaldehyde for 48 h, then preserved in 70% ethanol. Knees were scanned according to the guidelines for μCT analysis of rodent bone structure[29] (energy = 55 kVp, intensity = 114 mA, 10 μm nominal voxel size, integration time = 900 ms). Analysis of trabecular bone in the distal femoral epiphysis was performed by manually drawing contours on 2D transverse slices; the distal femoral epiphysis was delineated as the region of trabecular bone enclosed by the growth plate and subchondral cortical bone plate (Fig. 3). Using the manufacturer's analysis software, we quantified trabecular bone volume per total volume (BV/TV), trabecular thickness (Tb.Th), trabecular separation (Tb.Sp), trabecular number (Tb.N), bone tissue mineral density (Tissue BMD; mg HA/cm^3 BV), and apparent mineral density (Apparent BMD; mg HA/cm^3 TV). Osteophyte volume was calculated for each knee. For this analysis, manual contours were drawn to quantify all non-native mineralized tissue in and around the joint space, excluding naturally ossified structures (patella, fabella, anterior and posterior horns of the menisci; Fig. 3).

Whole-joint histology of articular cartilage

Following μCT imaging, knees from the same 8 male mice and 8 female mice were analyzed with whole-joint histology to quantify cartilage and joint deterioration. Knee joints were decalcified for 4 days in 10% buffered formic acid, and processed for standard paraffin embedding. From each joint, four sagittal slices of 6 μm

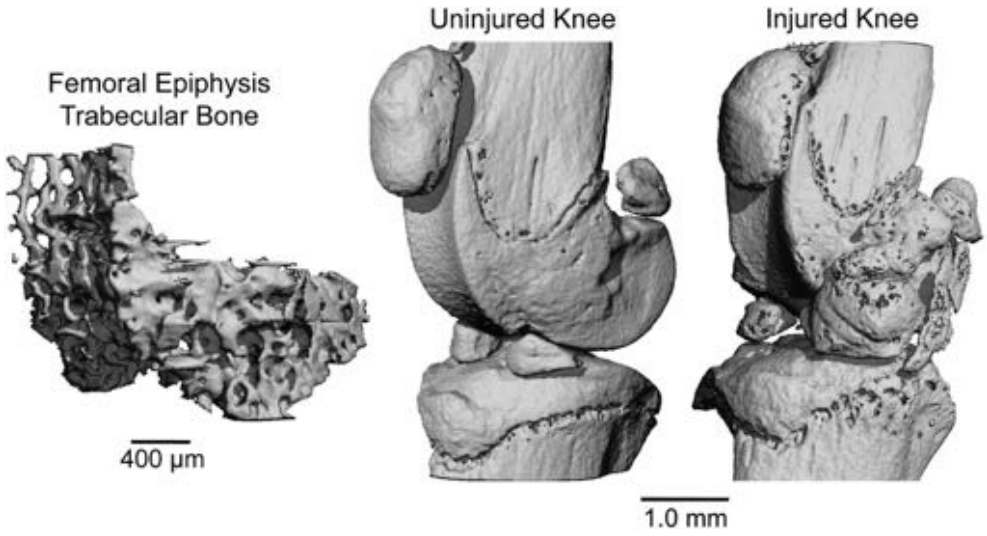

Fig. 3. (Left) Trabecular bone volume of interest from the femoral epiphysis. (Right) Uninjured and injured mouse knees at 56 days post-injury. Considerable osteophyte formation and joint degeneration are apparent on the injured knee.

thickness were sectioned from the medial joint, separated by 250 μm. The medial joint was analyzed since this is the primary site of joint degeneration in our previous studies, and in studies by other investigators using similar models[24,30]. Slides were stained with Safranin-O and Fast Green in order to assess proteoglycan content, articular cartilage degeneration, and overall joint integrity. Slides were blinded and graded by three independent readers using the semi-quantitative OARSI scale[31]. Grades were assigned to the medial tibial plateau and medial femoral condyle. Grades from the three readers were averaged for each section, and all gradable sections were averaged for each knee.

Statistical analysis

For all analyses, paired Student's *t*-tests were used within each experimental group in order to determine differences in injured vs uninjured knees. Differences in FRI readings between time points were analyzed with repeated measures ANOVA. FRI, μCT, and histology data were compared between male and female mice at each time point using unpaired *t*-test. Differences were considered statistically significant at $P < 0.05$ for all tests. All data is presented as mean ± 95% confidence interval. We also performed a statistical analysis to assess the effect of mouse position within the imaging chamber (left, right, center). We performed repeated-measures ANOVA on radiant efficiencies of mice imaged in the three positions, by delineating both the position on the stage and the position of a mouse leg with respect to the center as additional ordinal variables.

Results

FRI quantification of protease, MMP, and cathepsin K activity

Protease activity (ProSense 680), MMP activity (MMPSense 680), and cathepsin K activity (CatK 680 FAST) were all significantly increased in the injured knee compared to the contralateral (uninjured) knee at all time points (Figs. 4 and 5; $P < 0.05$). No significant differences were observed between male and female mice for any of the probes at any of the time points examined. Uninjured mice did not exhibit significant differences between the right and left knees at any time points. No differences in protease activity (ProSense 680) were observed between uninjured mice and contralateral knees at any time points except at 14 days post-injury, at which point protease activity of uninjured mice was significantly lower than contralateral knees, and significantly lower than all other time points for uninjured mice.

Normalization of fluorescence data (injured/contralateral for each mouse) indicated that MMPSense and ProSense were elevated 33–77% from days 1–14 post-injury, then decreased at

Fig. 4. Representative pseudo-colored images of male and female mice imaged with each of the fluorescent tracers at 3 and 14 days post-injury. Protease activity (ProSense 680), MMP activity (MMPSense 680), and cathepsin K activity (CatK 680 FAST) were all significantly increased in the injured knee compared to the contralateral knee at all time points.

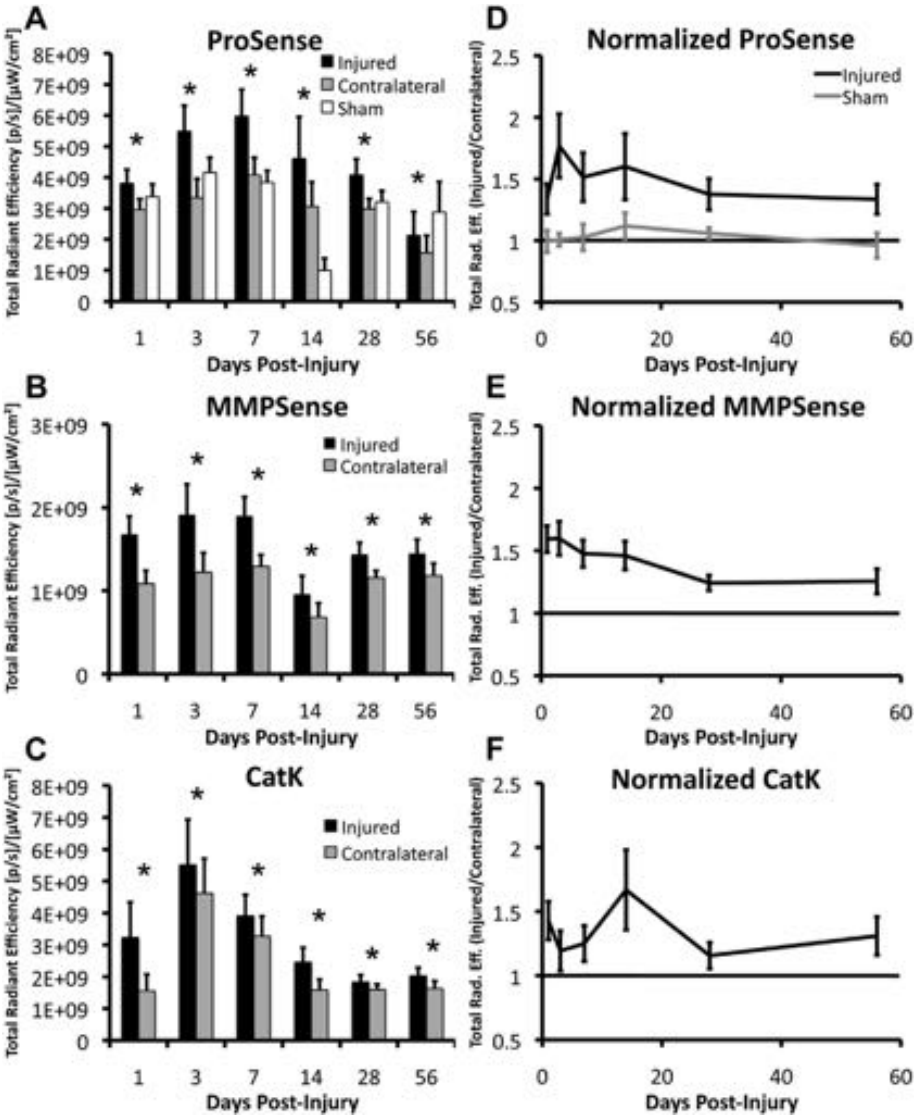

Fig. 5. (A–C) Total radiant efficiency values from each fluorescent activatable probe at each time point of interest ($n = 16$ mice/time point for Injured and Contralateral data, $n = 6$ for Sham data). (D–F) Normalized time course of total radiant efficiency (fluorescence intensity: injured knee/contralateral knee) for the three probes. Normalized fluorescence levels of MMPSense and ProSense were elevated from days 1 through 14, and decreased slightly at later time points while still remaining significantly elevated compared to uninjured limbs (above 1.0). CatK 680 FAST signals were increased in both the injured and contralateral knees at days 3–7, suggesting a systemic bone loss at these time points. All data presented as mean ± 95% confidence interval. *Injured > Contralateral ($P < 0.05$).

later time points while still remaining 24–37% greater than contralateral limbs until at least 56 days post-injury. Normalized data from the CatK probe exhibited a less consistent time course, with noticeable peaks in Cathepsin K activity at days 1 and 14. The raw (non-normalized) CatK 680 signal exhibited significant increases in both the injured and contralateral knees (Fig. 5), particularly at days 3 and 7 relative to other time points. Fluorescence intensity for ProSense and MMPSense of the contralateral knees also varied throughout the time course of the study, but did not exhibit the nearly 3-fold increase observed for the CatK probe at day 3.

Analysis of imaging positions within the IVIS Spectrum confirmed that there were significant differences in total radiant efficiency quantified between each of the respective positions ($P < 0.001$) due to slight differences in illumination intensity. To account for this, mouse position was included as a factor in all statistical analyses. Future studies will utilize only one imaging position (center) in order to eliminate this confounding factor.

Micro-computed tomography of femoral epiphysis

MicroCT analysis of injured and uninjured joints at Day 56 revealed a ~27% loss of trabecular bone volume and notable osteophyte formation in injured joints relative to uninjured joints, consistent with our previous findings[24,25] (Fig. 6). We observed no significant difference between males and females in osteophyte formation or trabecular bone adaptation, as injured-contralateral differences in trabecular bone volume fraction (BV/TV), connectivity density (Conn.Dens), structural model index (SMI), trabecular number (Tb.N), trabecular thickness (Tb.Th), and trabecular separation (Tb.Sp) were all similar for both sexes. We did, however, observe significant differences in the absolute values of some trabecular bone parameters between male and female mice (not considering adaptation to injury). For example, males exhibited significantly higher connectivity density ($P < 0.001$) and trabecular number ($P < 0.001$) than females, while females exhibited significantly higher trabecular thickness ($P < 0.001$) and trabecular

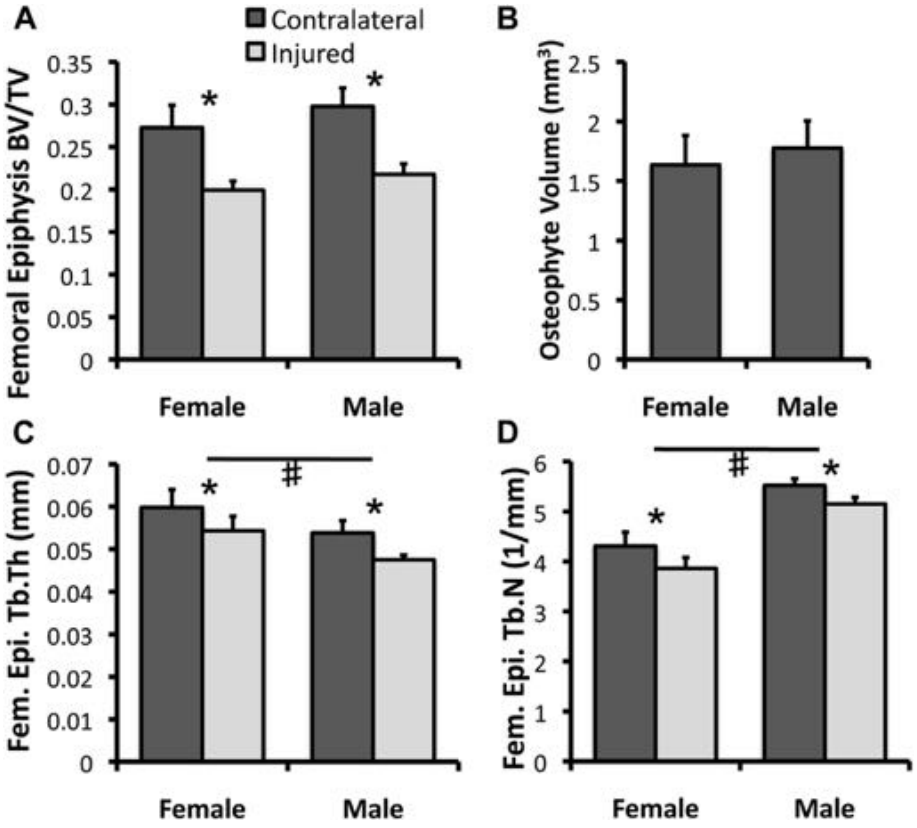

Fig. 6. (A, C, D) MicroCT analysis of femoral epiphysis trabecular bone structural parameters from injured and contralateral joints and (B) osteophyte volume of injured joints at 56 days post-injury ($n = 8$ mice/sex). No significant differences were observed for any parameters between males and females in adaptation to injury. All data presented as mean ± 95% confidence interval. *Injured vs Contralateral ($P < 0.05$), # Male vs Female ($P < 0.05$).

separation ($P < 0.001$) than male mice. This is consistent with previously published findings in mice[32].

Histological analysis of articular cartilage of the medial joint

Whole-joint histology of injured and uninjured knees revealed severe deterioration of articular cartilage and subchondral bone in injured knees, often including full loss of thickness and erosion of subchondral bone, representative of severe OA (Fig. 7). Degradation of cartilage often extended into the subchondral bone causing bone-to-bone contact. Osteophyte formation was also observed on the tibia and femur, along with growth of new mineralized cartilage from menisci. The anterior portion of the tibial plateau was not noticeably damaged, while the posterior tibial plateau exhibited erosion extending to the growth plate. This pattern of degeneration is similar to what we have observed at 12 and 16 weeks post injury[25]. Histological grading revealed significant differences between injured joints and uninjured control joints for both the tibial plateau ($P < 0.001$) and femoral condyle ($P < 0.001$). No significant differences were observed between male and female mice.

Discussion

In this study, we used FRI to visualize and quantify the time course of the biological response to traumatic joint injury in mice *in vivo* using near-infrared fluorescent activatable probes that report on protease activity, MMP activity, and cathepsin K activity. We confirmed that these processes are significantly increased in injured joints relative to uninjured joints, particularly at early time points (1–14 days post-injury), but contrary to our initial hypothesis, these processes did not return to control values at later time points. Rather, the increased protease activity observed in injured joints remained for the duration of the study (8 weeks).

This study used FRI to quantify and characterize the dynamic protease profile longitudinally in the same animals during the development of injury-induced PTOA. We were able to demonstrate that injured joints exhibited increased levels of protease activity, MMP activity, and cathepsin K activity compared to uninjured knees. ProSense 680 specifically reports on cysteine proteases such as Cathepsins B, L, and S, while CatK 680 reports specifically on Cathepsin K activity, and MMPSense reports on a family of MMPs involved in inflammation. A role for cathepsins (excluding Cathepsin K) is well-established in osteoarthritic progression, though they may not be the prime mediators of articular cartilage deterioration or bone turnover[33–36]. Cathepsin K plays a major role in bone resorption and aggrecan degradation; it has been recognized as one of the most abundant and primary proteases in osteoclastic activity. Additionally, Cathepsin K has shown the ability to degrade type II collagen, therefore it may also be directly involved in the degradation of articular cartilage in addition to its role in osteoclast function[37]. MMPs are the primary collagenolytic enzymes of osteoarthritic cartilage; MMP-13 is extremely active and MMP-3 is thought to be a collagenase activator[33], and MMP-9 is highly responsible for initiating osteoclastic resorption by removing the collagenous layer from the bone surface before demineralization begins[38].

In this study we observed increased Cathepsin K activity at days 3 and 7 post-injury relative to other time points in both injured and contralateral knees following injury. This is consistent with our previous study[24], in which we observed a decrease in trabecular

Fig. 7. Whole-joint histology of the medial aspect of injured and contralateral joints at 56 days post-injury ($n = 8$ mice/sex for Injured data, $n = 6$ mice for Uninjured data). Injured joints exhibited considerable deterioration of articular cartilage and subchondral bone, often including full loss of thickness and erosion of subchondral bone, representative of severe progressive OA (B–D). The anterior portion of the tibial plateau was not noticeably damaged, while the posterior tibial plateau exhibited erosion extended down to the growth plate. Articular cartilage grading revealed severe OA on both the tibial plateau and femoral condyle (A). No significant differences were observed between male and female mice. All data presented as mean ± 95% confidence interval. *Injured vs Contralateral ($P < 0.05$).

bone volume from the femoral epiphysis of both injured and contralateral knees by 7 days post-injury. Similarly, a study of injured and contralateral knees in human subjects following traumatic joint injury showed an increase in concentrations of aggrecan and cartilage oligomeric matrix protein (COMP) fragments and stromelysin-l in contralateral knees[39]. In the current study we did not observe significant increases in early protease activity or MMP activity in the contralateral knee relative to uninjured mice or later time points. However, this contralateral effect should be carefully considered for studies of OA using FRI, and future studies should more extensively utilize uninjured (sham) mice. It is common practice to use an internal control for normalizing fluorescent signals with FRI measurements, as this accounts for possible mouse-to-mouse differences in probe delivery. Systemic variations in fluorescent signal strength may be due to probe delivery, exact placement on the imaging stage, or illumination intensity. Normalizing by an internal control for each mouse can theoretically account for these systemic variations in difference in signal strength. However, taking into account the possible contralateral increases in these biological processes following an acute injury, this may not be a suitable analysis method for future studies of OA.

We did not detect any differences in PTOA development between male and female mice using any of the analysis methods in this study. It is well known that female athletes are 4–6 times more likely than male athletes to sustain an ACL rupture during exercise or sports[40–43], however studies of both humans and animal models suggest that males may have a greater tendency to develop PTOA following traumatic joint injury[44–46]. However, the specific mechanisms contributing to this sex-related disparity are unknown. In the current study we did not observe any sex-based differences in the protease profile at any of the time points. Furthermore, we did not observe any sex-based differences in articular cartilage or subchondral bone degeneration at 56 days post-injury. This may be due to examining a single time point when severe OA has already developed. An intermediate time point may be useful for detecting sex-based differences in OA progression, similar to those observed previously[45,46].

In vivo FRI was able to detect significant differences in fluorescent signal in injured vs contralateral knees using three different probes, however the high variability of this *in vivo* imaging technique may limit the capability to observe relatively small differences in fluorescence levels. For example, quantification of fluorescent signals using the IVIS Spectrum system exhibited large variance and a strong dependence on position of mice within the system. The IVIS Spectrum system produces a circular beam of light from the epi-illumination excitation light source above the stage. Because we imaged three mice at a time, the centrally located mouse received the most uniform illumination; whereas the mice on the left and right sides had more non-uniformity. An analysis of mouse position within the imaging system helped elucidate this issue, and by performing a repeated-measures ANOVA on radiant efficiencies on mice imaged in different positions, we confirmed that there was a significant difference in brightness between each respective position on the stage, as well as the position of each leg,

with respect to the center line. In addition, typical issues of autofluorescence and attenuation by tissue are continually a concern for *in vivo* imaging studies. In this respect, variations from mouse to mouse can make it difficult to quantify fluorescence with accuracy and reliability, as the depth of penetration of irradiated light can be considerably different. Future studies will minimize measurement variability by using only the center imaging position, however the precision of this imaging technique for detecting small differences in fluorescent signals remains unclear. However, despite these limitations, we were able to successfully track the time course of protease, MMP, and cathepsin K activity following knee injury in mice. This imaging method is non-invasive, time and cost effective, and provides longitudinal data from individual mice at multiple time points. In this way, FRI is a meaningful step forward for quantification of early biological processes in mouse models of PTOA.

This study is also somewhat limited because we did not validate our *in vivo* fluorescent signals with a histological "gold standard" such as immunohistochemistry or *in situ* hybridization. Therefore, we are unable to attribute the observed fluorescent signals to specific tissues associated with PTOA development. However, each of these fluorescent activatable probes has been extensively validated and compared to histological standards[12–19], and in particular have been validated for studies of musculoskeletal tissues[20–23], therefore we are confident that the fluorescent signals are indicative of cellular processes at the level of the whole joint. Our future studies will utilize histological techniques to further characterize the specific tissues in which these fluorescent signals originate following traumatic joint injury using this animal model.

Using commercially available fluorescent agents we were able to quantify the time course of protease activity, MMP activity, and cathepsin K activity following traumatic injury to the ACL, with noticeable peaks at early time points (1–7 days post-injury). This early response may point to a "window of opportunity" in which treatments may be administered to most efficiently stall the progression of OA. Cathepsin and MMP inhibitors have both been utilized experimentally, both in the molecular and transcriptional pathways, as potential therapies for hindering OA progression[33]. Future studies could investigate effective time periods for treatment in the murine model, which can then be extrapolated into larger animal models and human subjects.

Conclusions

Using *in vivo* FRI, we observed substantial increases in protease activity, MMP activity, and cathepsin K activity in injured joints compared to uninjured joints in mice following traumatic knee injury. We successfully described the dynamic protease profile following joint injury, and established FRI as a useful analysis method contributing to the quantification of OA progression in mice. This study provides crucial information about the time course of inflammation and cellular activity in a translatable mouse model of knee injury, and may inform future studies aimed at targeting early inflammation to reduce the development of PTOA.

Author contributions

All authors were fully involved in this study and in preparation of the manuscript.

Role of funding sources

Research reported in this publication was supported by the National Institute of Arthritis and Musculoskeletal and Skin Diseases, part of the National Institutes of Health, under Award Number AR062603 (BAC) and AR063348 (DRH). The content is solely the responsibility of the authors and does not necessarily represent the official views of the National Institutes of Health.

Competing interest statement

The authors have no potential conflicts of interest to disclose.

Acknowledgments

We would like to acknowledge Susan Stover and David Fyhrie for their meaningful contributions to this study.

References

1. Lawrence RC, Felson DT, Helmick CG, Arnold LM, Choi H, Deyo RA, *et al*. Estimates of the prevalence of arthritis and other rheumatic conditions in the United States. Part II. Arthritis Rheum 2008;58:26–35.
2. Lohmander LS, Englund PM, Dahl LL, Roos EM. The long-term consequence of anterior cruciate ligament and meniscus injuries: osteoarthritis. Am J Sports Med 2007;35:1756–69.
3. Gillquist J, Messner K. Anterior cruciate ligament reconstruction and the long-term incidence of gonarthrosis. Sports Med 1999;27:143–56.
4. Myklebust G, Bahr R. Return to play guidelines after anterior cruciate ligament surgery. Br J Sports Med 2005;39:127–31.
5. Madry H, Luyten FP, Facchini A. Biological aspects of early osteoarthritis. Knee Surg Sports Traumatol Arthrosc 2012;20:407–22.
6. Goldring MB, Goldring SR. Osteoarthritis. J Cell Physiol 2007;213:626–34.
7. Anderson DD, Chubinskaya S, Guilak F, Martin JA, Oegema TR, Olson SA, *et al*. Post-traumatic osteoarthritis: Improved understanding and opportunities for early intervention. J Orthop Res 2011;29:802–9.
8. Kurz B, Lemke AK, Fay J, Pufe T, Grodzinsky AJ, Schunke M. Pathomechanisms of cartilage destruction by mechanical injury. Ann Anat 2005;187:473–85.
9. Fitzgerald JB, Jin M, Dean D, Wood DJ, Zheng MH, Grodzinsky AJ. Mechanical compression of cartilage explants induces multiple time-dependent gene expression patterns and involves intracellular calcium and cyclic AMP. J Biol Chem 2004;279:19502–11.
10. Brophy RH, Rai MF, Zhang Z, Torgomyan A, Sandell LJ. Molecular analysis of age and sex-related gene expression in meniscal tears with and without a concomitant anterior cruciate ligament tear. J Bone Joint Surg Am 2012;94:385–93.
11. Irie K, Uchiyama E, Iwaso H. Intraarticular inflammatory cytokines in acute anterior cruciate ligament injured knee. Knee 2003;10:93–6.
12. Zhang H, Morgan D, Cecil G, Burkholder A, Ramocki N, Scull B, *et al*. Biochromoendoscopy: molecular imaging with capsule endoscopy for detection of adenomas of the GI tract. Gastrointest Endosc 2008;68:520–7.
13. Gounaris E, Tung CH, Restaino C, Maehr R, Kohler R, Joyce JA, *et al*. Live imaging of cysteine-cathepsin activity reveals dynamics of focal inflammation, angiogenesis, and polyp growth. PLoS One 2008;3:e2916.
14. Sheth RA, Mahmood U. Optical molecular imaging and its emerging role in colorectal cancer. Am J Physiol Gastrointest Liver Physiol 2010;299:G807–20.
15. Clapper ML, Hensley HH, Chang WC, Devarajan K, Nguyen MT, Cooper HS. Detection of colorectal adenomas using a bioactivatable probe specific for matrix metalloproteinase activity. Neoplasia 2011;13:685–91.

16. Nahrendorf M, Sosnovik DE, Waterman P, Swirski FK, Pande AN, Aikawa E, *et al*. Dual channel optical tomographic imaging of leukocyte recruitment and protease activity in the healing myocardial infarct. Circ Res 2007;100:1218–25.
17. Jaffer FA, Kim DE, Quinti L, Tung CH, Aikawa E, Pande AN, *et al*. Optical visualization of cathepsin K activity in atherosclerosis with a novel, protease-activatable fluorescence sensor. Circulation 2007;115:2292–8.
18. Jaffer FA, Libby P, Weissleder R. Optical and multimodality molecular imaging: insights into atherosclerosis. Arterioscler Thromb Vasc Biol 2009;29:1017–24.
19. Razansky D, Harlaar NJ, Hillebrands JL, Taruttis A, Herzog E, Zeebregts CJ, *et al*. Multispectral optoacoustic tomography of matrix metalloproteinase activity in vulnerable human carotid plaques. Mol Imaging Biol 2012;14:277–85.
20. Kozloff KM, Quinti L, Patntirapong S, Hauschka PV, Tung CH, Weissleder R, *et al*. Non-invasive optical detection of cathepsin K-mediated fluorescence reveals osteoclast activity in vitro and in vivo. Bone 2009;44:190–8.
21. Kozloff KM, Quinti L, Tung C, Weissleder R, Mahmood U. Non-invasive imaging of osteoclast activity via near-infrared cathepsin-K activatable optical probe. J Musculoskelet Neuronal Interact 2006;6:353.
22. Kozloff KM, Volakis LI, Marini JC, Caird MS. Near-infrared fluorescent probe traces bisphosphonate delivery and retention in vivo. J Bone Miner Res 2010;25:1748–58.
23. Kozloff KM, Weissleder R, Mahmood U. Noninvasive optical detection of bone mineral. J Bone Miner Res 2007;22:1208–16.
24. Christiansen BA, Anderson MJ, Lee CA, Williams JC, Yik JH, Haudenschild DR. Musculoskeletal changes following non-invasive knee injury using a novel mouse model of post-traumatic osteoarthritis. Osteoarthritis Cartilage 2012;20:773–82.
25. Lockwood KA, Chu BT, Anderson MJ, Haudenschild DR, Christiansen BA. Comparison of loading rate-dependent injury modes in a murine model of post-traumatic osteoarthritis. J Orthop Res 2013;32:79–88.
26. Barber PA, Rushforth D, Agrawal S, Tuor UI. Infrared optical imaging of matrix metalloproteinases (MMPs) up regulation following ischemia reperfusion is ameliorated by hypothermia. BMC Neurosci 2012;13:76.
27. Liu N, Shang J, Tian F, Nishi H, Abe K. In vivo optical imaging for evaluating the efficacy of edaravone after transient cerebral ischemia in mice. Brain Res 2011;1397:66–75.
28. Hoff BA, Chughtai K, Jeon YH, Kozloff K, Galban S, Rehemtulla A, *et al*. Multimodality imaging of tumor and bone response in a mouse model of bony metastasis. Transl Oncol 2012;5:415–21.
29. Bouxsein ML, Boyd SK, Christiansen BA, Guldberg RE, Jepsen KJ, Muller R. Guidelines for assessment of bone microstructure in rodents using micro-computed tomography. J Bone Miner Res 2010;25:1468–86.
30. Glasson SS, Blanchet TJ, Morris EA. The surgical destabilization of the medial meniscus (DMM) model of osteoarthritis in the 129/SvEv mouse. Osteoarthritis Cartilage 2007;15:1061–9.
31. Glasson SS, Chambers MG, Van Den Berg WB, Little CB. The OARSI histopathology initiative – recommendations for histological assessments of osteoarthritis in the mouse. Osteoarthritis Cartilage 2010;18(Suppl 3):S17–23.
32. Glatt V, Canalis E, Stadmeyer L, Bouxsein ML. Age-related changes in trabecular architecture differ in female and male C57BL/6J mice. J Bone Miner Res 2007;22:1197–207.
33. Troeberg L, Nagase H. Proteases involved in cartilage matrix degradation in osteoarthritis. Biochim Biophys Acta 1824;2012:133–45.
34. Woessner Jr JF. Purification of cathepsin D from cartilage and uterus and its action on the protein-polysaccharide complex of cartilage. J Biol Chem 1973;248:1634–42.
35. Fosang AJ, Neame PJ, Last K, Hardingham TE, Murphy G, Hamilton JA. The interglobular domain of cartilage aggrecan is cleaved by PUMP, gelatinases, and cathepsin B. J Biol Chem 1992;267:19470–4.
36. Hembry RM, Knight CG, Dingle JT, Barrett AJ. Evidence that extracellular cathepsin D is not responsible for the resorption of cartilage matrix in culture. Biochim Biophys Acta 1982;714:307–12.
37. Dejica VM, Mort JS, Laverty S, Antoniou J, Zukor DJ, Tanzer M, *et al*. Increased type II collagen cleavage by cathepsin K and collagenase activities with aging and osteoarthritis in human articular cartilage. Arthritis Res Ther 2012;14:R113.
38. Logar DB, Komadina R, Prezelj J, Ostanek B, Trost Z, Marc J. Expression of bone resorption genes in osteoarthritis and in osteoporosis. J Bone Miner Metab 2007;25:219–25.
39. Dahlberg L, Roos H, Saxne T, Heinegard D, Lark MW, Hoerrner LA, *et al*. Cartilage metabolism in the injured and uninjured knee of the same patient. Ann Rheum Dis 1994;53:823–7.
40. Arendt E, Dick R. Knee injury patterns among men and women in collegiate basketball and soccer – Ncaa data and review of literature. Am J Sports Med 1995;23:694–701.
41. Powell JW, Barber-Foss KD. Sex-related injury patterns among selected high school sports. Am J Sports Med 2000;28:385–91.
42. Hewett TE, Myer GD, Ford KR, Heidt Jr RS, Colosimo AJ, McLean SG, *et al*. Biomechanical measures of neuromuscular control and valgus loading of the knee predict anterior cruciate ligament injury risk in female athletes: a prospective study. Am J Sports Med 2005;33:492–501.
43. Zelisko JA, Noble HB, Porter M. A comparison of men's and women's professional basketball injuries. Am J Sports Med 1982;10:297–9.
44. Li RT, Lorenz S, Xu Y, Harner CD, Fu FH, Irrgang JJ. Predictors of radiographic knee osteoarthritis after anterior cruciate ligament reconstruction. Am J Sports Med 2011;39:2595–603.
45. van Osch GJ, van der Kraan PM, Vitters EL, Blankevoort L, van den Berg WB. Induction of osteoarthritis by intra-articular injection of collagenase in mice. Strain and sex related differences. Osteoarthritis Cartilage 1993;1:171–7.
46. Ma HL, Blanchet TJ, Peluso D, Hopkins B, Morris EA, Glasson SS. Osteoarthritis severity is sex dependent in a surgical mouse model. Osteoarthritis Cartilage 2007;15:695–700.

Elsevier Editorial System(tm) for Biochemical and Biophysical Research Communications
Manuscript Draft

Manuscript Number:

Title: In-vitro and in-vivo imaging of MMP activity in cartilage and joint injury

Article Type: Regular Article

Keywords: cartilage; in-vivo imaging; MMP activity; MMPSense750; osteoarthritis.

Corresponding Author: Dr. Dominik R Haudenschild, Ph.D.

Corresponding Author's Institution: University of California Davis

First Author: Tomoaki Fukui, M.D., Ph.D.

Order of Authors: Tomoaki Fukui, M.D., Ph.D.; Elizabeth Tenborg; Jasper H Yik, Ph.D.; Dominik R Haudenschild, Ph.D.

1. MMPSense750 is near-infrared fluorescent probe which can detect MMP activity.
2. MMPSense750 can detect human MMP-3, -9, and -13.
3. The reaction kinetics with MMPSense750 were different for the three MMPs.
4. MMPSense750 can reflect MMP activity in cartilage explants.
5. MMPSense750 can visualized real time MMP activity in mouse injured knees.
6. MMPSense750 is convenient tool to evaluate real-time MMP activity non-invasively.

*Manuscript
Click here to view linked References

In-vitro and *in-vivo* imaging of MMP activity in cartilage and joint injury

Tomoaki Fukui, Elizabeth Tenborg, Jasper H. N. Yik, *Dominik R. Haudenschild.

Lawrence J. Ellison Musculoskeletal Research Center, Department of Orthopaedic Surgery, University of California Davis Medical Center, 4635 Second Avenue Suite 2000, Sacramento CA 95817, USA

*Corresponding author:

Dominik R. Haudenschild

Lawrence J. Ellison Musculoskeletal Research Center, Department of Orthopaedic Surgery, University of California Davis Medical Center, 4635 Second Avenue Suite 2000, Sacramento CA 95817, USA

Tel: +1-916-734-5015

Fax: + 1-916-734-5750.

DRHaudenschild@ucdavis.edu

Running title: *In-vitro* and *in-vivo* MMP Imaging

Abstract

Non-destructive detection of cartilage-degrading activities represents an advance in osteoarthritis (OA) research, with implications in studies of OA pathogenesis, progression, and intervention strategies. Matrix metalloproteinases (MMPs) are principal cartilage degrading enzymes that contribute to OA pathogenesis. MMPSense750 is an in-vivo fluorimetric imaging probe with the potential to continuously and non-invasively trace real-time MMP activities, but its use in OA-related research has not been reported. Our objective is to detect and characterize the early degradation activities shortly after cartilage or joint injury with MMPSense750. We determined the appropriate concentration, assay time, and linear range using various concentrations of recombinant MMPs as standards. We then quantified MMP activity from cartilage explants subjected to either mechanical injury or inflammatory cytokine treatment in-vitro. Finally, we performed in-vivo MMP imaging of a mouse model of post-traumatic OA. Our in-vitro results showed that the optimal assay time was highly dependent on the MMP enzyme. In cartilage explant culture media, mechanical impact or cytokine treatment increased MMP activity. Injured knees of mice showed significantly higher fluorescent signal than uninjured knees. We conclude that MMPSense750 detects human MMP activities and can be used for in-vitro study with cartilage, as well as in-vivo studies of knee injury, and can offering real-time insight into the degradative processes that occurring within the joint before structural changes become evident radiographically.

Keywords: cartilage, in-vivo imaging, MMP activity, MMPSense750, osteoarthritis

Introduction

Osteoarthritis (OA) is a degenerative disease of the whole joint organ characterized by cartilage degradation,[1] and the number of OA patients continues to increase, estimated at nearly 27 million in the United States.[2] and there is no effective treatment to prevent OA or restore joints after the onset of OA. At this time, the gold standard for clinical OA diagnosis and evaluation are morphologic assessments, such as radiography[3,4,5], computed tomography (CT)[5,6], and magnetic resonance imaging (MRI)[3,5,6]. These imaging technologies primarily reveal the morphological changes that become evident at the later stages of OA, but do not offer insight into the process of cartilage degradation. As the field of OA research moves toward OA prevention it is becoming important to also measure the biological processes responsible for joint degradation, processes that precede the morphological and structural changes.

It is generally accepted that enzymatic activities contribute to cartilage degradation and loss in OA, and that elevated enzymatic activity precedes morphological joint space narrowing.[7,8] The ability to non-destructively image and quantify enzymatic activity would be an important tool to assess OA initiation and progression, and the efficacy of intervention strategies. While primary OA is considered idiopathic, in post-traumatic OA (PTOA) the time point of OA initiation (trauma) can be easily identified, and this is therefore an appropriate model to study the enzymatic activities during the early phases of OA.

Matrix metalloproteinases (MMPs) are a family of zinc-dependent degradative proteinases with roles in the enzymatic cartilage degradation and OA progression. MMP-mediated degradation of type II collagen fibrils is considered one of the first irreversible steps in OA pathogenesis (reviewed in [9]), and the presence of MMPs correlates with OA symptoms, including joint effusion and pain[10,11]. Although serum level of MMP-3 is used as a biomarker for rheumatoid arthritis (RA), there is no clinically established MMP biomarker for OA[12]. Most studies inves-

tigating MMP activity in OA rely on assays such as ELISA[13,14] or Western Blotting[14,15], and RT-PCR[14,16] to estimate protein levels and mRNA expression, respectively. However, these assays are not suitable for in-vivo use, and can only measure the amount of MMP protein but do not directly assay MMP activity. Direct measurements of MMP activity include zymography[14,16,17] and more recently fluorimetric MMP assays[14,16], but again these assays are generally not suited for *in-vivo* imaging. The development of a method to visualize MMP activities *in-vivo* hence may offer new insight into OA initiation and treatment efficacy.

An *in-vivo* fluorimetric probe was recently developed that allows non-destructive imaging of activity from a broad spectrum of MMPs (MMPSense^{TM}750 FAST PerkinElmer, Inc., Boston, MA). This near-infrared fluorescent probe is a peptide substrate that enables the detection of MMP activities by exhibiting fluorescent signal when cleaved by MMPs[13,15,18]. In-vivo imaging with this reagent has the potential to continuously measure real-time MMP activities non-invasively. This probe has been successfully used to detect tumor progression[13,18] or ischemia reperfusion in brain[15] with *in-vivo* mouse model, but to our best knowledge there is no previous report investigating MMPSense750 for the assessment of MMP activity in cartilage or joint injury. Moreover, although this probe is expected to be utilized for human patients in clinical setting in future, no paper has studied the kinetics of this substrate using human MMPs. The objective of the present study is to investigate the potential of MMPSense750 for detection of human MMPs and to use in an assay with cartilage explants, as well as an *in-vivo* mouse model of knee injury leading to PTOA.

Methods

Assessment of optimal MMPSense750 concentration

We first wanted to determine the appropriate MMPSense750 concentration for *in-vitro* studies using purified recombinant human MMPs. Human MMP-3, -9, and -13 were chosen based on their established importance in OA[11,19,20]. To achieve comparable results between the different enzymes, the amount of active enzyme in each assay was normalized using the specific activity (Units of enzyme activity per weight) provided by the manufacturer (Supplementary information 1). MMPSense750 was added to media containing the active proteases, the reactions were incubated at 37°C, and the resulting fluorescent signal was measured at different time points as described in detail below.

Recombinant human MMP-3 (Enzo Life Sciences, Farmingdale, USA) was reconstituted to various concentrations in assay buffer consisting of 50mM sodium acetate, 10mM $CaCl_2$, 150mM NaCl and 0.05% Brij-35 at pH 6.0.[9] Recombinant human MMP-9 and MMP-13 (Enzo Life Sciences) were reconstituted in the assay buffer consisting of 50mM HEPES, 10mM $CaCl_2$ and 0.05% Brij-35 at pH 7.5.[21]

MMPSense750 (24 nmol per vial) was reconstituted in 1200µl sterile phosphate-buffered saline (Invitrogen) as recommended by the manufacturer, then added into the MMP solutions at 0.2, 0.7 and 2.0µM final concentration. Imaging was performed on an IVIS-Spectrum imaging system at multiple time points for up to 72 hours after adding MMPSense750.

Cartilage explants

Cartilage explants were harvested from the weight-bearing area of the femoral articular surfaces of bovine stifle knee joints purchased from a local slaughterhouse (Petaluma, CA). A 6mm dermal biopsy punch was used to isolate cartilage cylinders, which were then cut to 2mm height from the articular surface using a custom jig. Explants were cultured for 3 days in DMEM with 10% FBS and 1% penicillin-streptomycin (all from Invitrogen, Carlsbad, CA) at 37°C and

5% CO_2. Six joints were used, and 1 or 2 explants from each joint was randomly assigned to one of three treatment groups; IL-1β, mechanical injury, or control. There was no significant difference among the cartilage weights of each group. The IL-1β group was treated with 10ng/ml IL-1β (R&D Systems, Minneapolis, MN). The explants in the mechanical injury group were mechanically compressed with an Instron 8511.20 digital servo-hydraulic mechanical testing device using displacement control. A compressive preload of ~0.5N was applied, and then the explant was loaded to 30% strain at a strain rate of 100%/s, held at 30% strain for 100ms, then unloaded. Following compression, all loaded explants were transferred to fresh culture medium and returned to an incubator at 37°C and 5% CO_2 until the termination of the experiment. In the control group, the explants were given a preload of ~0.5N and then returned to the culture media. The culture media were replenished at day 3. The media were collected at 3 and 6 days after IL-1β stimulation or mechanical injuries. MMPSense750 was added to a final concentration of 0.7μM, and the fluorescence measured at 60 minutes and 24 hours after adding MMPSense.

Animal model of joint injury

Eight adult male BALB/cByJ mice (9-week-old at time of injury) were obtained from Jackson Laboratory (Bar Harbor, Maine). All animals were maintained and used in accordance with National Institutes of Health guidelines on the care and use of laboratory animals. This study was approved by our Institutional Animal Care and Use Committee (IACUC). The right knees of the mice were injured with a single mechanical compression as previously described in our PTOA model [22]. Briefly, the tibial compression system consists of two custom-built loading platens; the bottom platen that holds the knee flexed, and the top platen that holds the heel. The platens were aligned vertically and positioned within an electromagnetic materials testing ma-

chine (Bose ElectroForce 3200) (Eden Prairie, MN). Mice were anesthetized using isoflurane inhalation, then the right leg of each mouse was subjected to a single dynamic axial compression (1mm/s loading rate) to a target load of 12N. This causes a transient anterior subluxation of the tibia, which injures the anterior cruciate ligament and leads to PTOA within 8 weeks. The contralateral uninjured knees served controls, and were used to normalize the data within each animal.

All mice received an injection of 2nmol of MMPSense750 via the orbital sinus at 24-hours post-injury, and IVIS imaging was performed 24 hours after the injection (48-hours post-injury). Mice were euthanized immediately after the imaging and both knees were dissected for isolation of total RNA and analysis of mRNA expression.

Quantitative real-time RT-PCR

Total RNA was extracted from injured and uninjured knees using the miRNeasy Mini Kit (Qiagen Valencia, CA) and reverse transcribed by the QuantiTect Reverse Transcription Kit (Qiagen). 2µl of cDNA was used for quantitative RT-PCR (in a final volume of 10µl) performed in triplicate in a 7900HT RT-PCR system with gene-specific probes according to the manufacturer's conditions. Results were normalized to the 18s rRNA and calculated as fold-change in mRNA expression relative to the untreated control, using the $2^{-\Delta\Delta CT}$ method. The probes used are shown in Supplementary information 2.

IVIS imaging

An IVIS Spectrum imaging system (Perkin Elmer) was utilized to monitor fluorescent signal of MMPSense750. For imaging of media cultured with cartilage explants, the samples were placed in black plates. For *in-vivo* imaging of mice, the hairs from the lower trunk and both

legs were removed, and then imaging was performed under general anesthesia by isoflurane inhalation. The excitation and emission wavelengths were set to 745 and 800nm, respectively. The fluorescence intensities were analyzed by Living Image software 4.2(Perkin Elmer). Grid type and circle type of regions of interest (ROI) were set for plates and mice, respectively. Average radiant efficiency [p/s/cm^2/sr] / [μW/cm^2] in the ROI was measured as an index of intensity of fluorescent signal. For the experiment with MMP enzymes, normalized average radiant efficiency was calculated by subtracting the value of average radiant efficiency with 0(m)U of MMPs from that with each concentration of MMPs and used for the assessment. For the purpose of clarity, we use the term "fluorescence intensity" to indicate normalized average radiant efficiency in the ROI.

Statistical analysis

The results were statistically analyzed using a software package (GraphPad Prism; MDF Software, Inc.). Values of all measurements were expressed as the mean with error bars representing the 95% confidence interval. Correlation between MMP concentration and MMPSense signal was evaluated with Pearson correlation coefficient. Differences of MMPSense signal with MMP enzymes and *in-vivo* study were analyzed by paired t tests. Comparison of MMPSense signal between different concentrations of MMPs and of MMPSense signal with cartilage explants were analyzed by unpaired t test. Comparison of mRNA expression was analyzed by Wilcoxon signed rank test.

Results

Determination of the optimal MMPSense750 concentration for *in-vitro* experiments

To examine how well the normalized fluorescent signal correlated to the MMP activity at each time point, Pearson's correlation coefficients (R) were calculated for each combination of

MMPSense and time (Figure 1). For all MMPs, the best correlation between MMP activity and fluorescent signal occurred at the higher concentrations of MMPSense probe, 0.7 or 2.0μM. Perhaps more surprisingly the best time to measure fluorescence intensity was highly dependent on the types of MMP enzyme. For MMP-13, high correlations were observed as early as 15 minutes, while MMP-3 started to become significant after 60 minutes, and MMP-9 not until after 24 hours. At the later time points the MMP activity and fluorescent signal were highly correlated for all three MMP enzymes.

To estimate the detection limit of the assay at each concentration of MMPSense750 over time, we statistically analyzed the differences between fluorescent intensity for each concentration increase of MMP (Supplementary Figure 1). The intermediate concentrations of MMP generated significantly different fluorescence signal in all conditions, but there were variations in the lower and upper detection limits. With respect to the upper detection limit, we examined the fluorescent signal over time for each enzyme and the higher MMPSense probe concentrations (Figure 2). While higher concentrations of MMPSense yielded greater absolute fluorescence signals, the statistical analysis showed no benefit of the 2μM compared to 0.7μM MMPSense probe.

Taken together, these results indicate that 0.7μM of MMPSense750 at a 24 hour time point would yield the best assay to measure the activities of the three MMPs over the greatest range of concentrations

MMP activity in IL-1β-treated cartilage explants

Three days of IL-1β treatment caused a significant increase in fluorescence intensity of culture media, indicating elevated MMP activity in cartilage explants (Figure 3A). Specifically, the fluorescence signal of the IL-1β group at day 3 was significantly greater than that of the con-

trol group both at 60 minutes and 24 hours after adding MMPSense750. At day 6, fluorescence intensity in the IL-1β-treated group was significantly greater than that of the control group at 24 hours (but not 60 minutes) after adding MMPSense750.

MMP activity in mechanically injured cartilage explants

As observed with the IL-1β treatment, the fluorescence of the mechanical injury group at day 3 was significantly greater than that of the control group at both 60 minutes and 24 hours after adding MMPSense750. At day 6, the trends are similar to the IL-1β treatment, with greater fluorescence at the 24 hour, although this did not reach statistical significance (Figure 3B).

MMP activity *in-vivo* after knee injury

The non-surgical joint injury caused a substantial increase in the fluorescence intensity in the injured right knee relative to the uninjured left knee of the same animal, indicating that injury increased the local MMP activity (Figure 4A). The real-time RT-PCR results showed elevated mRNA expression of MMP-3 in the injured knee at this time point (48 hours after injury), while the expression of MMP-9 and -13 were not statistically different in the injured and contralateral limb at this time point (Figure 4B).

Discussion

Imaging technologies used in OA primarily measure structural morphology rather than the biological processes that contribute to joint degradation. The results in the present study demonstrate that the MMPSense750 is useful with human MMPs, providing insight into the parameters to consider when interpreting the data, and show a good response of the assay in *in-vitro* stu-

dies of cartilage explants and in a mouse model of joint injury. Although there are a few previous reports using MMPSense680, precedent product of MMPSense, to investigate MMP activity in OA or RA with human cartilage or mouse model,[23,24,25] this article is the first studying OA-related assay with cartilage and joint injury using MMPSense750. This is an important contribution because MMPSense680 and MMPSense750 have different substrate specificities and different in-vivo kinetics, and MMPSense750 has the advantage that it enables a shorter time between injection and imaging (6 hours versus 24 hours for MMPSense680). Although human MMPs, bovine cartilage and mice were used in the current study, MMPs share a high degree of orthology among most vertebrates [26,27] and we do not expect significant species-related differences in the substrate-enzyme interactions.

With all MMPs tested, the fluorescent signal increased as the MMP activity increased. Interestingly, the reaction kinetics of the enzymes were different for the three MMPs. Namely, recombinant human MMP-13 caused a rapid increase in fluorescence within 15 minutes even at low enzyme concentrations, and longer incubations past 24 hours decreased the assay linearity. In contrast, human MMP-9 required at least 24 hours to show a dose-dependent increase in substrate activation, and longer incubations out to 3 days improved the assay linearity. Human MMP-3 was intermediate, showing linear response after 1 hour out to 2 days, but decreasing at 3 days. The experiments were all performed within the reported tissue half-life of 72 hours for the MMPSense750 reagent. MMPSense produces fluorescent signal upon MMP-mediated hydrolysis, and the discrepancy of the detection time between MMPs may suggest the kinetics of cleavage differs between MMPs. We examined MMP-3, -9 and -13 in the current study, but according to the manufacturer MMPSense750 can also detect the activities of MMP-2, -7, and -12. In summary, it is important to recognize that a fluorescent signal indicates activities from multiple MMPs with differing sensitivities and reaction kinetics.

The result from cartilage explants assay provides a novel non-destructive method to quantify the MMP activity. At day 6, significantly higher fluorescence was detected in the IL-1β group when compared with the control group, while there was no significant difference between the mechanical injury group and the control group at both 60 minutes and 24 hours after adding MMPSense. A possible reason for this difference could be the continuous presence of IL-1β during the 6 days, compared to a single mechanical injury at day 0.

In the *in-vivo* mouse model, injured knees showed significantly higher signals of MMPSense750 than the contralateral uninjured knees, indicating that MMP activity was elevated 48 hours after injury. This provides a novel real-time non-destructive imaging method to quantify knee injury response and the progression of cartilage degradation and OA based on MMP activity. Interestingly, when we examined MMP mRNA expression at 48 hours after injury, we found that only MMP-3 was still elevated. In a separate study, we found that mRNA up-regulation of MMP expression after injury peaked at 4 hours after injury and returned to baseline after 24 hours using the same animal model (data not shown). MMPs are secreted as inactive pro-enzymes that are later activated in the extracellular matrix, which may explain the apparent discrepancy between the mRNA expression and the protease activity and highlight the importance of quantifying the enzymatic activity.

A limitation of the imaging technology is that we did not have sufficient resolution to determine the exact tissue source of MMP activity. It is likely that MMPs are active in multiple tissues, including cartilage, bone, and synovium. In our explant experiments we were able to detect activity of MMP secreted by cartilage, but not within the cartilage itself. Based on these observations we speculate that the *in-vivo* source of fluorescent signal might be joint tissues other

than cartilage, although this does not preclude the MMP activity in the cartilage. In future experiments we would like to localize the source of MMP activity more precisely.

In conclusion, we established experimental parameters to use the MMPSense750 imaging reagent to quantify MMP activity *in-vitro* in cartilage explants, and *in-vivo* in a mouse joint injury model. The advantages of MMPSense750 over other techniques to evaluate MMP activity include its non-destructive nature, enabling repeated measurements on the same samples. This provides an imaging opportunity to monitor the destructive enzymatic processes that contribute to OA progression, and complements traditional imaging technologies that quantify the resulting structural changes.

Acknowledgements

This work was funded by NIH/NIAMS grant AR063348 to Dominik R. Haudenschild.

The authors declare that they have no competing interests.

Imaging work was performed at the Center for Molecular and Genomic Imaging (CMGI), University of California, Davis. We would like to acknowledge Douglas Rowland and Jennifer Fung for help with the in-vivo and in-vitro imaging on the IVIS-Spectrum instrument.

References

[1] R.F. Loeser, S.R. Goldring, C.R. Scanzello, M.B. Goldring, Osteoarthritis: a disease of the joint as an organ, Arthritis Rheum 64 (2012) 1697-1707.

[2] E. Losina, A.M. Weinstein, W.M. Reichmann, S.A. Burbine, D.H. Solomon, M.E. Daigle, B.N. Rome, S.P. Chen, D.J. Hunter, L.G. Suter, J.M. Jordan, J.N. Katz, Lifetime risk and age at diagnosis of symptomatic knee osteoarthritis in the US, Arthritis Care Res (Hoboken) 65 (2013) 703-711.

[3] T.P. Lozito, R.S. Tuan, Endothelial cell microparticles act as centers of matrix metalloproteinsase-2 (MMP-2) activation and vascular matrix remodeling, J Cell Physiol 227 (2012) 534-549.

[4] K. Yoshida, R.J. Barr, S. Galea-Soler, R.M. Aspden, D.M. Reid, J.S. Gregory, Reproducibility and Diagnostic Accuracy of Kellgren-Lawrence Grading for Osteoarthritis Using Radiographs and Dual-Energy X-ray Absorptiometry Images, J Clin Densitom (2014).
[5] A. Guermazi, F. Eckstein, M.P. Hellio Le Graverand-Gastineau, P.G. Conaghan, D. Burstein, H. Keen, F.W. Roemer, Osteoarthritis: current role of imaging, Med Clin North Am 93 (2009) 101-126, xi.
[6] A. Williams, J.R. Smith, D. Allaway, P. Harris, S. Liddell, A. Mobasheri, Carprofen inhibits the release of matrix metalloproteinases 1, 3, and 13 in the secretome of an explant model of articular cartilage stimulated with interleukin 1beta, Arthritis Res Ther 15 (2013) R223.
[7] L. Troeberg, H. Nagase, Proteases involved in cartilage matrix degradation in osteoarthritis, Biochim Biophys Acta 1824 (2012) 133-145.
[8] P. Verma, K. Dalal, ADAMTS-4 and ADAMTS-5: key enzymes in osteoarthritis, J Cell Biochem 112 (2011) 3507-3514.
[9] P.E. Di Cesare, D.R. Haudenschild, J. Samuels, S.B. Abramson, Pathogenesis of Osteoarthritis, in: G.S. Firestein, W.N. Kelley (Eds.), Kelley's Textbook of Rheumatology, 2013, pp. 1617-1635.
[10] N.M. Cattano, J.B. Driban, E. Balasubramanian, M.F. Barbe, M. Amin, M.R. Sitler, Biochemical comparison of osteoarthritic knees with and without effusion, BMC Musculoskelet Disord 12 (2011) 273.
[11] P.I. Mapp, D.A. Walsh, J. Bowyer, R.A. Maciewicz, Effects of a metalloproteinase inhibitor on osteochondral angiogenesis, chondropathy and pain behavior in a rat model of osteoarthritis, Osteoarthritis Cartilage 18 (2010) 593-600.
[12] H. Yamanaka, Y. Matsuda, M. Tanaka, W. Sendo, H. Nakajima, A. Taniguchi, N. Kamatani, Serum matrix metalloproteinase 3 as a predictor of the degree of joint destruction during the six months after measurement, in patients with early rheumatoid arthritis, Arthritis Rheum 43 (2000) 852-858.
[13] C.P. Hollis, H.L. Weiss, B.M. Evers, R.A. Gemeinhart, T. Li, In Vivo Investigation of Hybrid Paclitaxel Nanocrystals with Dual Fluorescent Probes for Cancer Theranostics, Pharm Res (2013).
[14] M. Hufeland, M. Schunke, A.J. Grodzinsky, J. Imgenberg, B. Kurz, Response of mature meniscal tissue to a single injurious compression and interleukin-1 in vitro, Osteoarthritis Cartilage 21 (2013) 209-216.
[15] P.A. Barber, D. Rushforth, S. Agrawal, U.I. Tuor, Infrared optical imaging of matrix metalloproteinases (MMPs) up regulation following ischemia reperfusion is ameliorated by hypothermia, BMC Neurosci 13 (2012) 76.
[16] M.H. Moon, J.K. Jeong, Y.J. Lee, J.W. Seol, C.J. Jackson, S.Y. Park, SIRT1, a class III histone deacetylase, regulates TNF-alpha-induced inflammation in human chondrocytes, Osteoarthritis Cartilage 21 (2013) 470-480.
[17] R. Schure, K.D. Costa, R. Rezaei, W. Lee, C. Laschinger, H.C. Tenenbaum, C.A. McCulloch, Impact of matrix metalloproteinases on inhibition of mineralization by fetuin, J Periodontal Res 48 (2013) 357-366.
[18] B. Waschkau, A. Faust, M. Schafers, C. Bremer, Performance of a new fluorescence-labeled MMP inhibitor to image tumor MMP activity in vivo in comparison to an MMP-activatable probe, Contrast Media Mol Imaging 8 (2013) 1-11.
[19] U. Vaatainen, L.S. Lohmander, E. Thonar, T. Hongisto, U. Agren, S. Ronkko, H. Jaroma, V.M. Kosma, M. Tammi, I. Kiviranta, Markers of cartilage and synovial metabolism in

joint fluid and serum of patients with chondromalacia of the patella, Osteoarthritis Cartilage 6 (1998) 115-124.
[20] T.P. Misko, M.R. Radabaugh, M. Highkin, M. Abrams, O. Friese, R. Gallavan, C. Bramson, M.P. Hellio Le Graverand, L.S. Lohmander, D. Roman, Characterization of nitrotyrosine as a biomarker for arthritis and joint injury, Osteoarthritis Cartilage 21 (2013) 151-156.
[21] Y.C. Lu, C.H. Evans, A.J. Grodzinsky, Effects of short-term glucocorticoid treatment on changes in cartilage matrix degradation and chondrocyte gene expression induced by mechanical injury and inflammatory cytokines, Arthritis Res Ther 13 (2011) R142.
[22] B.A. Christiansen, M.J. Anderson, C.A. Lee, J.C. Williams, J.H. Yik, D.R. Haudenschild, Musculoskeletal changes following non-invasive knee injury using a novel mouse model of post-traumatic osteoarthritis, Osteoarthritis Cartilage 20 (2012) 773-782.
[23] E.F. Jones, J. Schooler, D.C. Miller, C.R. Drake, H. Wahnishe, S. Siddiqui, X. Li, S. Majumdar, Characterization of human osteoarthritic cartilage using optical and magnetic resonance imaging, Mol Imaging Biol 14 (2012) 32-39.
[24] J. Zhou, Q. Chen, B. Lanske, B.C. Fleming, R. Terek, X. Wei, G. Zhang, S. Wang, K. Li, L. Wei, Disrupting the Indian hedgehog signaling pathway in vivo attenuates surgically induced osteoarthritis progression in Col2a1-CreERT2; Ihhfl/fl mice, Arthritis Res Ther 16 (2014) R11.
[25] C.L. Galligan, E.N. Fish, Circulating fibrocytes contribute to the pathogenesis of collagen antibody-induced arthritis, Arthritis Rheum 64 (2012) 3583-3593.
[26] B.C. Jackson, D.W. Nebert, V. Vasiliou, Update of human and mouse matrix metalloproteinase families, Hum Genomics 4 (2010) 194-201.
[27] I. Massova, L.P. Kotra, R. Fridman, S. Mobashery, Matrix metalloproteinases: structures, evolution, and diversification, FASEB J 12 (1998) 1075-1095.

Figure Legends

Figure 1 Correlation between MMP Activity and MMPSense750 Signal. R^2 (R: Pearson correlation coefficient) as indices of correlation of the relationship between MMPs concentration and fluorescent signals at each time point were shown in tables and figures. R^2 greater than 0.8 were shown in the table with bold letters and shaded background.

Figure 2 Substrate Activation over Time. The normalized average radiant efficiency of the greatest and the second greatest concentration of each MMP with 0.7 or 2.0μM of MMPSense750. p-values vs. the second greatest concentrations at the same time points. (n=3)

Figure 3 Increased MMP Activity in Models of Cartilage Explant Injury. The average radiant efficiency in culture media at day 3 of the IL-β group (A) and the mechanical injury group (B) measured at 60 minutes and 24 hours after adding MMPSense was significantly greater than that of the control group. As for the media collected at day 6, the average radiant efficiency of the IL-1β group measured at 24 hours was significantly greater than the other, while there was no significant difference in the radiant efficiency measured at 60 minutes of the IL-1β group and at 60 minutes and 24 hours of the mechanical injury group compared to the control group. M. Inj.: mechanical injury group, Ctrl: control group. (n=10)

Figure 4 Increased MMP Activity and mRNA in a Mouse Model of Joint Injury

A. Representative IVIS imaging of knees after MMPSense750 injection are shown. The image is a merged picture of fluorescent signal in color and a grayscale picture of the mouse. Blue circles on both knees are ROI with same shape and size as each other. The graph shows that average radiant efficiency in injured knees was significantly higher than the controls. (n=8)
B. mRNA expression of MMP-3 in injured knees were significantly greater than in uninjured knees. No significant difference in MMP-9 and MMP-13 mRNA expression was detected between the knees at this time point. (n=8)

Supplementary Figure 1 Normalized average radiant efficiency from MMPs solution with several concentration at 60 minutes and 24 hours after adding MMPSense750 were shown in graphs. Representative IVIS imaging is shown below each graph with logarithmic scale for average radiant efficiency not normalized average radiant efficiency. Difference between the adjacent nor-

malized average radiant efficiency was analyzed statistically.(n=3) #: normalized average radiant efficiency of MMP concentration required for hydrolysis of equivalent substrate in 1 nmol/minute. (MMP-3: 1mU, MMP-9: 10U, MMP-13: 10U)

Figure1
Click here to download high resolution image

Figure2
Click here to download high resolution image

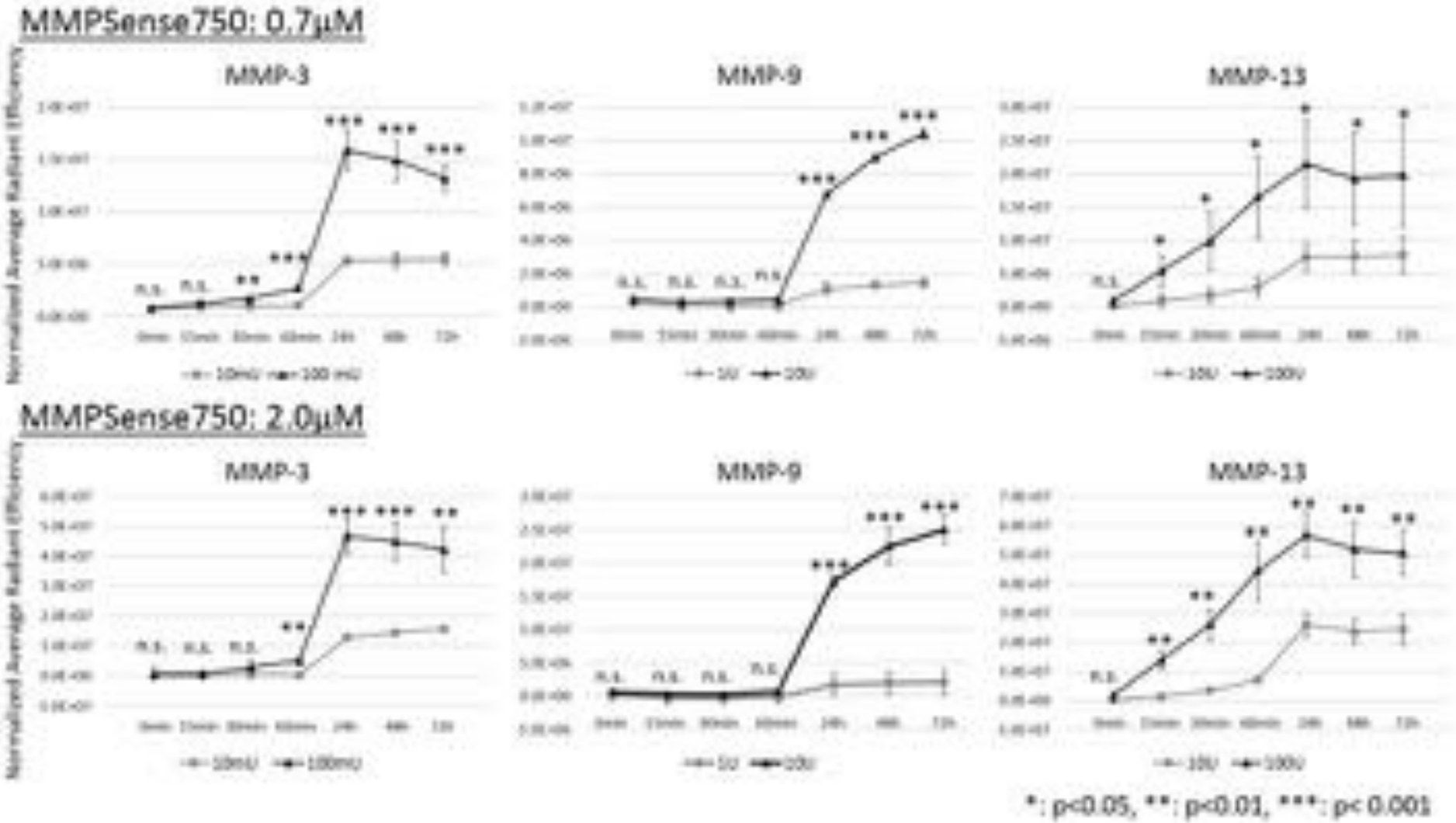

Figure3
Click here to download high resolution image

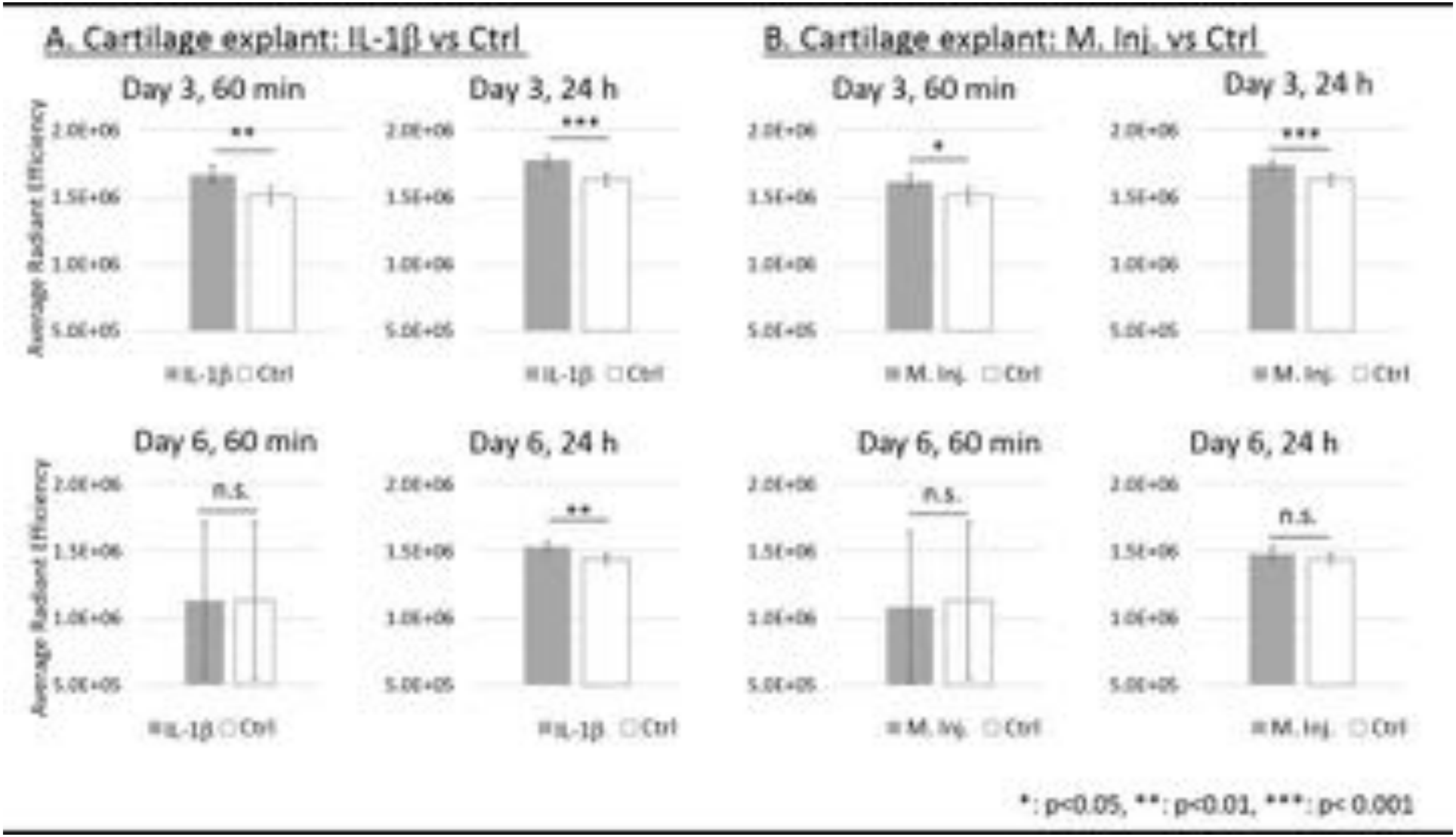

Figure4
Click here to download high resolution image

Running Head:

Title: **Inhibition of CDK9 prevents mechanical injury-induced inflammation, apoptosis, and matrix degradation in cartilage explants**

Authors: Zi'ang Hu, M.D.[1,2,#]

Jasper H. N. Yik, Ph.D. [2,#]

Derek D. Cissell, V.M.D.[3]

Kyriacos A. Athanasiou, Ph.D. [3,1,]

Dominik R. Haudenschild, Ph.D. [2,*]

Grants: Arthritis Foundation 2012 IRG Award to DRH
DOD PRMRP IIRA Award #PR110507 to DRH
R21-AR063348 NIAMS/NIH to DRH
Departmental Startup Funds to DRH
National Natural Science Fund of China (81271971) to ZH
T32 OD 011147 to DDC

No author received any financial support or other benefits from commercial sources for the work reported on in this manuscript, and no author has any other financial interest that could create a potential conflict of interest or the appearance of a conflict of interest with regard to the work.

1, Department of Orthopaedic Surgery,
Sir Run Run Shaw Hospital,
School of Medicine,
Zhejiang University,
Hangzhou, 310016 PR China

2, * Address correspondence to
Dominik R. Haudenschild
University of California Davis
Department of Orthopaedic Surgery
Lawrence J. Ellison Musculoskeletal Research Center
Research Building 1 Suite 2000
4635 Second Avenue
Sacramento, CA 95817
Tel: 916-734-5015
Fax: 916-734-5750
Email: Dominik.Haudenschild@ucdmc.ucdavis.edu

3, Department of Biomedical Engineering,
College of Engineering,
University of California,
Davis, California95618
#These two authors contributed equally

Abstract

Introduction: Joint injury is often associated with the development of post-traumatic osteoarthritis. Mechanical and physical damages to the cartilage and the surrounding joint tissues can induce the expression of pro-inflammatory cytokines (e.g. IL-1, IL-6, and TNF) and catabolic enzymes (e.g. MMPs, ADAMTSs), which promote cartilage matrix degradation and chondrocyte apoptosis. Recent advances have established that the rate-limiting step for the transcriptional activation of primary response genes is controlled by the elongation factor cyclin-dependent kinase 9 (CDK9). Upon inflammatory stimulus, CDK9 is recruited to target genes and phosphorylates RNA Polymerase II to stimulate transcription of full-length mRNAs. Therefore, targeting CDK9 may be an effective strategy to globally and effectively suppress inflammatory response. Our objective in this study is to determine the therapeutic potential of CDK9 inhibition in suppressing the inflammatory response and preventing chondrocyte apoptosis in mechanically injured cartilage explants, thereby preserving their biological and mechanical property. Our study may lead to a novel strategy to protect cartilage from traumatic mechanical injury, and in turn may prevent or delay the onset of post-traumatic osteoarthritis.

Methods: Cartilage explants (6mm diameter by 3mm height) with the articular surfaces intact were harvested from the femoral chondyles of bovine stifled joints and cultured in DMEM+10% FBS for 24 hrs. The explants (n=6/condition) were then mechanically

injured by a single load of 30% strain compression (Bose), and then placed into culturing media with or without 300 nM of the pharmacological CDK9 inhibitor Flavopiridol (Santa Cruz Biotech). At different time points, the explants were harvested for mRNA expression of inflammatory cytokines and catabolic enzymes, as determined by qPCR using gene-specific probes and normalized to 18s rRNA (ABI). Chondrocytes viability was determined by Live/Dead Viability/Cytotoxicity kit (Invitrogen); chondrocytes apoptosis was determined by DeadEnd Fluorometric TUNEL system (Progema) of paraformaldehyde-fixed cartilage sections. Glycosaminoglycan (GAG) released into the culturing media was determined by the dimethylmethylene blue (DMMB) assay. After 4 weeks of culture, mechanical properties were measured in a sample of the cartilage (3mm diameter by 2mm height). A Bose Enduratec instrument was used to apply 10% and 20% compressive strain and custom MatLab software to estimate the instantaneous and relaxation moduli. One-way ANOVA with LSD correction for multiple comparisons within group between conditions was used to determine significance (*: $P<0.05$).

Results: After receiving a single impact loading, the injured explants showed an increase in the mRNA expression of the pro-inflammatory cytokine IL-6, and the catabolic enzymes ADAMTS4 and MMP1 in a time-dependent manner; however, their induction was markedly reduced by the CDK9 inhibitor Flavopiridol (Fig.1, $p<0.05$). In contrast, the baseline expression of IL-6, ADAMTS4 and MMP1 in uninjured controls (Fig 1), and in anabolic genes such as Col2a1 and aggrecan (not shown), was not significantly affected by Flavopiridol. Moreover, mechanical injuries resulted in increased chondrocytes death, and TUNEL staining showed most of them were apoptotic; the mRNA expression of apoptotic genes also proved this. However, this progress was

reduced by Flavopiridol (Fig 2). Mechanical injuries also enhanced the amount of GAG released into the culturing media (Fig 3), but the increase in matrix degradation was reduced to baseline by Flavopiridol (Fig 3). Lastly, the mechanical property of the explants was lowered in the injured group when compared to the control, but was reversed by Flavopiridol (Fig 4). Collectively, these results indicate that CDK9 inhibition by Flavopiridol prevents inflammation-induced apoptosis and protects cartilage from the deleterious effects of mechanical injuries.

Conclusion: Our results demonstrate that CDK9 inhibition by Flavopiridol significantly reduces the inflammatory and apoptotic response in cartilage explants to mechanical injuries. CDK9 inhibition also prevents degradation of GAG in the cartilage matrix and preserves their mechanical properties after injuries. Our data thus indicate that CDK9 is a novel target for preventing the initiation of matrix degradation after mechanical injuries. Further studies are needed to test if Flavopiridol could prevent the onset of post-traumatic osteoarthritis in vivo.

Key words: CDK9, flavopiridol, inflammatory cytokines, chondrocytes, cartilage

Introduction

Osteoarthritis (OA) is a disease characterized by progressive articular cartilage degradation and loss of mechanical properties, joint pain and dysfunction[1, 2]. Although most OA cases are idiopathic, a major risk factor is traumatic joint injury such as an ACL or meniscus tear. Roughly half of the people with these types of knee injury will develop post-traumatic osteoarthritis (PTOA) in 5-20 years[3]. Shortly after an injury, an acute inflammatory response is triggered at the cellular level to prevent infection and to initiate healing. However, excessive inflammation can lead to adverse secondary effects, such as cartilage and subchondral bone erosion that is not detected at the time of injury but becomes apparent a few days later in our mouse knee injury model[4, 5]. Activation of the inflammatory cascade can disrupt joint tissue homeostasis through augmentation of the catabolic response, causing overexpression of extracellular enzymes[6], such as the various matrix metalloproteinases and aggrecanases that degrade the cartilage matrix[7]. In addition, the inflammatory response can also trigger chondrocytes apoptosis[8, 9] that further accelerates cartilage erosion. Therefore, a strategy to prevent excessive inflammation-induced secondary damage after knee injury may prevent or delay the onset of PTOA.

Inflammation is initiated at the cellular level by the activation of the primary response genes involved in the inflammatory process. Recent advances demonstrate that the rate-limiting step in primary response gene activation is controlled by the general transcription factor cyclin-dependent kinase 9 (CDK9). A unique feature of primary response genes is their instant activation upon stimulation without de-novo protein synthesis. In order to achieve instant activation, the basal transcription of primary

response genes is already pre-initiated by RNA Polymerase II (Pol II), even in the absence of inflammatory signals. However, only truncated mRNA transcripts are produced because Pol II is paused shortly after the transcription start site (reviewed in[10, 11]). This promoter proximal pausing of Pol II at a basal resting state is currently recognized as a hallmark for all primary response genes[12] Upon inflammatory signal activation, the transcription factor CDK9 is rapidly recruited to the transcription complex, where it phosphorylates Pol II to induce a conformational change that allows Pol II to overcome promoter pausing and continue to produce full-length mRNA transcripts[10] Hence, the kinase activity of CDK9 is the rate-limiting step, and a common requirement for the activation of all primary response genes. Thus CDK9 represents a novel attractive target to efficiently and effectively inhibit the acute inflammatory response regardless of the source of inflammation.

In a recent report we highlighted the effectiveness of CDK9 inhibitors in protecting chondrocytes and cartilage explants from the catabolic effects of pro-inflammatory cytokines[13]. In the presence of exogenously added inflammatory cytokines, we found that the small molecule CDK9 inhibitor Flavopiridol[14] significantly suppressed the transcriptional activation of inflammatory response genes as well as catabolic genes, resulting in reduced cartilage matrix degradation[13] While this study demonstrates the feasibility of targeting CDK9 as a viable strategy for protecting cartilage from exogenously added pro-inflammatory cytokines, the experimental conditions may not accurately represent the physical damage and inflammatory stimulation that the cartilaginous tissues may experience in the event of an actual traumatic knee injury. Various ex-vivo impact injury models have been used for studying

the effects of mechanical loading on cartilage explants[6-9, 15-17]. Mechanical over-loading in cartilage explants can lead to chondrocyte cell death via both necrosis and apoptosis, and cause an inflammatory/catabolic response that damages the cartilage matrix and alter its physical properties[18, 19]. Therefore, these ex-vivo impact injury models are an invaluable tool to study the injury response in cartilage, since they recapitulate the physical injury and the subsequent biological response in the cartilage during traumatic knee injury.

In this study we examined the therapeutic potential of the CDK9 inhibitor Flavopiridol in a single impact injury model with bovine cartilage explants. The ability of Flavopiridol to prevent the activation of the injury-induced inflammatory and catabolic responses, chondrocytes apoptosis, and cartilage matrix degradation was determined.

Materials and methods

Cartilage explants - Bovine calf stifle joints were obtained from a local slaughterhouse (Petaluma, CA) within 1 day of slaughtering. 6-8 cylindrical cartilage explants were harvested from each femoral condyle with a 6 mm biopsy punch inserted perpendicular to the weight bearing area of the articular surface. The explants were then trimmed into ~3 mm thickness (with the articular surface intact) using a custom measuring block. The explants were washed with phosphate buffered saline and cultured for 24 hours in high-glucose Dulbecco's Modified Eagle's Medium (DMEM) supplemented with 10% fetal bovine serum (Invitrogen), penicillin (1×10^4 units/ml) and streptomycin (1×10^4 ug/ml) at 37 °C, 5% CO_2, and 95% relative humidity.

Single impact ex-vivo injury model - After a 24-hours recovery and equilibration period, the cartilage explants were subjected to a single impact mechanical injury. The precise thickness of the individual explant was measured by a caliper before it was placed onto a custom-built unconfined loading chamber, with the articular surface facing upward. A 20mm diameter stainless steel platen was lowered onto the explant surface to a pre-load of 0.5N (~17.7 kPa). All explants including the uninjured controls were subjected to this 0.5N pre-loading step. To avoid potential variation due to the positional differences from where the explants were harvested on the condyles, two adjacent explants were purposefully matched as a control and injured pair for later comparison. After pre-loading, the Enduratec was then calibrated to deliver to the cartilage explant a single compression of 30% strain in one second, followed by immediate release. After the single impact loading, the explant was sliced in half and weighed. One half of the explant was placed in 3 ml regular media and the other half placed in media containing 300 nM Flavopiridol (Sigma) and cultured for various times (see Fig. 1A). The media was changed every other day with fresh Flavopiridol added. The explants and the culturing media were then subjected to further processing and analysis as described below.

Quantitative real-time PCR - At 2-, 6-, and 24-hours post-injury, the explants were frozen in liquid nitrogen and then pulverized with a pestle and mortar while remained frozen. Total RNA was isolated with the miRNeasy Mini Kit (Qiagen) according to the manufacturer's instruction, with the exception that the RNA was extracted twice with the Qiazol reagents to adequately remove the cartilage matrix constituents. The quantity and quality of the total RNA were determined by a Nanodrop-2000 spectrophometer. 2.5 ug

of total RNA from each sample was used for reverse transcription with the SuperScript First-Strand RT kit (Invitrogen). Individual mRNA expression was determined with quantitative real-time PCR performed in triplicates in a 7900HT system (Applied Biosystem). Results were normalized to the 18s rRNA (cat# 4319413E from Applied Biosystem) and calculated as fold-change in mRNA expression relative to control, using the $2^{-\Delta\Delta CT}$ method. Probes used for individual bovine genes were custom made from Integrated DNA Technologies.

Chondrocyte viability – The live and dead cells in the explants 5 days after mechanical injury were stained using a Live/Dead Viability/Cytotoxicity kit (catalog no. L3224; Invitrogen) according to the manufacturer's protocol. The percentages of live and dead cells were determined by counting the cell numbers in 3 random fields of the cross-sectional images of the explants (n=6 for each sample group) captured using a Nikon TE2000 inverted fluorescence microscope and a 20x objective.

Staining for apoptotic cells – After 1, 3, and 5 days after injury, the explants were fixed with 4% paraformaldehyde for 24 hours and transferred to 75% ethanol, followed by sectioning for histological analysis. In situ detection of apoptosis was performed on 5 um-thick whole explant cross-section using the DeadEnd Fluorometric TUNEL system kit (Promega). This kit measures the fragmented DNA of apoptotic cells by catalytically incorporating fluorescein-12-dUTP at 3'-OH DNA ends using the Terminal Deoxynucleotidyl Transferase recombinant enzyme (rTdT). All nuclei were also counter stained with DAPI. The sections were then mounted and examined under a fluorescence microscope. Percent apoptotic cells (n=3 different donors) was determined by counting the number of TUNEL positive cells (green) and calculated as a percentage of the total

cells (DAPI). Sections incubated with DNase I were used as positive control while those incubated with buffer only were used as negative control.

GAG release – At 5-days post-injury, the culturing media was collected and the amount of glycosylaminoglycan (GAG) present was determined by the dimethyl-methylene blue (DMMB) colorimetric assay with chondroitin sulfate as the standard. Total GAG released into the medium was calculated and normalized to the wet weight of the explant (determined at the day of injury).

Cartilage mechanical properties – To test if CDK9 inhibition preserves the mechanical properties of cartilage explants after injury, injured and control explants were cultured for 4 weeks in media with or without Flavopiridol. Cartilage sample compressive properties were assessed by stress-relaxation testing in unconfined compression using a mechanical testing system (Instron 5565, Norwood, MA). Prior to testing, a 3mm diameter, 2mm thick compression sample was prepared using a dermal biopsy punch, then placed in phosphate buffered saline and centered beneath a 16mm stainless steel platen. The platen was slowly lowered until a preload of 0.2N was observed, indicating contact between the platen and the cartilage sample. The sample was then preconditioned via fifteen cycles of 5% strain. All strains, including the preconditioning, were applied at a strain rate of 10% per second. Immediately following preconditioning, the sample was subject to 10% compressive strain; the 10% strain was held constant and the load recorded for 380 seconds. At the end of the 10% strain application, the compressive strain was increased to 20% and held constant while the load was recorded for an additional 530 seconds. The compressive properties- instantaneous modulus, relaxation modulus, and coefficient of viscosity- were calculated from the individual stress-relaxation curves using data analysis

software (MATLAB R2013a, Natick, MA) according to a standard linear solid model of viscoelasticity as previously described {Allen, K.D. and K.A. Athanasiou, 2006, Journal of Biomechanics. This mechanical test and model were chosen for their simplicity and accuracy in approximating the viscoelastic behavior of cartilage.

Statistical analysis - Values of all measurements were expressed as the mean +/- standard deviation. Changes in gene expression were analyzed by one-way ANOVA with SPSS 16.0 software. The fold-change in mRNA was used as variables to compare samples between different treatment groups. The least significant difference post-hoc analysis was conducted with a significance level of $P<0.05$.

Changes in compressive properties were analyzed by one-way ANOVA with Tukey's *post hoc* test using JMP Pro software (version 11.2.0) with a significance level of $P<0.05$.

Results

CDK9 inhibition suppresses injury-induced pro-inflammatory and catabolic genes - CDK9 controls the rate-limiting step of inflammatory gene activation [14, 15] and we have previously shown that in vitro CDK9 inhibition protects chondrocytes and cartilage from the catabolic effects of exogenously added pro-inflammatory cytokines [10]. However, the effects of CDK9 inhibition on cartilage that receives a direct impact injury, similar to what may happen in a knee injury, have not been examined. We hypothesize that CDK9 inhibition in mechanically injured cartilage will prevent an inflammatory response, this in turn will reduce the subsequent deleterious effects on chondrocytes and the cartilage matrix. To test our hypothesis, bovine cartilage explants were mechanically

injured by subjecting them to an impact loading at a 30% strain rate (Fig 1A). This magnitude of loading has been shown to induce chondrocyte apoptosis and cartilage matrix degradation [8, 9, 15, 18]. The injured explants were then cultured in media in the presence or absence of 300 nM CDK9 inhibitor Flavopiridol for various times. The mRNA expression of inflammatory cytokines and catabolic genes were then determined by qPCR. The results showed that the mRNA expression of the pro-inflammatory cytokine IL-1 □ was induced i controls (C) at the 2- and 24-hour time points (Fig 1B, open bars), while the addition of Flavopiridol reduced the induction of IL-1b mRNA by injury (Fig 1B, grey bars). This effect was more pronounce in the expression of IL-6 mRNA, which was significantly induced by injury at all time point tested (Fig 1C, open bars), but the IL-6 induction was markedly suppressed by Flavopiridol (Fig. 1C, grey bars). These data indicate that as expected, CDK9 inhibition in cartilage explants suppresses inflammatory cytokine induction in response to mechanical injury.

We next examined the mRNA expression of the catabolic genes MMP-1 and MMP-13, and ADAMTS4, which are induced by inflammatory cytokines and degrade the cartilage matrix. The results showed that when compared to uninjured controls, injury induced MMP-1 and ADAMTS4 expression significantly at all time points, and MMP-13 at the 2-hour time point (Fig 1D-F, open bars). However, CDK9 inhibition effectively prevented the induction of these genes in the injured samples at all time points tested (Fig 1D-F, grey bars). In contrast, the mRNA expression of the anabolic genes Aggrecan and Col2a1 were not affected by injury whether or not Flavopiridol is present (Fig 1G-H).

Taken together, these results indicate that CDK9 inhibition suppressed injury-induced expression of pro-inflammatory cytokines and catabolic genes, while the basal levels of anabolic genes are not affected by either injury or Flavopiridol.

CDK9 inhibition reduces injury-induced chondrocyte apoptosis – Besides inducing an inflammatory response, mechanical injury also causes chondrocytes apoptosis in cartilage explants[8, 9, 15, 18], we therefore investigated the effects of CDK9 inhibition on apoptosis using our explant injury model. The mRNA expression of three selected genes (P53, Bcl-2 and PTEN) central to the apoptotic process were examined in the cartilage explants 24-hour post-injury. P53 initiates apoptosis when DNA damage is irreparable [20], Bcl-2 is the founding member of anti-apoptotic factors [21]and PTEN is a crucial regulator of apoptosis [22]. The results showed that mechanical injury itself did not significantly change the mRNA expression of P53, Bcl-2, and PTEN (Fig 2, open bars). However, Flavopiridol significantly decreased the expression of these three apoptotic mediators in both the injured and uninjured groups (Fig 2, grey bars), thus reducing the basal levels of these apoptotic mediators. This result has prompted us to directly examine the apoptotic chondrocytes in the cartilage explant harvested 5-day post-injury. The cross section of the entire explant with TUNEL (green) with nuclei counter stain (blue) was shown in Fig 3A. As expected, when compared to the uninjured explant (Fig 3A, left panel), a significant increase in apoptotic cells was detected in the injured sample, especially around the center of the explant (Fig 3A, middle panel). In contrast, Flavopiridol treatment markedly reduced the number of apoptotic cells in the explant (Fig 3A, right panel). Next, multiple explants from three different donors collected at 1-, 3-,

and 5-day post-injury were examined by TUNEL stain and the percentage of apoptotic cells relative to the total number of nuclei in each sample was determined. The results showed that injury increased the percentage of apoptotic chondrocytes at day 1 to ~ 20%, and that percentage further increased significantly in day 3 (~60%) and day 5 (~65%) injured explants (Fig 3B). In contrast, CDK9 inhibition significantly reduced the percentage of apoptotic cells in the injured explants in all time points tested (Fig 3B). These results were further collaborated by the data on live/dead staining of cartilage explants collected 5-day post-injury (Fig 3C). The live/dead stain showed that injury significantly reduced the number of live chondrocytes from ~80% to ~55% (Fig 3C, open bars). On the other hand, Flavopiridol treatment did not affect cell survival in uninjured explants but enhanced cell survival in the injured explants (Fig 3C, grey bars). Taken together, the above results indicate that CDK9 inhibition prevents injury-induced apoptosis in cartilage explants and enhance chondrocyte survival after impact injury.

CDK9 inhibition prevents injury-induced cartilage matrix degradation – Since injury induced catabolic response leads to upregulation of matrix degrading enzymes that damage the cartilage matrix, we next investigated if CDK9 inhibition could prevent cartilage matrix degradation after injury. The cartilage explants were continuously cultured for 5 days in the presence or absence of 300 nM Flavopiridol after injury, the culturing media was then collected and the GAG content determined as a measure of matrix degradation. The data showed that GAG released into the media was significantly increased after injury (Fig 4, open bars); however, the concentration of GAG was reduced

to baseline level by Flavopiridol. This result indicates that the CDK9 inhibition prevents cartilage matrix degradation induced by mechanical injury.

CDK9 inhibition preserves the mechanical properties of cartilage explants after injury - Compressive properties of the cartilage explants following four weeks of culture demonstrate increased 10% relaxation modulus, 10% instantaneous modulus, and 10% coefficient of viscosity in samples treated with Flavopiridol compared to injured, untreated samples (Fig 5). Similar results were observed for the moduli and coefficients of viscosity calculated from the 20% strain stress-relaxation curves (not shown). The positive effect of Flavopiridol on compressive properties was observed in both injured and uninjured cartilage samples; no significant difference was observed for any compressive property between injured and uninjured cartilage samples when treated with Flavopiridol. Although injured, untreated cartilage samples exhibited the lowest compressive properties among all groups, there was no significant difference between injured and uninjured cartilage samples in the absence of Flavopiridol. Interestingly, cartilage samples treated with Flavopiridol exhibited greater relaxation moduli than untreated, uninjured controls. Furthermore, injured cartilage samples treated with Flavopiridol also have greater instantaneous moduli and coefficients of viscosity than untreated, uninjured controls. These results indicate that Flavopiridol has a beneficial effect on the compressive properties of cartilage samples cultured *in vitro*.

Discussion

This study examined the effects of CDK9 inhibition on the biological and mechanical properties of cartilage explants after loading injury, which caused a significant induction of pro-inflammatory cytokines (IL-1 -6) and matrix degrading enzymes (MMP-1, MMP-13 and ADAMTS4) (Fig 1) within the first 24 hours. Although apoptotic genes were unchanged within this period (Fig 2), apoptotic chondrocytes could be detected in the explants at 1 day following injury and peaked after 5 days (Fig 3). Injury also accelerated cartilage matrix degradation in terms of GAG release (Fig 4) and deteriorated the mechanical properties of the explants (Fig 5). However, CDK9 inhibition by Flavopiridol suppressed all those changes, thus effectively protecting the chondrocytes and the cartilage from the harmful effects of physical injury and the inflammatory response that follows.

Flavopiridol has a beneficial effect on the compressive, viscoelastic properties of cartilage explants after four weeks of culture. Specifically, both injured and uninjured cartilage samples treated with Flavopiridol have increased stiffness upon initial compression (instantaneous modulus) and upon reaching equilibrium during prolonged static compression (relaxation modulus) compared to injured, untreated samples. The increased instantaneous and relaxation moduli are likely associated with preservation of glycosaminoglycans (GAG) in the cartilage extracellular matrix (ECM) and of the elastic stiffness of the ECM, respectively. Furthermore, injured samples treated with Flavopiridol exhibit a slower rate of relaxation toward equilibrium following compression compared to injured, untreated samples as evidenced by a greater coefficient of viscosity in the treated samples. An increased coefficient of viscosity is also likely associated with retention of GAG in the ECM, which resists movement of water out of

cartilage during compression. Overall, treatment with Flavopiridol maintains the viscoelastic, compressive properties of cultured cartilage samples close to values observed for uncultured native cartilage samples. Flavopiridol may preserve cartilage mechanical properties *in vivo* following injury as well as *in vitro* during culture.

The lack of difference between injured cartilage explants and uninjured control explants was an unexpected finding of this study. Although the injured explants cultured without Flavopiridol had the lowest instantaneous modulus and coefficient of viscosity among all treatment groups, the difference between injured and uninjured samples was not statistically significant ($P > 0.05$). Cartilage degradation and loss of GAG known to occur during prolonged culture of immature cartilage[23] may have caused the loss of cartilage compressive properties observed in the untreated, uninjured cartilage explants. We suspect that testing samples after shorter culture duration may demonstrate a greater difference between the injured and uninjured cartilage.

A high incidence of OA is associated with traumatic knee injury and hence the term post-traumatic OA (PTOA). Although the pathology of the development of PTOA from injury remains unclear, several lines of evidence point to the involvement of the inflammatory response in this process. Elevated levels of the inflammatory cytokines IL-1 [6] and IL- detected in the human joints within 24 hours after an ACL injury[24]. Ko et al demonstrate that inflammation and the accompanying dysregulated cytokines activities likely contribute to the disruption of the balance between anabolism and catabolism in OA[25]. In vitro and in vivo studies have implicated pro-inflammatory cytokines, particularly IL-1 [25, 26]. In the destruction of articu cartilage, chondrocytes are the main target of pro-inflammatory cytokines, which

dysregulate the expression of catabolic and anabolic genes. Cytokine-stimulated chondrocytes produce a variety of matrix-degrading enzymes, like MMP-1, -3, -13 and the aggrecanase ADAMTS-4, -5[6, 27]. All these data suggest implicate the involvement of the inflammatory response in cartilage matrix degradation.

Our results demonstrate that in cartilage explants single impact injury model, CDK9 inhibition by Flavopiridol effectively suppressed the acute response of pro-inflammatory cytokines IL-1b and IL-6, as well as catabolic genes that contribute to the degradation of the cartilage matrix. IL-1b, IL-6, ADAMTS-4 and MMP-1 expression in this study showed an increase with time-dependent manner, with their peak at 24 hours. 300 nM Flavopiridol tremendously suppressed the induction and almost return to baseline. Meanwhile, neither of the two selected anabolic genes, aggreacan and col2a1, was impacted by mechanical injury or Flavopiridol treatment.

The influences of mechanical injury on chondrocytes anabolic gene expression are still controversial. It has been reported that Il-1b suppresses the expression of Col2a1 in chondrocytes in vitro[28], however, evidence of anabolism in OA studies, on the other hand, showed enhanced aggrecan and col2a1 gene expression and biosynthesis in human osteoarthritic cartilage compared to normal cartilage[29, 30]. Our results showed no significant change of anabolic gene expression in injured cartilage in the early 24 hours, which is supported by lately large-scale expression profiling studies use full-thickness cartilage like us, demonstrating that many anabolic genes, including clo2a1, are only enhanced in late-stage OA[31, 32]. More importantly, our result for the first time demonstrates that Flavopiridol has no impact on anabolic gene expression in the first 24 hours after mechanical injury.

Mechanical loading and inflammation in joints cause responsive protein synthesis, which not only stimulate the production of enzymes that break down the cartilage but also impair the ability of the chondrocytes to repair the damage[33]. D'Lima et al created a single mechanical injury model at 30% strain using full-thickness cartilage explants, 34% percent of apoptotic chondrocytes were observed at 96 hours in injured group when compare to 4% apoptosis in the non-loaded group[8]. In fact, OA is characterized by the destruction of the articular cartilage due to dysregulation of chondrocytes, and the change in the homeostatic control of synthesis and degradation of matrix components[34, 35]. So it is possible that loss of chondrocytes following injury impairs the ability of the cartilage to maintain or repair the extracellular matrix[15].

Theoretically, if chondrocytes apoptosis can be shown to play a role in cartilage degeneration following joint injury, then the development of drugs designed to block this self destructive mechanism could help minimize cartilage degeneration[8, 15]. D'Lima et al treated mechanical injured explants with z-vad.fmk, which is a caspase inhibitor, a 50% percent reduction of in apoptosis rate was seen[8]. However, little study has been seen focused on correlation between injury induced early stage inflammation and followed apoptosis. Pro-inflammatory cytokines like IL-1b and IL-6 have the capacity to activate a diverse array of intracellular signaling pathways such as JNK, p38 MAPK and NF-kB[33], and further induce the expression of various pro-apoptotic genes like p53[20], BCL-2 [21]and PTEN[22]. In chondrocytes, JNK and p38 signaling pathway are thought to be pro-apoptotic post-injury[9]. Our results in this study further demonstrate that the enhancement of IL-1b and IL-6 expression was followed by a remarkably increase of

chondrocytes apoptosis, and suppression of those pro-inflammatory cytokines with CDK9 inhibition by Flavopiridol, rescued chondrocytes from apoptosis significantly.

In contrast to the anti-apoptosis property in this study, Flavopiridol has been reported to pro-apoptotic in many cancer cells. Notably. Flavopiridol was originally known for its anti-proliferation properties by suppressing cell-cycle progression in rapidly dividing cells (e.g. cancers)[14]. Chondrocyte, as the unique cellular component of avascular cartilage tissue and maintain low-turnover replacement of the extracellular matrix, do not normally divide[26]. Thus, chondrocyte itself was not influenced by Flavopiridol, which was also supported by our anabolic gene expression determination.

In summary, out data for the first time demonstrated the effectiveness of CDK9 inhibition in the suppression of pro-inflammatory cytokine induced by mechanical injury and prevention of chondrocyte apoptosis in cartilage explants. In addition, our data strongly indicate that Flavopiridol is an effective agent to prevent cartilage degradation and save cartilage mechanical properties. Thus CDK9 inhibition by Flavopiridol may provide a new strategy to prevent or delay OA.

Competing interest

The authors declare that they have no competing interest.

Acknowledgements

This study was supported by an Arthritis Foundation 2012 IRG award to DRH, a DOD PRMRP IIRA award #PR110507 to DRH, R21-AR063348 from NIAMS/NIH to DRH, Departmental Funds to BAC and DRH, and the National Natural Science Fund of China (81271971) to ZH

References

1. Blumberg, T.J., R.M. Natoli, and K.A. Athanasiou, Effects of doxycycline on articular cartilage GAG release and mechanical properties following impact. Biotechnol Bioeng, 2008. 100(3): p. 506-15.
2. Guilak, F., et al., The role of biomechanics and inflammation in cartilage injury and repair. Clin Orthop Relat Res, 2004(423): p. 17-26.
3. Lohmander, L.S., et al., The long-term consequence of anterior cruciate ligament and meniscus injuries: osteoarthritis. Am J Sports Med, 2007. 35(10): p. 1756-69.
4. Christiansen, B.A., et al., Musculoskeletal changes following non-invasive knee injury using a novel mouse model of post-traumatic osteoarthritis. Osteoarthritis Cartilage, 2012. 20(7): p. 773-82.
5. Lockwood, K.A., et al., Comparison of loading rate-dependent injury modes in a murine model of post-traumatic osteoarthritis. J Orthop Res, 2014. 32(1): p. 79-88.
6. Lee, J.H., et al., Mechanical injury of cartilage explants causes specific time-dependent changes in chondrocyte gene expression. Arthritis Rheum, 2005. 52(8): p. 2386-95.
7. Imgenberg, J., et al., Estrogen reduces mechanical injury-related cell death and proteoglycan degradation in mature articular cartilage independent of the presence of the superficial zone tissue. Osteoarthritis Cartilage, 2013. 21(11): p. 1738-45.
8. D'Lima, D.D., et al., Human chondrocyte apoptosis in response to mechanical injury. Osteoarthritis Cartilage, 2001. 9(8): p. 712-9.
9. Rosenzweig, D.H., et al., Mechanical injury of bovine cartilage explants induces depth-dependent, transient changes in MAP kinase activity associated with apoptosis. Osteoarthritis Cartilage, 2012. 20(12): p. 1591-602.
10. Hargreaves, D.C., T. Horng, and R. Medzhitov, Control of inducible gene expression by signal-dependent transcriptional elongation. Cell, 2009. 138(1): p. 129-45.
11. Zippo, A., et al., Histone crosstalk between H3S10ph and H4K16ac generates a histone code that mediates transcription elongation. Cell, 2009. 138(6): p. 1122-36.
12. Fowler, T., R. Sen, and A.L. Roy, Regulation of primary response genes. Mol Cell, 2011. 44(3): p. 348-60.
13. Yik, J.H., et al., Cyclin-dependent kinase 9 inhibition protects cartilage from the catabolic effects of proinflammatory cytokines. Arthritis Rheumatol, 2014. 66(6): p. 1537-46.
14. Wang, L.M. and D.M. Ren, Flavopiridol, the first cyclin-dependent kinase inhibitor: recent advances in combination chemotherapy. Mini Rev Med Chem, 2010. 10(11): p. 1058-70.
15. Borrelli, J., Jr., et al., Induction of chondrocyte apoptosis following impact load. J Orthop Trauma, 2003. 17(9): p. 635-41.
16. Ni, W., et al., Flavopiridol pharmacogenetics: clinical and functional evidence for the role of SLCO1B1/OATP1B1 in flavopiridol disposition. PLoS One, 2010. 5(11): p. e13792.
17. Ko, F.C., et al., In vivo cyclic compression causes cartilage degeneration and subchondral bone changes in mouse tibiae. Arthritis Rheum, 2013. 65(6): p. 1569-78.
18. Hembree, W.C., et al., Viability and apoptosis of human chondrocytes in osteochondral fragments following joint trauma. J Bone Joint Surg Br, 2007. 89(10): p. 1388-95.
19. Murray, M.M., D. Zurakowski, and M.S. Vrahas, The death of articular chondrocytes after intra-articular fracture in humans. J Trauma, 2004. 56(1): p. 128-31.
20. Amaral, J.D., et al., The role of p53 in apoptosis. Discov Med, 2010. 9(45): p. 145-52.
21. Czabotar, P.E., et al., Control of apoptosis by the BCL-2 protein family: implications for physiology and therapy. Nat Rev Mol Cell Biol, 2014. 15(1): p. 49-63.

22. Zheng, T., et al., PTEN- and p53-mediated apoptosis and cell cycle arrest by FTY720 in gastric cancer cells and nude mice. Journal of Cellular Biochemistry, 2010. 111(1): p. 218-228.
23. Bian, L., et al., Effects of dexamethasone on the functional properties of cartilage explants during long-term culture. Am J Sports Med, 2010. 38(1): p. 78-85.
24. Irie, K., E. Uchiyama, and H. Iwaso, Intraarticular inflammatory cytokines in acute anterior cruciate ligament injured knee. Knee, 2003. 10(1): p. 93-6.
25. Goldring, M.B. and F. Berenbaum, The regulation of chondrocyte function by proinflammatory mediators: prostaglandins and nitric oxide. Clin Orthop Relat Res, 2004(427 Suppl): p. S37-46.
26. Kobayashi, M., et al., Role of interleukin-1 and tumor necrosis factor alpha in matrix degradation of human osteoarthritic cartilage. Arthritis Rheum, 2005. 52(1): p. 128-35.
27. Nishimuta, J.F. and M.E. Levenston, Response of cartilage and meniscus tissue explants to in vitro compressive overload. Osteoarthritis Cartilage, 2012. 20(5): p. 422-9.
28. Okazaki, K., et al., CCAAT/enhancer-binding proteins beta and delta mediate the repression of gene transcription of cartilage-derived retinoic acid-sensitive protein induced by interleukin-1 beta. J Biol Chem, 2002. 277(35): p. 31526-33.
29. Bau, B., et al., Bone morphogenetic protein-mediating receptor-associated Smads as well as common Smad are expressed in human articular chondrocytes but not up-regulated or down-regulated in osteoarthritic cartilage. J Bone Miner Res, 2002. 17(12): p. 2141-50.
30. Hermansson, M., et al., Proteomic analysis of articular cartilage shows increased type II collagen synthesis in osteoarthritis and expression of inhibin betaA (activin A), a regulatory molecule for chondrocytes. J Biol Chem, 2004. 279(42): p. 43514-21.
31. Aigner, T., et al., Large-scale gene expression profiling reveals major pathogenetic pathways of cartilage degeneration in osteoarthritis. Arthritis Rheum, 2006. 54(11): p. 3533-44.
32. Ijiri, K., et al., Differential expression of GADD45beta in normal and osteoarthritic cartilage: potential role in homeostasis of articular chondrocytes. Arthritis Rheum, 2008. 58(7): p. 2075-87.
33. Goldring, M.B., et al., Roles of inflammatory and anabolic cytokines in cartilage metabolism: signals and multiple effectors converge upon MMP-13 regulation in osteoarthritis. Eur Cell Mater, 2011. 21: p. 202-20.
34. Goldring, M.B. and K.B. Marcu, Cartilage homeostasis in health and rheumatic diseases. Arthritis Res Ther, 2009. 11(3): p. 224.
35. Goldring, M.B., et al., Defining the roles of inflammatory and anabolic cytokines in cartilage metabolism. Ann Rheum Dis, 2008. 67 Suppl 3: p. iii75-82.

Fig 1

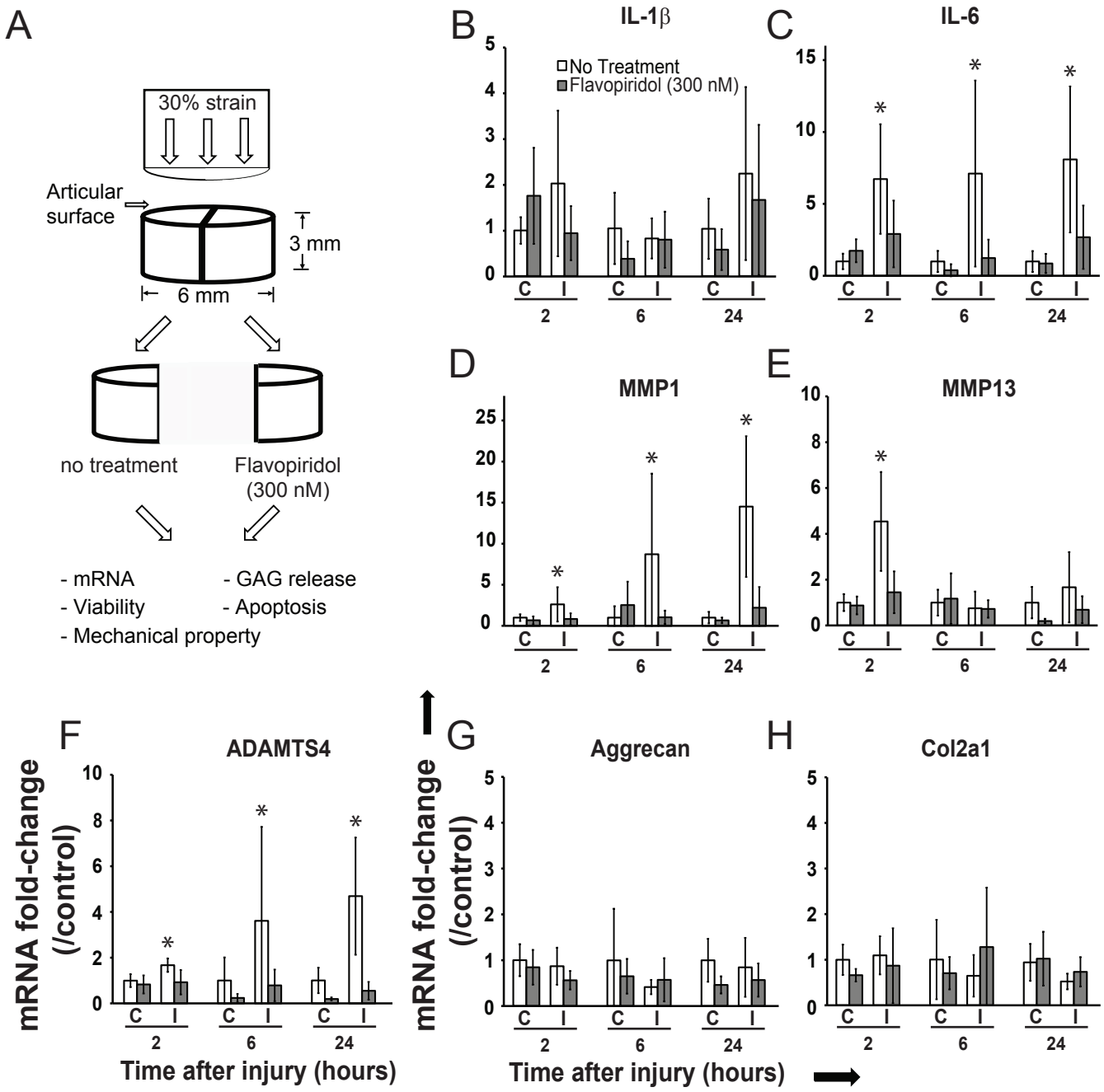
A
30% strain
Articular surface
3 mm
6 mm
no treatment
Flavopiridol (300 nM)
- mRNA
- Viability
- Mechanical property
- GAG release
- Apoptosis
B
IL-1β
No Treatment
Flavopiridol (300 nM)
C
IL-6
D
MMP1
E
MMP13
F
ADAMTS4
G
Aggrecan
H
Col2a1
mRNA fold-change (/control)
C I
2
6
24
Time after injury (hours)

Fig 2

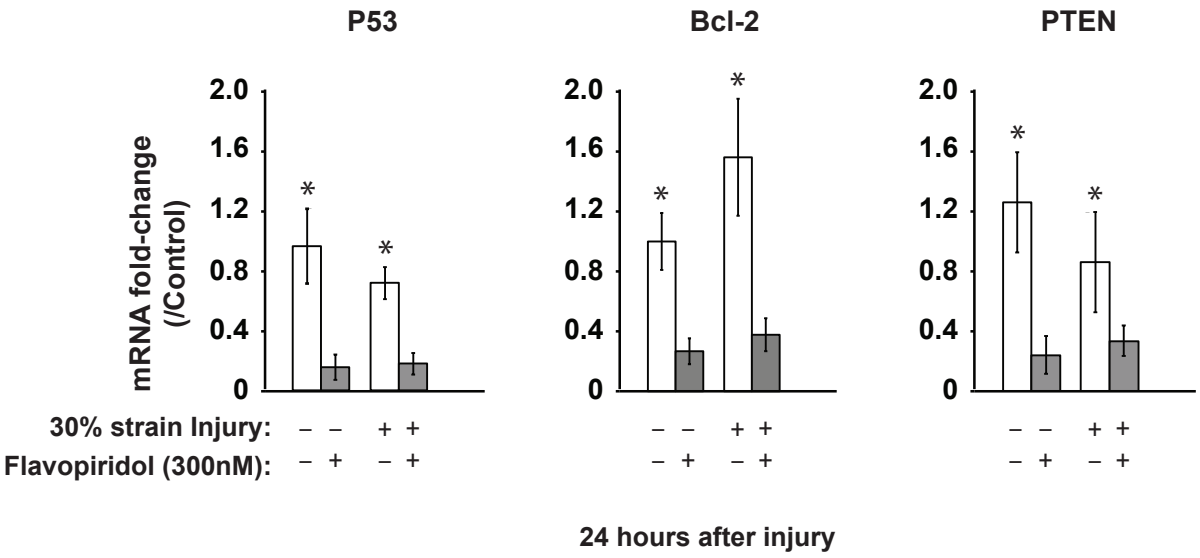
P53
Bcl-2
PTEN
mRNA fold-change (/Control)
2.0
1.6
1.2
0.8
0.4
0
*
30% strain Injury: – – + +
Flavopiridol (300nM): – + – +
24 hours after injury

Fig 3

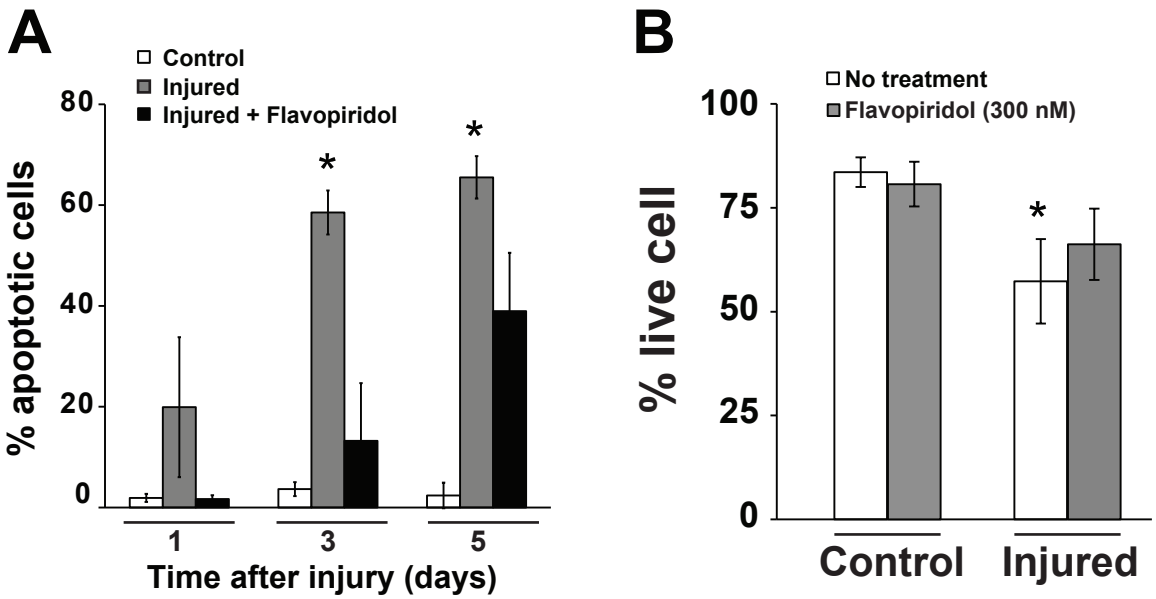
A
Control
Injured
Injured + Flavopiridol
% apoptotic cells
80
60
40
20
0
*
*
1
3
5
Time after injury (days)
B
No treatment
Flavopiridol (300 nM)
% live cell
100
75
50
25
0
*
Control
Injured

Fig 4

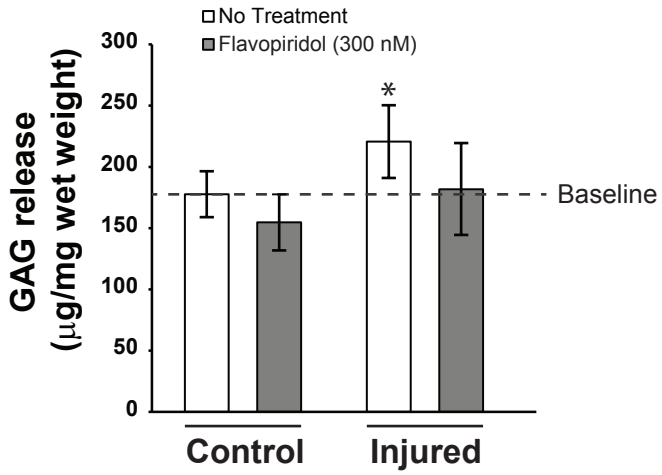
No Treatment
Flavopiridol (300 nM)
GAG release
(μg/mg wet weight)
300
250
200
150
100
50
0
*
Baseline
Control
Injured

Figure 5. Effect of Flavopiridol on compressive properties of cartilage explants following four weeks of culture after injury.

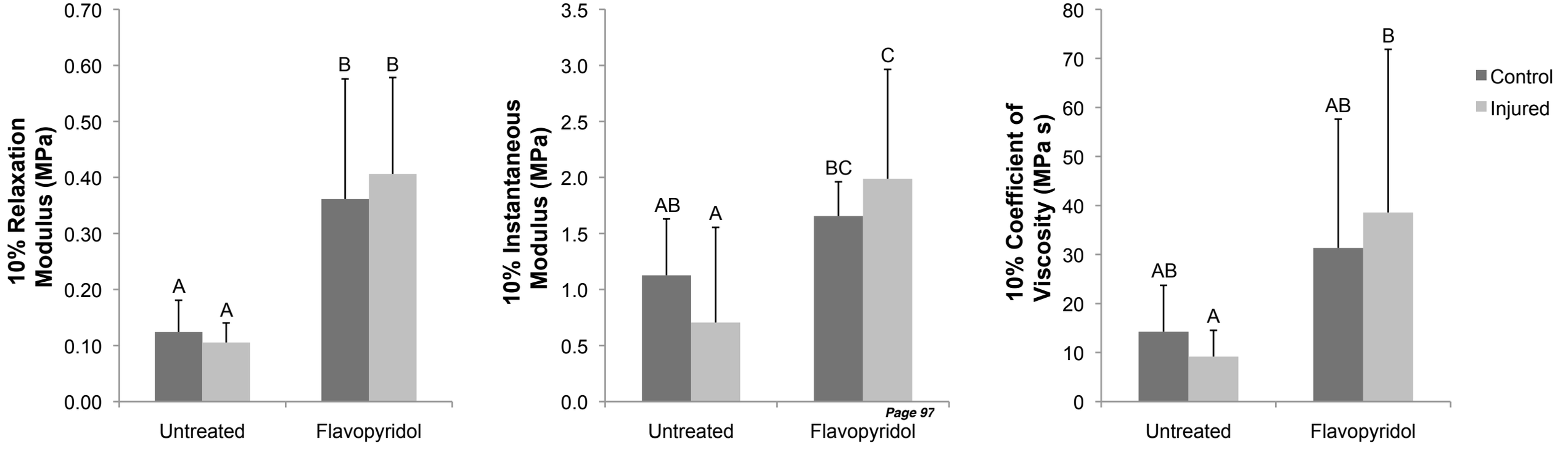

Cdk9 Inhibitors Preserve the Mechanical Properties of Osteochondral Explants After Prolonged Storage

Yik, J.H.N.; Liu, N.; Shidara, K.; Cissell, D.; Athanasiou, K.A.; and Haudenschild, D. R.

Department of Orthopaedic Surgery, UC Davis Medical Center, Sacramento, CA
Dominik.haudenschild@ucdmc.ucdavis.edu

Introduction: Osteochondral allograft transplantations are becoming increasingly popular for the treatment of articular cartilage lesions. A major challenge in this technology is maintaining cell viability and cartilage matrix integrity during extended storage. Cellular and inflammatory stress is introduced during the harvesting and prolonged storage of osteochondral tissues, leading to activation of primary inflammatory response genes that causes cell death and catabolic matrix degradation. Numerous studies using inhibitors of caspases or pro-inflammatory cytokines to better preserve osteochondral tissues have met with varying degrees of success. Recent studies reveal that the rate-limiting step in transcriptional activation of inflammatory response genes is control by cyclin-dependent kinase 9 (cdk9). We have previously shown that cdk9 activity is an absolute requirement for the stress-induced activation of primary inflammatory response genes in human chondrocytes (1). Our hypothesis is that inhibition of cdk9 will protect cartilage from the deleterious effects of inflammatory stress during extended storage of osteochondral allografts. The objective of this study is to test whether cdk9 inhibitors can enhance chondrocyte viability and prevent cartilage matrix degradation during prolonged storage of osteochondral explants at either 37 or 4°C.

Methods:

Harvesting and storage of osteochondral explants - Eight bovine stifle joints from 2-months old calves were obtained from a local slaughterhouse. For each knee, a total of eight osteochondral explants (~20mm height by 8mm diameter) were excised from the weight bearing area of the femoral condyles (four explants from each condyle) by gently inserting an OATS harvesting device (Arthrex Inc.) perpendicular to the articular surface while assisted by a hammer. The excised osteochondral plug was then separated from the harvester core with a core extruder to avoid damage to the articular cartilage surface. The explants were then washed with PBS and cultured at either 37 or 4°C in DMEM containing 1% ITS, 50ug/ml ascorbate, 0.1mM dexamethasone, 40ug/ml proline and 15mM HEPES, and in the presence or absence of 300 nM of CDK9 inhibitor Flavopiridol (Sigma). Each explant was placed individually in a 50ml tube with 20ml media with the tube cap tightly closed. Media with fresh Flavopiridol was changed weekly. At 2 and 4 weeks, the culturing media and the osteochondral explants were harvested. The cartilage was separated from the subchondral bone and weighed.

Chondrocyte viability - The chondrocytes were stained using the LIVE/DEAD Viability/Cytotoxicity kit (Invitrogen, cat# L3224) according to the manufacturer's protocol. The percentages of live and dead cells were determined by counting the cell numbers at three random fields of the cross-section images of the explants captured using a fluorescence microscope with a 40X objective.

GAG assay - Degradation of cartilage matrix was determined by measuring the amount of glycosaminoglycan (GAG) released into the culturing media by the colorimetric dimethylmethylene blue dye-binding assay, using chondroitin sulfate as standards. The total amount of GAG released into the media was normalized to the weight of the individual explants.

Mechanical properties - Mechanical properties were measured in a sample of the cartilage trimmed to 2mm height by 3mm diameter with a scalpel and biopsy punch. Freshly isolated cartilage was used to establish the baseline values of native cartilage. A Bose Enduratec materials testing instrument was used to apply 10% and 20% compressive strain at 100%/second and custom MatLab software was used to estimate the instantaneous and relaxation moduli.

Statistics – All data were shown as mean (n=8 donors) with standard deviation. Statistical analysis was performed by two-tailed paired Student's t-test with a p value of <0.05 to be considered as significant.

Results:

Effects of Cdk9 inhibitors on chondrocyte viability. The viability of chondrocyte in explants cultured for 2 weeks at 4°C was reduced compared to those cultured at 37°C (Fig. 1). Inclusion of 300nM Flavopiridol restored the viability of the 4°C cultures to a level similar to that of the 37°C cultures. At 4 weeks, there was no change in the viability of the explants cultured at 37°C compared to the 2 weeks counterpart in the absence of Flavopiridol. However, Flavopiridol reduced the viability of the 37°C cultures from ~42% to ~28%. Flavopiridol did not significantly alter the viability of the 4°C cultures, whose viability at ~25% is already at the lowest among all samples (Fig 1).

Cdk9 inhibition prevents cartilage matrix degradation. At the 2 week time point, the amounts of GAG released into the media among all samples were between ~320-520 ng/mg cartilage, and the GAG contents were not significantly affected by the addition of cdk9 inhibitors (Fig 2). On the other hand, the overall GAG contents were substantially higher (10-30 fold) in all sample groups at 4 weeks, indicating that there was an acceleration of GAG degradation beyond the 2-week time point. When compared to the 37°C cultures, GAG release was reduced in the 4°C cultures, indicating low temperature is favorable in preserving the integrity of the GAG structure within the matrix. In the presence of Flavopiridol, GAG release was the lowest regardless of the culturing temperature, indicating cdk9 inhibition can prevent GAG degradation during extended storage of cartilage explants.

Cdk9 inhibition preserves the mechanical properties of cartilage. At 2 and 4 weeks, the stiffness of the 37°C explant cultures, but not the 4°C cultures, was lower than that of the native cartilage, as illustrated by a reduction in both the 20% instantaneous and relaxation moduli (Fig 3). This indicates that low temperature is better suited to preserve cartilage integrity during long term storage. However, the addition of Flavopiridol restored the mechanical properties of the 37°C explant cultures to levels comparable to the native cartilage and the explants stored at 4°C, indicating that cdk9 inhibitors have a protective effects on cartilage stored at 37°C.

Discussion: Our data indicate that cdk9 inhibition enhances the viability of osteochondral explants stored at 4°C for up to 2 weeks. Cdk9 inhibition also prevents the loss of GAG from the cartilage matrix and preserves the mechanical properties of the osteochondral explants during long term storage. These observed effects are likely due to the ability of Flavopiridol to suppress the inflammatory response and activation of the catabolic pathways in cartilage.

Significance: Our study provides a novel method to preserve the cartilage matrix integrity during extended storage of osteochondral explants.

References:

1. Yik et al., Arthritis Rheumatology 2014, 66 (6), 1537-1546

Fig 1. Cdk9 inhibition prevents cell death at 4°C.

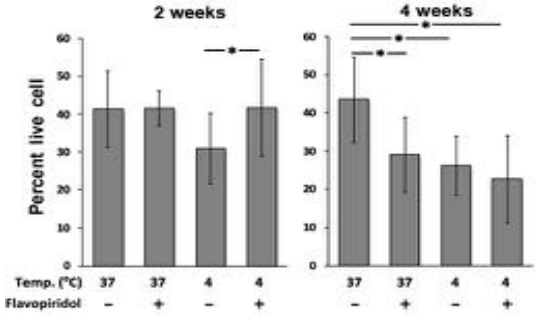

Fig 2. Cdk9 inhibition reduces GAG released into the culture media.

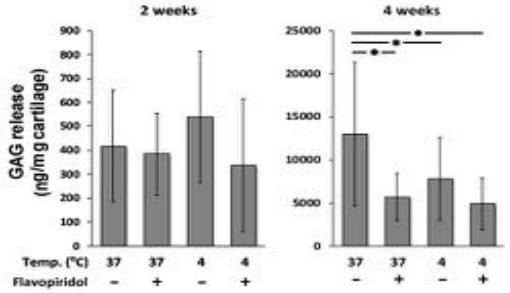

Fig 3. Cdk9 inhibition preserves cartilage mechanical properties at 37 °C.

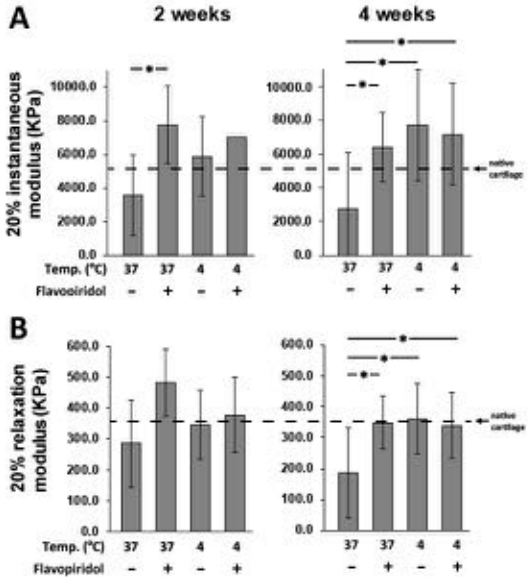

Mouse plasma ELISA

		Plasma			
				50ul	5ul
				1X	1:10
Std(pg/ml)	absorbance	Sample #	absorbance	absorbance	
0.00		UnInjured 1			
31.25		UnInjured 1			
62.50		UnInjured 2			
125.00		UnInjured 2			
250.00		8h 1			
500.00		8h 1			
1000.00		8h 2			
2000.00		8h 2			

		Plasma			
				50ul	5ul
				1X	1:10
Std(pg/ml)	absorbance	Sample #	absorbance	absorbance	
0		JnInjured 1			
31.25		JnInjured 1			
62.5		JnInjured 2			
125		JnInjured 2			
250		8h 1			
500		8h 1			
1000		8h 2			
2000		8h 2			

single-analyte ELISArray kit
Qiagen

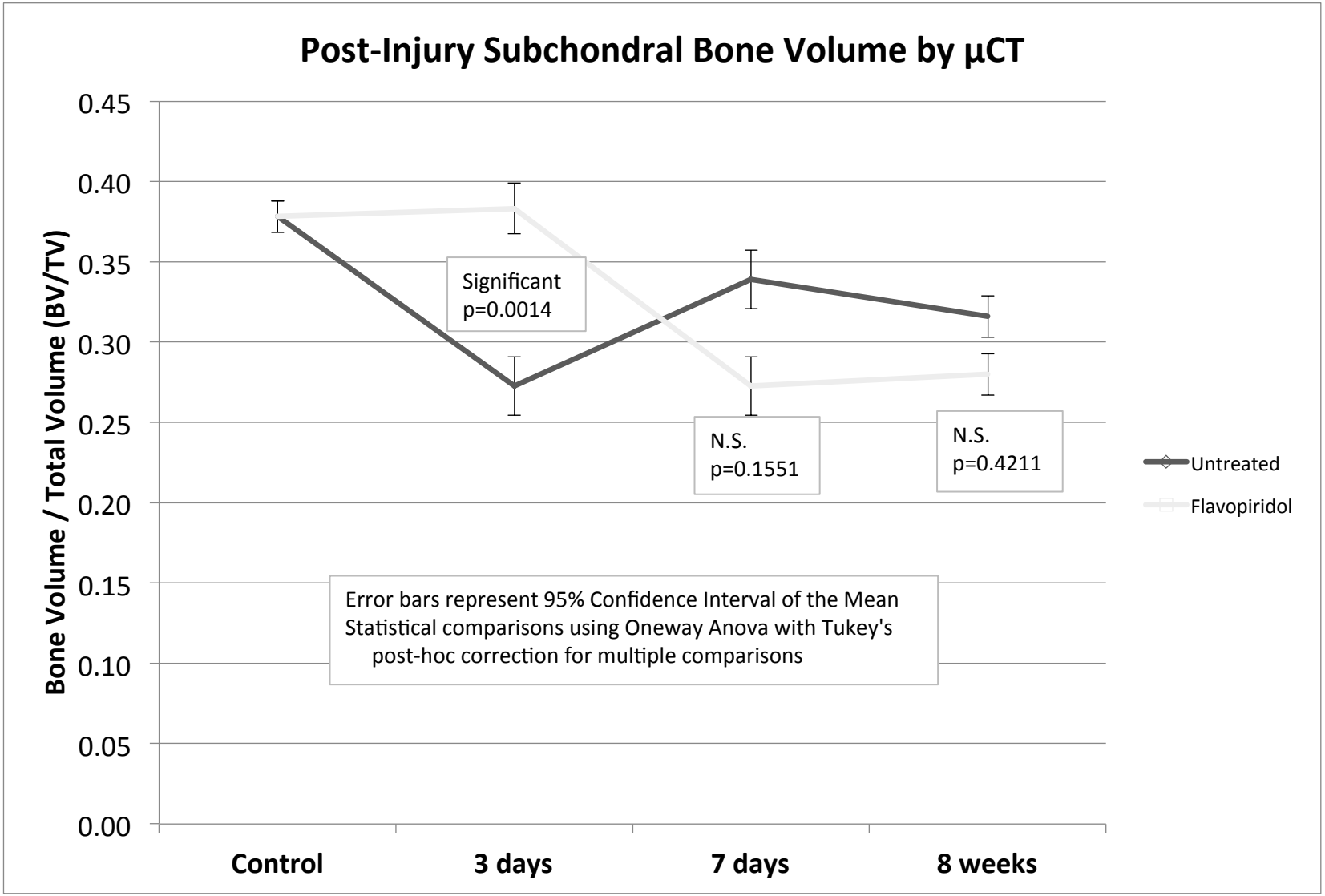
Post-Injury Subchondral Bone Volume by µCT
Bone Volume / Total Volume (BV/TV)
0.45
0.40
0.35
0.30
0.25
0.20
0.15
0.10
0.05
0.00
Control
3 days
7 days
8 weeks
Significant
p=0.0014
N.S.
p=0.1551
N.S.
p=0.4211
Untreated
Flavopiridol
Error bars represent 95% Confidence Interval of the Mean
Statistical comparisons using Oneway Anova with Tukey's
post-hoc correction for multiple comparisons